



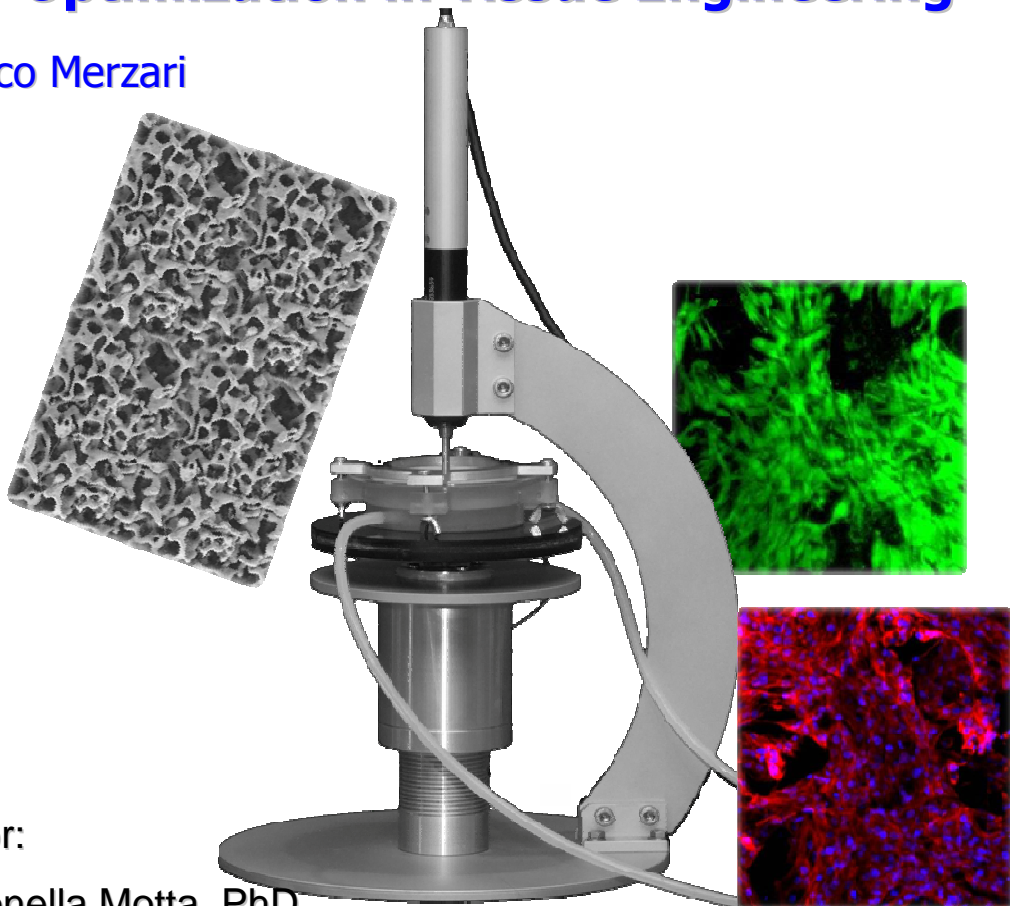
UNIVERSITY
OF TRENTO - Italy

Department of Materials Engineering
and Industrial Technologies

Doctoral School in Materials Engineering – XXIII cycle

Bioreactor Design for Dynamic Process Optimization in Tissue Engineering

Enrico Merzari



Tutor:

Antonella Motta, PhD

Claudio Migliaresi, Prof.

April 2011

Publications:

Papers

1. Motta A, Maniglio D, **Merzari E**, Foss C, Bella E, Migliaresi C. Multicomponent scaffold for osteochondral defects tissue engineering. *Tissue Engineering Part A* 2008, 14 (5): 883-883.

Conference Acta

1. C. Foss, D. Maniglio, **E. Merzari**, C. Migliaresi, A. Motta. Silk fibroin-based multicomponent scaffold for osteochondral defects tissue engineering. VII Convegno nazionale INSTM sulla Scienza dei Materiali. 9-12 Giugno 2009, Tirrenia (PI).
2. A. Motta, C. Foss, **E. Merzari**, D. Maniglio, C. Migliaresi. Silk fibroin-based scaffolds for osteochondral defect regeneration. BIOMED 2009, 15th International Biomedical Science and Technology Symposium. 16-19 August METU, Northern Cyprus Campus, Guzelyurt, TRNC.
3. M. Floren, **E. Merzari**, E. Carletti, A. Motta, C. Migliaresi. Osteoblast genotypic response and matrix formation: Effect of scaffold morphology and mechanical stimuli in vitro – Preliminary evaluation. Proceedings of TERMIS-EU, Gallway, Ireland, June 13-17 2010.
4. A. Motta, C. Foss, **E. Merzari**, Y. Wang, Z. Schwartz, BD Boyan, C. Migliaresi. Silk Fibroin/Hyaluronic acid 3D matrices for cartilage tissue engineering. Proceedings of TERMIS-NA, Orlando, (F), USA, December 5-8 2010.

Abstract	8
1. INTRODUCTION	10
1.1 Cartilage	10
1.2 Cartilage types	11
1.3 Hyaline Articular Cartilage	11
1.4 Composition of Hyaline Cartilage	12
1.5 Anatomy and Function of Articular Cartilage	16
1.6 Organization and Hierarchical Structure of Cartilage	18
1.7 Mechanical behaviour of articular cartilage	20
1.8 Viscoelastic Analysis of Articular Cartilage and Meniscus	22
1.8.1 Solid Matrix Properties	
1.8.2 Compressive Fluid-Solid Properties	
1.9 State of the art in articular repair and regeneration	29
1.9.1. Hyaline Articular Cartilage Injuries and defects	
1.9.2 Cartilage Healing Techniques	
1.9.2.1 Arthroscopic repair: abrasion and drilling arthroplasty (Marrow-stimulating procedures)	
1.9.2.2 Periosteal and Perichondral Implants	
1.9.2.3 Osteochondral transplantation (MosaicPlasty)	
1.9.2.4 Tissue Engineering	
1.9.3 Brief Considerations	
1.10 Bone	40
1.11 Bone composition	40
1.12 Bone Structure	42
1.13 Structural complexity and mechanical properties	44
1.14 Remodelling	46
1.15 Bone Repair and Regeneration Techniques	47
1.15.1 Bone transfer through fixators	
1.15.2 Distraction osteogenesis	
1.15.3 Bone-Grafting	
1.15.4 Bone Tissue Engineering	
2. TISSUE ENGINEERING	53
2.1 Scaffold	60

2.2 Polymer scaffold process techniques	64
2.3 Bioreactors, from static 2D to dynamic 3D culture	68
2.4 Bioreactor stimuli	71
2.4.1 Low/High oxygen partial pressure	
2.4.2 Mechanical stresses and shear stress induced by fluid	
2.4.3 Growth factors	
2.5 Bioreactors used in tissue engineering	76
2.6 Mechanical stimulation in tissue engineering cartilage	85
2.7 Bioreactor used in bone tissue engineering	100
3. MATERIALS AND METHODS	107
3.1 Materials & Methods part 1: Device description	108
3.1.1 Culture Chambers	
3.1.2 Mechanical components	
3.1.3 Controller and Software	
3.1.3.1 Hardware description	
3.1.3.2 Software Description	
3.1.4 Stimulation setting description	
3.2 Materials & Methods part 2: Scaffold characterization	137
3.2.1 Cartilage tissue engineering: Silk fibroin sponges	
3.2.2 Bone tissue engineering: P(d,l)LA sponges	
3.2.3 Characterization techniques	
3.2.3.1 Mechanical properties	
3.2.3.2 SEM and ESEM microscopy	
3.2.3.3 Porosity evaluation	
3.2.3.4 Statistical analysis	
3.3 Materials & Methods part 3: <i>in vitro</i> Experiment	144
3.3.1 <i>in vitro</i> experiment description	
3.3.1.1 Cartilage tissue engineering: validation experiment	
3.3.1.2 Cartilage tissue engineering: condition investigations	
3.3.1.3 Bone tissue engineering: validation experiment	
3.3.1.4 Bone tissue engineering: dynamic hydrostatic pressure, condition investigations	

3.3.1.5 Bone tissue engineering: dynamic hydrostatic pressure, long experiment	
3.3.2 Biological evaluation Techniques	
3.3.2.1 XTT proliferation test	
3.3.2.2 Histology	
3.3.2.3 ESEM & SEM microscopy	
3.3.2.4 Confocal laser microscopy (CLM)	
3.3.2.5 Alamar Blue Assay	
3.3.2.6 Real time-polymerase chain reaction (RT-PCR)	
4. RESULTS AND DISCUSSIONS	158
4.1 Results & Discussions Part1: Device Development	158
4.1.1 Peristaltic Pump Calibrations	
4.1.2 Pressure Gauge Calibrations	
4.1.3 Load Cell Calibrations	
4.1.4 Motor Calibrations	
4.1.5 Device testing	
4.2 Results & Discussions part 2: Scaffold characterization	169
4.2.1 Silk fibroin and PDLA sponges	
4.2.2 Electron Microscopy characterization	
4.2.3 Porosity characterization	
4.2.4 Mechanical properties characterization	
4.3 Results and Discussions part 3: <i>in vitro</i> Experiment	184
4.3.1 Cartilage tissue engineering: validation experiment	
4.3.2 Cartilage tissue engineering: condition investigations	
4.3.3 Bone tissue engineering: validation experiment	
3.3.1.4 Bone tissue engineering: dynamic hydrostatic pressure, condition investigations	
3.3.1.5 Bone tissue engineering: dynamic hydrostatic pressure, long experiment	
5. FINAL REMARKS	212
6. REFERENCES	214

Abstract

Tissue engineering(**1**) is an interdisciplinary field in which cell biology, biomaterials science, and surgery are combined and its main goal is to repair, replace and reproduce tissues and organs.

Following this procedure, cells are seeded on proper scaffolds and induced in sequence to adhere, eventually differentiate, proliferate and finally to produce the wanted extracellular matrix (ECM). During cell culture, the usefulness of applying proper physiological-like stimuli, i.e., biochemical but also mechanical signals to drive and accelerate both cell differentiation and ECM production has been demonstrated(**2**).

Tissue regeneration can be either conducted entirely *in vivo* or assisted by a previous *in vitro* phase. Considering the latter situation, a bioreactor can be defined as any apparatus that attempts to mimic physiological conditions in order to maintain and encourage tissue regeneration in dynamic conditions(**3**). Dynamic cell cultures using bioreactors can be considered a good intermediate step between the conventional *in vitro* static approach and *in vivo* studies. Therefore it is possible to promote the formation of the specific tissue by simulating physiological conditions via the application of specific mechanical and biochemical stimuli.

ABSTRACT

The proposed work is focused on the design and development of bioreactors for bone and cartilage regeneration, in which optimal cell culture conditions are controlled (temperature, nutrients, carbon dioxide and oxygen levels), and mechanical stimuli are applied on the cell constructs. This study presents a wide investigation concerning these mechanical stimulations in order to understand the best cell culture parameters for the activations of cells, naturally accustomed to similar stresses inside the joint. In particular, direct compression, change in hydrodynamic pressure and perfusion modes are compared and analyzed.

1. INTRODUCTION

1.1 Cartilage

Cartilage is a connective tissue highly specialized to guarantee support functions, load bearing behaviour, low friction and viscoelastic properties to absorb stresses and shocks. Cartilage properties leads to a complex structure characterized by low capability of self-regeneration and absence of vascular, neural and lymphatic systems, making cartilage completely different from other tissues(4).

Cartilage is composed by cells, called chondrocytes, and extracellular matrix ECM. Chondrocytes are immersed in the ECM and nutrient transfer, oxygen supply, cellular signaling are ensured by synovial fluid diffusion throughout the matrix. In fact, due to the absence of direct systems, biological substance exchange occurs only by diffusion mechanisms causing a low tendency to regenerate spontaneously after damages. During the organism development, especially in fetal life, most of the skeleton is cartilaginous and subsequently mineralizes. In fact, even if cartilage and bone are both connective tissues, bone has a higher content of calcium phosphate and is also vascularized.

INTRODUCTION

1.2 Cartilage types

In human body, three main types of cartilage can be found: elastic cartilage, fibrocartilage and hyaline cartilage. Elastic cartilage appears opaque and yellowish, and it is principally present in the epiglottis, Eustachian tube, outer ear and larynx. This tissue is composed by elastin fibers, and results to be more flexible than hyaline cartilage, although they are histologically very similar. Fibrocartilage is found permanently in the intervertebral disc, temporomandibular joint, pubic symphysis and meniscus; moreover it is often present temporary in fracture sites. It appears as a dense and fibrous tissue. The third type, hyaline cartilage, mainly exists in ribs, larynx, trachea, bronchi and on articular surfaces covering the proximal part of long bones involved in the joint area. In addition, hyaline cartilage also forms the epiphyseal plate which is replaced by long bones during the childhood growth. In general, articular cartilage appears as a thin coating, thick approximately between 1 and 5 mm, on the contact surface of the joint and it looks like a ivory coloured tissue with a very smooth surface. In this chapter, the hyaline cartilage characteristics are discussed in detail, concerning the structure and the biomechanical behaviour of this tissue in the joints and in the meniscus of the knee.

1.3 Hyaline Articular Cartilage

The main function of hyaline articular cartilage is to ensure a viscoelastic structure which can sustain mechanical loads in the joints and reduce the bone deformation during movement, allowing relative sliding between

INTRODUCTION

articular surfaces. Therefore the contact region must have a low coefficient of friction and the stresses must be transferred along the interface at the same time. In summary, the main cartilage features are friction reducing, relative motion transferring, load bearing and distribution. However, the shock or stress absorption profiles result to be quite different compared to damper behaviour, as described in the next paragraph.

1.4 Composition of Hyaline Cartilage

The mechanical properties of articular cartilage are given by the presence of synovial fluid, which may flow out from the porous matrix when cartilage is stimulated by compression. The basic components of articular cartilage can be divided in two different phases, solid and liquid. The solid structural components include chondrocytes, collagen, proteoglycans of the extracellular matrix and other proteins, while the liquid part consists of synovial fluid and water. The distribution of each component may change within four distinct histological zones: superficial, middle, deep and calcified zone. In figure 1.1, it is possible to observe the typical composition of articular cartilage in meniscus or intervertebral discs. As previously mentioned, chondrocytes (from Greek *chondros* cartilage and *kytos* cell) are the only cells found in cartilage tissue. Cells, when their maturity is reached, occupy only a small fraction of the total volume and are trapped in capsules, called "lacunae". Chondrocytes present a rounded shape which may change slightly along the tissue section, acquiring a little orientation. Chondrocytes are also characterized by a limited mitogenic capacity, especially in old

INTRODUCTION

cells, and by a very slow anaerobic metabolism. Chondrocytes present a membrane with numerous protrusions, having an highly developed Golgi apparatus, and may be binucleated. These cells produce and maintain the extracellular matrix, which is principally composed by collagen and proteoglycans. The extracellular matrix ECM represents the 90-95% of the total dry volume, while cells only the 5-10%. The extracellular matrix is macroscopically homogeneous, although at microscopic level, the structural and compositional characteristics change, moving from outer surface to bone.

Tissue	Collagen (% dry wt.)	Proteoglycan (% dry wt.)	H ₂ O (% wet wt.)
Articular cartilage	50-73	15-30	58-78
Meniscus	75-80	2-6	~70
Intervertebral disc - nucleus pulposus	15-25	~50	70-90
- annulus fibrosus	50-70	10-20	60-70

Fig.1.1. Composition of articular cartilage, meniscus and intervertebral disc(5, 6,192).

Collagen is the main protein of animal connective tissues, and is the most abundant protein in mammals (25-30% of the total protein amount), representing approximately the 6% of human body weight. The tropocollagen is the collagen structural unit, a protein with a molecular mass of approximately 285 kDa, composed by three polypeptide chains in alpha-

INTRODUCTION

helical conformation. The collagen biosynthesis can be carried out by different cell types depending on the tissue. The biosynthesis begins through the gene transcription and the subsequent mRNA maturation. However, the process is completed outside the cell where tropocollagen can be synthesized. The tropocollagen molecules are spontaneously arranged in parallel staggered rows through hydrogen bonds and chemical cross-linking, forming semicrystalline *fibrils*. Finally, fibrils may aggregate in waved or parallel fibers. Collagen has a high level of structural organization and several types of collagens can be found. Collagen type I and type II are predominant in articular cartilage. Collagen type I is mainly present in the fibrocartilage and in the main connective tissues such as skin, tendons, bones and cornea, and represents nearly the 90% of the total collagen in the body. Instead, collagen type II can be found mostly in hyaline cartilage, intervertebral discs and in the vitreous humor. Due to its structure, composed by fibers and fiber threads, collagen improves the tensile and shear strength, providing stiffness to the tissue.

Proteoglycans, which are immersed in the collagen network, are another important component of cartilage. Proteoglycans are composed by a proteic axis, called *core*, where long chains of disaccharides or glycosaminoglycans (GAG) are linked through covalent bonds. Proteoglycans can be divided in two types, sulfate and non-sulfate compounds. The first group is constituted by chondroitin sulfate, keratan sulfate, heparan sulfate and dermatan sulfate. The second consists mainly of hyaluronic and chondroitin acid. The main property of these polymeric molecules are given by acidic sulfonic acid SO_3^-

INTRODUCTION

and carboxylic acid COO^- terminal groups mostly deprotonated, which thus introduce a strong negative charge. Proteoglycans possess the ability to interact with other elements or with each other, forming a network structure with densified meshes, providing a filtering action. In fact, GAGs are located in the extracellular matrix in order to filter cell nutrients and other substances; in addition, a large amount of water can be stored thanks to the negative charge, regulating the hydration level in the tissue.

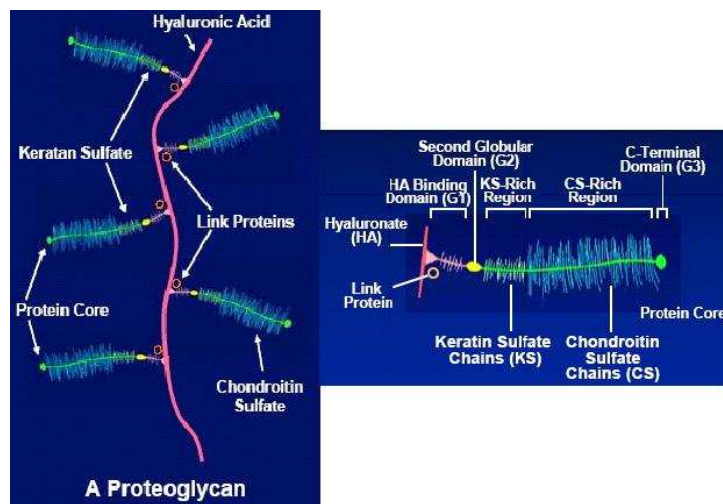


Fig.1.2. Proteoglycan structure(7,193).

Consequently, water retention and the described GAG network can also perform a support function to compressive forces, giving up a resistance 65 times the human body weight. Figure 1.2 shows the proteoglycan structure in two different sections. Water and synovial fluid are the last main component of articular cartilage, representing a significant volume fraction

INTRODUCTION

of the tissue, between 58% and 78%. In articular cartilage, water provides the chondrocyte nutrition by diffusion and also contains inorganic ions in solution, such as Ca^{++} , Na^+ , K^+ and Cl^- . The 70% of water binds to proteoglycans, while the remaining 30% to collagen. Water is usually concentrated on the surface. Thanks to the interaction between the molecules in the extracellular matrix, viscoelastic behaviour can be achieved. Therefore, water may freely move in the matrix and between the fibrils, providing mechanical and tribological properties to cartilage and adjusting tissue deformation during load. In synovial fluid, hyaluronic acid and glycoprotein, such as lubricin, proteinases, and collagenases, are also contained.

1.5 Anatomy and Function of Articular Cartilage

The cartilage can also be seen as a biphasic elastic and porous material, with a heterogeneous structure at a microscopic level, in which it is possible to distinguish layers with different properties related to different collagen fiber orientations. As previously mentioned, almost 80% of the tissue is composed by water. The mechanical properties are guaranteed by the network of collagen type II and proteoglycans, in which collagen fibrils ensure the tensile strength and biomechanic resistance, while proteoglycans promote viscoelastic behaviour allowing also compression strength and recovery properties. Subsequently, depending on the required properties and functions, the component distribution must be organized. The extracellular matrix ECM must provide a specific organization and distribution starting

INTRODUCTION

from chondrocytes, which synthesizes the molecules. In addition, low mobility, induced by ECM, prevent the migration of other cell types within the tissue, such as macrophages. Chondrocytes are distributed in the micropores of the tissue exhibiting several connections with the matrix, to evaluate the status and the biomechanical behaviour of the tissue.

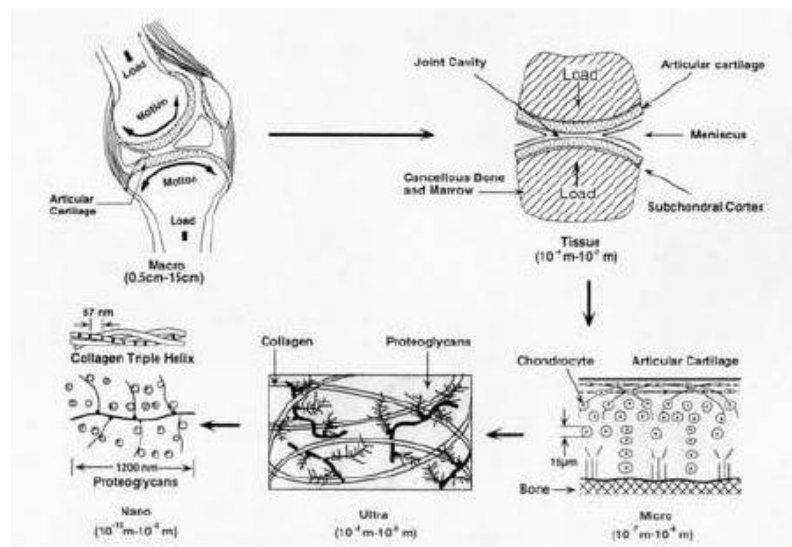


Fig.1.3. Hierarchical level of articular cartilage(8).

These connections are crucial to maintain the normal phenotype, and explain the cell low mobility. The articular cartilage presents a complex structure hierarchically organized. In figure 1.3 it is possible to observe the hierarchical nature of articular cartilage in the joint, which is divided into five levels depending on the analyzed scale dimensions. The first level (fig- 1.3 top left), shows the macroscopic composite structure of the joint, which

INTRODUCTION

is composed by bone, cartilage, ligaments, tendons, muscles and joint capsule. The next level (fig.1.3 top right) reports a sketch of the joint surface, in particular it describes where the stresses are transferred between bones. In the third level, between 1 μm and 100 μm , cartilage does not appear as a homogeneous matrix anymore, but a specific organization, which contains chondrocytes and collagen type II fibrils, is present. In the fourth and fifth levels, the micro- and submicroscopic organization of the main solid components is shown. It is possible to observe the individual collagen fibrils and the proteoglycan network between 0.01 μm and 1 μm , while at a nanometer level the molecular structures of proteoglycans and collagen are schematized. This brief description is not enough to explain the complex mechanical behaviour of cartilage, in fact, an important key to understand the tissue properties is to consider the interaction between structures, water and the electrolytes. Thus, the fluid-solid interaction may be considered the main cause of the cartilage mechanical characteristics.

1.6 Organization and Hierarchical Structure of Cartilage

The cartilage organization at a microstructural level can be summarized considering 4 regions: the superficial or tangential zone, the middle zone, the deep zone and the tide mark or calcified zone, where cartilage is joined to the subchondral bone. The summary layout is reported in figure 1.4. The highest amount of collagen is contained in the surface zone, about 85% of the dry weight. Collagen fibrils are packed and oriented parallel to the surface, which underlines how the main function of the first zone in hyaline

INTRODUCTION

articular cartilage is to withstand shear stresses. The collagen content generically decreases up to the tide mark, reaching a value of about 68% in the middle zone. The surface zone is a fraction of the total thickness, between 10% and 20%. In this surface region, the produced proteins behave as a lubricant, further reducing the shear stresses.

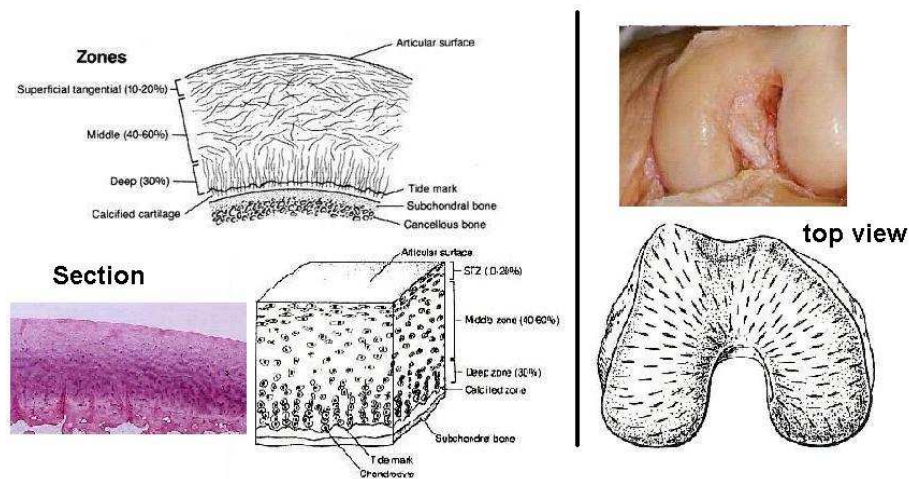


Fig.1.4. Cartilage section (left) and top view (right)(5, 6, 8-10, 191-193).

The middle zone has a high content of proteoglycans and a randomly distributed collagen fibers which appear to be thicker. The middle zone represents the 60% of the thickness. In the deep zone, which is about 30% of the thickness, collagen fibers are longer and vertically oriented, in order to improve the stress distribution and the compressive strength. The tide mark is the interfacial region of junction between cartilage and bone. Thanks to the fiber disposition, stresses at the interface are reduced. In fact, this calcified region presents collagen fibers anchored to the subchondral

INTRODUCTION

bone. The scheme described in this section and photos achieved by optical microscopy are shown in figure 1.4 as well as the top view of the collagen fibers distribution on the articular cartilage of the knee. In the outer zone of articular cartilage and meniscus, the collagen fibrils are arranged in a circular way and are more organized compared with middle zone fibers. This orientation can increase considerably the tensile strength in the outer cartilage.

1.7 Mechanical behavior of articular cartilage

As previously described, the hyaline cartilage composition presents two main phases, fluid and solid one. The first contains water and electrolytes, and the second is composed by collagen (type I in the meniscus and type II in the joint), proteoglycans, glycoproteins and chondrocytes (191). The specific constituent contents are shown in the table of figure 1.5.

<u>Tissue</u>	<u>Water</u>	<u>Collagen</u>	<u>Proteoglycans</u>
Articular Cartilage	68-85%	10-20% (type I)	5-10%
Meniscus	60-70%	15-25% (type II)	1-2%

Fig.1.5. Component contents in articular cartilage and Meniscus(5, 6, 193).

The three components reported in the table (water, collagen and proteoglycans) interact with each other determining the mechanical behavior of cartilage. A variation of component contents of a specific tissue portion, for example due to diseases or degenerations, can lead to significant changes in mechanical properties.

INTRODUCTION

In the extracellular matrix, proteoglycans are aggregated in the collagen network, also absorbing about 30% of the total water content. The water content, but also the collagen fiber diameters, are determined by the swelling pressure due to accumulation of negative charge density (fixed charge density FCD) on proteoglycans. The swelling pressure is the developed pressure inside the tissue, which allows the water absorption. In other words, thanks to the strong negative charges given by proteoglycans, repulsion forces are generated, which can only be neutralized by positive ions contained in the surrounding fluid. The difference in ion concentrations can be considered the driving force determining the swelling pressure. In this way an increase in repulsion forces and swelling pressure can be achieved when water is released such as by compression. Water content finally depends on various factors related to proteoglycan concentrations (which also influence the FCD and the swelling pressure) and to the organization, distribution, stiffness and strength of the collagen network playing a retained function on the tissue and maintaining the structure compact. In fact, cartilage tensile strength is commonly attributed to collagen. Thus, cartilage is a dynamic system which responds to the external environment. The collagen network must resist to the swelling pressure of the articular cartilage. When the collagen network degradation occurs, such as in osteoarthritis, water content in cartilage increases due to an increase of negative charge. Fluid variation can significantly alter the mechanical behaviour of cartilage.

1.8. Viscoelastic Analysis of Articular Cartilage and Meniscus

As widely described, the three main factors, which contribute to influence the articular cartilage mechanical behaviours, are the swelling pressure, the elastic properties of the solid matrix and the fluid-solid interaction in cartilage under compression. In this chapter, the influence of ECM structure on mechanical properties is examined.

1.8.1 Solid Matrix Properties(191)

As a first analysis, the tensile properties and the solid matrix behaviours will be considered. Considering most of the soft tissues, characterized by low stiffness matrix and randomly orientated fibers, the solid matrix mechanical behavior is determined by the collagen fiber content and by their arrangement in the cartilage matrix. In figure 1.6 it is possible to observe the classic J-shape stress-strain curve for a soft material. The graph also shows clearly the first non-linear trend and the fracture end. The first region corresponds to the re-orientation and alignment of fibers, principally composed by the biological macromolecules previously described. In general, elastic modulus is calculated using the linear slope which coincides in first approximation with the stiffness of the aligned collagen fibers. This assumption may also be applied for the fracture behaviour . In figure 1.6(a), a typical specimen to test the mechanical properties is reported. It is possible to observe how a variation in collagen content can affect the mechanical properties of cartilage, in terms of structural behaviours. In figure 1.7(a), some experimental data found in literature are summarized, in which the

INTRODUCTION

reported elastic moduli correspond to the linear portion of the measured tensile curves in different regions of cartilage.

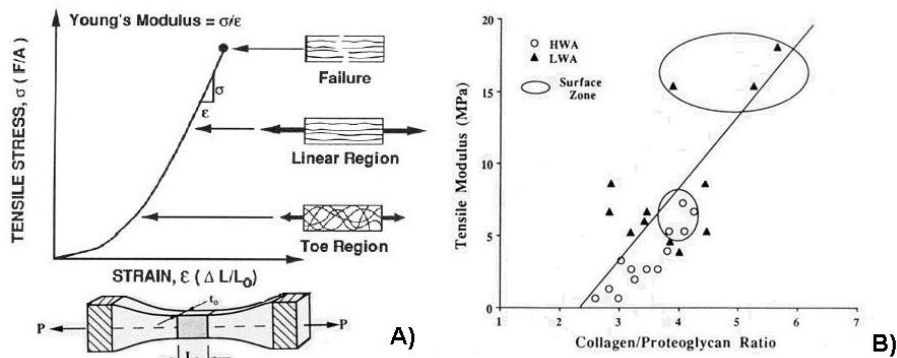


Fig.1.6. (A) J-shape curve and test specimen; (B) Graph: Tensile Modulus vs Collagen/proteoglycans ratio(9, 191).

The results listed in the table (figure 1.7(a)) can be confirmed analyzing the graph in figure 1.6(b), which plots the measured tensile modulus as a function of the ratio between collagen and proteoglycan contents in cartilage matrix.

	Bovine		Canine		Human	
	Glenoid Condyle	Humerus	Femoral Groove	Femoral Condyle		
Groove						
Superficial	5.9	13.4	27.4	23.3	13.9	7.8
Middle	0.9	2.7			3.4	4.0
Deep	0.2	1.7			1.0	

A)

	Normal (MPa)	Fibrillated (MPa)	OA (MPa)
Surface	7.8	7.2	1.4
Subsurface	4.9	7.5	0.85
Middle	4.0	4.9	2.11

B)

Fig.1.7. (A) Elastic Moduli of different part of cartilage; (B) Tensile modulus during tissue degeneration(9,191).

INTRODUCTION

Osteoarthritis (OA) are the main cartilage diseases in which tissue degeneration and a significant change in solid matrix mechanical properties are found. As explained by histological analysis, this dysfunction is caused by the collagen fibers breakdown. The table (figure 1.7(b)) shows how the elastic modulus decreases with the pathology degeneration; *Fibrillated* corresponds to an intermediate situation where the defect is filled with fibrocartilage. Being a soft tissue, cartilage cannot show a linear trend and can be considered hyperelastic. Consequently, it is also possible to derive the strain energy function to calculate the relationship between stress and strain. The following function can be assumed:

$$W = k(e^{BE} - E) \quad (1)$$

where k and B are material constants and E is the Green-Lagrange deformation. Differentiating the function on the strain E , the stress S can be obtained:

$$S = \frac{\partial W}{\partial E} = Bk(e^{BE} - 1) \quad (2)$$

1.8.2 Compressive Fluid-Solid Properties

As previously introduced, the fluid-solid phase interaction plays a crucial role in the mechanical behaviour of cartilage. The water flow out determines the tissue behaviour, in fact the compression properties strongly depend on the fluid ability to flow in or out from the tissue. This behaviour can be described by the cartilage permeability. The matrix permeability is governed by Darcy's law. Darcy's law relates the expelled fraction volume through the

INTRODUCTION

porous solid (discharge) with the applied pressure gradient and the hydraulic permeability coefficient k . Darcy's law is expressed mathematically by the relation(191):

$$Q = \frac{k \cdot A \cdot \Delta P}{h} \quad (3)$$

where Q is the volumetric flow rate [m^3/s], k is the permeability coefficient [m^4/Ns], A is the surface [m^2], ΔP is the pressure gradient [N/m^2] and h is the sample thickness [m]. The permeation rate V can be obtained by differentiating Q on the surface. The diffusion resistance coefficient K , which can be defined as the resistance generated by the liquid on the solid, is determined through the equation 4:

$$K = \frac{(\Phi_v)^2}{k} \quad (4)$$

where K is the mentioned resistance, k is the permeability and the remaining term Φ_v is the fluid volume fraction. The permeability and load distribution between liquid and solid phases are the basic concepts of the biphasic theory in articular cartilage, and can be summarized as follows(191):

- the isotropic or anisotropic matrix can assume elastic or hyperelastic behaviours;
- the solid and fluid phases are considered incompressible. Thus, it is clear how cartilage can be compressed only when the fluid is completely expelled from the tissue;
- the dissipated energy corresponds to the energy consumption during fluid expulsion through the matrix;

INTRODUCTION

- the friction caused by the fluid-solid resistance is proportionally related to the relative velocity, through the coefficient K .

The equations of dynamic equilibrium (5) can be written according to the biphasic theory, as follows:

$$\frac{\partial \sigma^s_{ij}}{\partial x_j} + K(v^s - v^f) = 0 \quad ; \quad \frac{\partial \sigma^f_{ij}}{\partial x_j} + K(v^f - v^s) = 0 \quad (5)$$

where σ^s_{ij} and σ^f_{ij} are the stresses along the i-j principal directions, respectively for the solid and the fluid, K is the resistance coefficient, v_s is the solid speed and v_f is the fluid speed. This theory summarizes the cartilage mechanical behaviour under compression. As example, it is possible to observe figure 1.8. In this specific case fluid can not immediately leave the matrix due to the resistance (*point A*); therefore the system has a tendency to retain a high level of stresses. In this way, the cartilage at *point B* can no longer deform and an increase in the total stress can be observed. When the fluid leaves the tissue (*points C-D*), stresses are transferred to the solid matrix and hence are significantly reduced. Equilibrium modulus and permeability coefficient are two key material properties in the described theory. The equilibrium modulus corresponds to the cartilage stiffness after the total fluid flow out (*point E*).

However, under normal conditions, the GAGs contained in proteoglycans possess a sufficient negative surface charge to draw in water and ions from outside, causing an increase of the internal pressure. The generated swelling

INTRODUCTION

pressure is counteracted by the collagen network and by the applied compression.

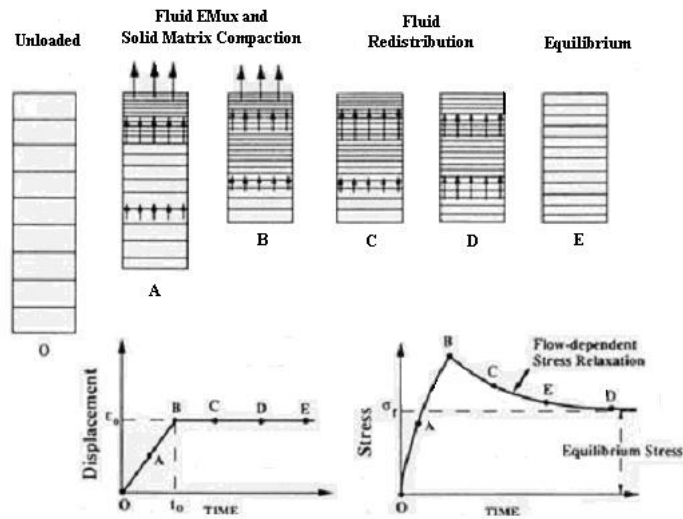


Fig.1.8. In figure the loading and unloading behaviours are reported(4).

In advanced osteoarthritis (OA), the permeability increases due to collagen fibers loss; consequently the maximum stress achieved during the fluid flow out decreases, causing a rise of the stress exerted on the solid phase. The increased stress on the solid matrix can increase the tissue damage, creating a “*vicious loop*” which leads to a further tissue degeneration. In figure 1.9 ECM structure and collagen network are reported. The articular cartilage viscoelastic behaviour can be summarized as follows:

- the liquid flow out, due to the compression, may alter the viscoelastic properties of cartilage (Figure 1.8);

INTRODUCTION

- the stress-strain relationship is not linear, and depends on water content in the system;
- different behaviour of the tissue when it is subjected to compression or tensile stresses;
- resilience: low permeability prevents a quick water squeeze out from the cartilage. Thus, the fluid phase "protects" the solid one during impacts or shocks, preventing matrix damage;
- anisotropy;
- very low friction coefficient: ankle 0.005 - 0.02; hip: 0.01 - 0.04; graphite on steel: 0.1, UHMWPE (Ultra High Molecular Weight PolyEthylene) on cobalt-chromium: 0.01 to 0.05.

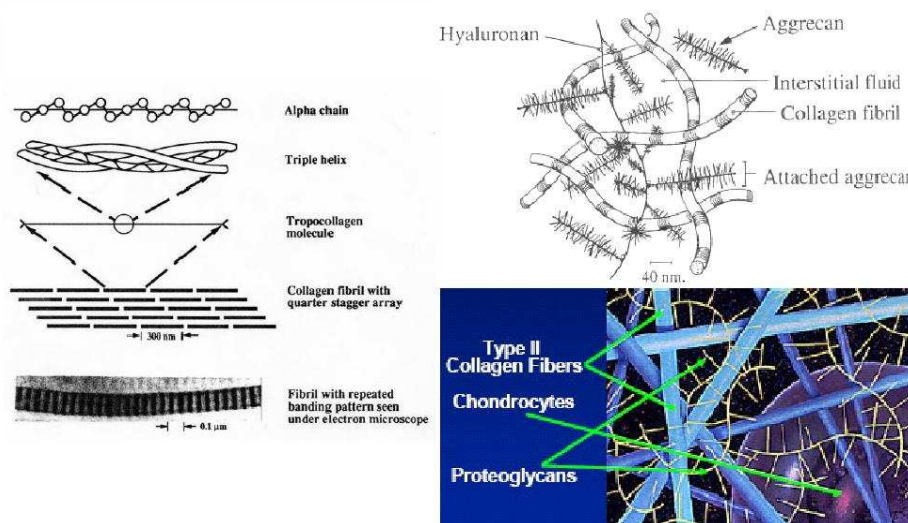


Fig1.9. ECM structure, both collagen and proteoglycans are shown(7-9).

1.9. State of the art in articular repair and regeneration

1.9.1. Hyaline Articular Cartilage Injuries and defects

Articular cartilage is a highly specialized connective tissue which must sustain considerable mechanical stresses while ensuring an extreme smoothness between articular heads. Due to the complete absence of blood vessels and nerves, cartilage exhibits little self-regenerative capacity when an injury or a disease occurs. Cartilage lesions can be classified as full or partial thickness defects, depending on the injury depth the subchondral is respectively exposed or not(II). Cartilage damages are usually caused by an excessive load, which leads to an alteration and loss of the macromolecule organization in the tissue. In fact, traumatic injuries can occur due to a sudden impact or movement and can be direct or caused by other events (indirect), such as ligament tears. Repeated external actions can also lead to wear damages or to osteochondral fractures, which consists of the detachment or laceration of cartilage-subchondral bone interface. Other lesions may take place by congenital or metabolic diseases, such as Paget's disease, hamemophilia and acromegaly. Cartilage defect can also be acute or chronic. The natural tissue degeneration caused by a pathology, old age of the patient or as a result of a mechanical action, also known as osteoarthritis, is the deterioration of the proteoglycan gel, which leads to a reduction in water content, a decrease in the mechanical properties and finally a consequent wear. The healing capacity of a partial thickness disease depends principally on the defect dimension (width and depth), on

INTRODUCTION

the position on the joint and on the patient age. In fact, the articular cartilage has not a strong inclination to a spontaneous regeneration. It is well known how only small lesions may be filled with fibrocartilaginous tissue, while larger defects are rarely self-healed, incurring in a progressive complete degeneration. Full thickness lesions induce a vascular proliferation response which produces only fibrocartilage. This natural process of cartilage is mainly based on the effusion of mesenchymal stem cells from bone marrow. Several techniques for partial defect care take the advantage of this natural mechanism. After the surgical drilling, the subchondral bone occurs infiltration of stem cells from the bone, resulting in tissue formation which mainly consists of fibrocartilage. Although fibrocartilage fills and covers the defect, the newly formed tissue is not the correct material in terms of biomechanical properties. Fibrocartilage is a weak substitute of hyaline cartilage and tends to degrade rapidly with time. In fact, fibrocartilage principally may resist under tensile stresses, while the main function of hyaline cartilage is to counteract compression stresses, long and variable load cycles and finally shear stresses. In addition, during the regeneration, the fibrocartilage close to the normal tissue may become necrotic, with a none or a slight remodelling in hyaline cartilage only in the centre of the defect. Several studies (*12*) have demonstrated how the 40% of patients, treated with arthroscopic knee surgery, in order to fill the defect with fibrocartilaginous tissue, have reported a strong degeneration of the formed tissue. For many years, the main cartilage healing techniques were more focused on the repair or regeneration of the damaged tissue, rather than the

INTRODUCTION

filler properties. However, these techniques have shown poor successful due to the complex properties and histological characteristics of the cartilage(13). Now, it is important to distinguish between the concepts of "repair" and "regeneration" in order to choose the most appropriate healing technique to use with a specific type of injury(1, 11, 14-18).

Repair: generally it is related to the healing or replacement process which involves the damaged tissue by cell proliferation and new extracellular matrix synthesis. Typically, the repaired tissue shows different structure and composition and worse functions if compared to the normal cartilage.

Regeneration: it refers to the formation of new ECM which essentially duplicates the original hyaline articular cartilage.

1.9.2 Cartilage Healing Techniques

Several problems can occur during the healing process of cartilage tissue, but it is possible to summarize these considering two different approaches. The defect can be either filled with a material matching the natural cartilage properties or else the formed tissue and the surrounding hyaline cartilage can be integrated together. Even small defects may fail during the filling and consolidation processes, leading to tissue degeneration and consequently to osteoarthritis. Repair cartilage procedures can include open surgical or arthroscopic techniques, allogenic or autogenic tissue transplantation procedures, and finally tissue engineering. The arthroscopic techniques can be summarized as arthroscopic lavage, shaving and debridement (drilling), abrasion chondroplasty (abrasion), Pride drilling and microfracture

INTRODUCTION

technique. Open surgical techniques have only limited applications, such as osteotomies and osteodistraction in which bone orientation and position is externally modified in order to shift the maximum stressed region, preventing further damages. Other open surgical procedures involve autograft or allograft transplantation, including chondral or osteochondral implants (mosaicplasty), perichondral and periosteal grafts. Tissue engineering is a very promising technique in which autologous chondrocyte implantation ACI, or the application of mesenchymal stem cells MSCs, scaffolds, growth factors and cytokines are considered.

Currently, different surgical techniques were proposed for articular cartilage treatment. However, there are not clear results which show long-lasting repair or regeneration, in terms of composition, structure, functions and finally integration. The previously listed techniques are explained and divided into reparative techniques, such as drilling, abrasion or microfracture; and regeneration techniques, such as mosaicplasty, perichondrium or periosteum transplantation, or tissue engineering.

1.9.2.1 Arthroscopic repair: abrasion and drilling arthroplasty (Marrow-stimulating procedures)

The main arthroscopic techniques include lavage, debridement and abrasion arthroplasty, Pride drilling and microfracture techniques. These techniques consist mainly in defect cleaning, removing any obstacle which mechanically precludes a correct joint motion and also aiming to promote blood effusion from subchondral bone, practicing accesses for stem cells,

INTRODUCTION

which penetrate and stimulate the formation of fibrocartilaginous new tissue. Arthroscopic repair techniques are minimal invasive procedures which can induce a significant pain relief, nevertheless these methods cannot be considered curative techniques, but only palliative. The main problems regarding these techniques are tissue degeneration and necrosis, resulting in cell death induced by the heating during abrasion and drilling processes. In addition, subchondral bone may be compromised affecting any future operation in repairing or regenerating the tissue. Finally, fibrocartilage does not present the basic properties to guarantee the needed mechanical performance, such as wear resistance and mechanical interface strength. In fact, the results cannot be considered satisfactory in most cases(11, 12).

1.9.2.2 Periosteal and Perichondral Implants

Periosteal (a vascular layer which covers the bone), and perichondral (a fibrous layer on cartilage) grafts were widely used as implants to fill full thickness defects in articular cartilage repair. The periosteum is a highly vascularized connective tissue. Currently, periosteal implants are preferred, considering the highest availability and the experimental data which do not report different results when the grafts are compared. The formed tissue are generally synthesized by chondrocyte precursor cells from both the subchondral bone and the grafts. Clinical experiences have shown poor results, in terms of hyaline cartilage content and long-lasting stability, while graft calcification probably occurs causing an high number of failures.

1.9.2.3 Osteochondral transplantation (MosaicPlasty)

Osteochondral transplantation (or mosaicplasty) is a widely used technique for the osteochondral defect treatment. The implants can be divided in two categories, autologous grafts, from the same organism, and allografts, when the allogenic implants are harvested from other organisms. Autologous grafts are obtained from an unstressed articular portion. Obviously, autotransplantation is only applied for small lesion treatments, while allografts are preferred in larger defects. This technique presents several advantages, such as low cost, it's minimally invasive and may be conducted either via arthroscopic or via open surgery. Furthermore, there is no immune rejection for autografts, it is one-stage operation and it does not depend on cell proliferation. It is very useful for joint defect associated to ACL (Anterior Cruciate Ligament) tears and finally can give good and promising results, in terms of structural and composition properties of the filler material.

However, integration problems are not resolved due to the incomplete geometric filling of the defect, where a minimum gap between the natural tissue and the graft is difficult to eliminate; in addition, cell necrosis and death are induced during graft harvesting.

1.9.2.4 Tissue Engineering

The aim is to produce a new hyaline cartilage-like tissue, starting from chondrogenic cells. Following, ACI (Autologous Chondrocyte

INTRODUCTION

Implantation) and MACI (Matrix-Induced Autologous Chondrocyte Implantation) techniques are briefly described.

Autologous Chondrocyte Implantation (ACI)

ACI technique is currently used as treatment of chondral and osteochondral symptomatic defects of the knee and it is developed following two main stages. ACI technique involves the use of chondrogenic cells harvested from the patient and then expanded to induce proliferation. The obtained chondrocytes are finally reimplanted ($\sim 3 \cdot 10^7$ cells/mL) in the patient's knee to promote the formation of hyaline cartilage-like tissue and defect regeneration. In surgical practice, the defect is enlarged to reach the subchondral bone and washed to prepare the cell container. Cells are finally deposited or injected in the prepared site and the defect is sealed with a periosteal or a collagen membrane by suturing or gluing. A linear dependence between the seeded chondrocyte number and the relative biosynthetic activity can be identified. Growth factors are also injected to enhance cell proliferation, induce cell differentiation and ECM synthesis; in fact a different MSC contribution from subchondral bone and periosteum can be found. Studies on molecular mechanisms have shown a low collagen type II mRNA expression, suggesting how transcription process is not fully activated, such as Sox-9, Egr-1 and Aggrecan expression. Other technical limitations of conventional ACI are the chondrocyte non homogeneous distribution, making necessary the use of a suspension and increasing the risk of external effusion. The experimental results in ACI treatment are only

INTRODUCTION

updated for few years, with uncertain long-term data. Figure 1.10 shows the ACI technique. However, in clinical practice, ACI procedures have given satisfactory results, in terms of pain relief, formed ECM structure and function properties. Most of the ACI treated patients (often over 70% of the analyzed patients) presents an improvement of articular cartilage and a better quality of life; while studies, which compare ACI and mosaicplasty techniques, have reported contradictory results(*II*).

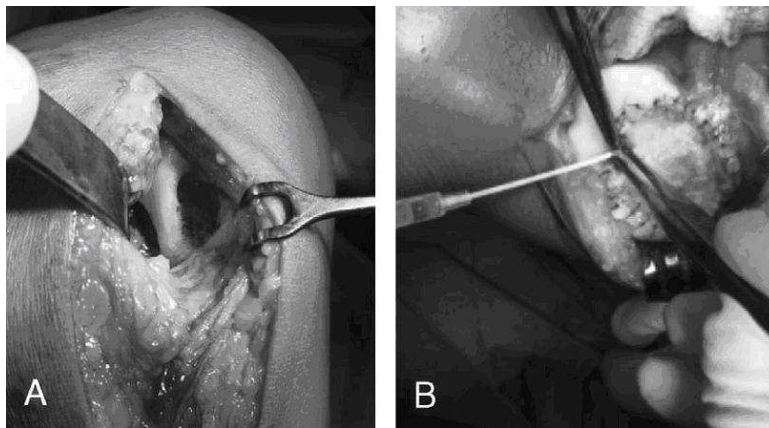


Fig.1.10. ACI Technique: A) defect opening; B) suturing.

These data indicate how the described treatment techniques are still heavily dependent on the defect type, size and extension, patient's age and other external factors able to affect the result goodness, suggesting how it is still necessary to improve these treatment methods.

INTRODUCTION

Matrix-Induced Autologous Chondrocyte Implantation (MACI)

Although ACI techniques have shown remarkable results especially in the articular cartilage regeneration, a new method to improve ACI techniques was developed. In MACI technique (matrix-induced autologous chondrocyte), cell culture is favoured through the transplantation of a preseeded bioreabsorbable polymer matrix. So, biodegradable scaffolds are studied to resolve the observed problems by ACI. In fact, scaffolds can also act as a barrier against the migration of fibroblasts derived from subchondral bone, which may cause a fibrous repair, while maintaining a homogeneous chondrocyte distribution. MACI implant presents several advantages, such as the absence of sutures, it does not require the harvesting of a periosteal portion and can be carried out quickly and without an extended exposure. The preliminary performed tests are promising, but limited in the patient number. In addition, the long-term evaluations are not yet reported, considering how MACI is still a recent technique. However, the MACI procedure is currently considered the most promising approach.

MSCs, Scaffolds, Growth Factors and Cytokines

The MSCs are widely used in the articular cartilage regeneration due to their chondrogenic potential. MSCs are pluripotent cells with the ability to differentiate in various cell type of the connective tissues, such as chondral tissue, bone, muscle and tendon. So, the bone marrow derived MSCs can differentiate in several cell types, such as osteoblasts, adipocytes, and chondrocytes. Currently in tissue engineering, a common practice is to

INTRODUCTION

combine the use of stem cells and scaffolds. Scaffold materials may satisfy certain specific characteristics of biocompatibility, strength and structural stability. In addition, these matrix must be able to induce cell maturation and differentiation, as well as sustain cell growth and ECM synthesis. Finally, cell culture stimulation by cytokines and growth factors is commonly used to promote cell proliferation and synthesis of extracellular matrix. For example, Matsusaki and Kawasaki have found respectively the positive effect of hyaluronic acid (HA) and transforming growth factor α (TGF- α) on cell proliferation and chondroitin-sulfate synthesis by seeded chondrocytes(II).

1.9.3 Brief Considerations

Currently, many promising techniques and procedures are employed for articular cartilage repair and regeneration. All the described techniques are widely used in clinical practice for injury treatment. However, researchers have shifted to the production of hyaline cartilage-like tissue. In addition, it is necessary to search new strategies in order to promote the integration with the native tissue. The use of arthroscopic techniques combined with products derived from tissue engineering, such as *Hyalograft C*, seems to be the best promising approach. In fact, tissue engineering is still a medicine field involved in strong and rapid improvements. Pluripotent mesenchymal stem cells, embryonic stem cells, reabsorbable biomaterials, growth factors and biomechanical stimuli can be considered useful tools, while their combination can lead to good results for the articular cartilage treatment.

INTRODUCTION

However, the summarized strategies for cartilage repair and regeneration generally fail to prevent the future degeneration, probably caused by the nature of the formed tissue. The hyaline cartilage often presents an immature form and does not show correct mechanical and surface properties, resulting in an inevitable future implant failure. For this reason, further investigations are needed, such as the application of MACI technique combined with different type of scaffolds and seeded cells(*11, 12, 19-21*).

1.10 Bone

Bone(22) is a mineralized connective tissue. The main function of bone is to sustain and protect the soft tissues of the body, while also allowing movements through the joints. The intercellular matrix is mainly formed by mineral crystals, principally calcium phosphate. The presence of minerals combined with an appropriate distribution of collagen fibers in the extracellular matrix provides strong mechanical properties in terms of hardness, and compressive, tensile, torsion strength. The calcium diffusion and deposition in bone are driven by endocrine mechanisms, contributing substantially to the ion regulation of plasma levels. Bones can be classified as long bones (e.g. femur, tibia), short (e.g. carpal, tarsal), flat (e.g. cranium, scapula), irregular (e.g. vertebra) and sesamoid bones (e.g. patella), while there are two main types considering the macrostructure, the compact bone and the trabecular (also known as cancellous or spongy) bone with a sponge-like porous structure. The bone structure is generally composed by inorganic substance, hydroxylapatite (65-70%w), water (about 9%w); cell amount represents the 1%w of the total weight, while the remaining 20-25% is made up by the extracellular matrix, which can be divided in collagen (90-96%w), proteoglycans and glycoproteins (4-10%w).

1.11 Bone composition

Collagen type I is predominant in bone. According to the collagen arrangement and size, two types of bone can be considered, primary fibrous bone and secondary lamellar bone. The fibrous or immature bone is formed

INTRODUCTION

by relatively long 5-10 μm collagen fibers, randomly oriented. The fibrous bone is normally found only in the periosteum; even if it is the first deposited tissue both in physiological growth and during healing process, it is then rapidly reabsorbed and replaced by lamellar bone. The lamellar bone is the most common structure, constituting nearly all the collagen content of compact and spongy bone. It is characterized by the ordered arrangement of collagen fibers in layers, called lamellae. In bone, proteoglycans are mainly formed by short glycosaminoglycans, byglican and decorin. The bone glycoproteins include different molecules, which are considered crucial in the regulation of mineralization processes. Among them *osteonectina*, having an high calcium affinity, is responsible for the nucleation of mineral crystals; *alkaline phosphatase* enzyme is capable of hydrolyzing phosphate groups attached to organic substrates and it is involved in the synthesis of bone organic matrix; *fibronectin* molecule drives cell adhesion thanks to the high affinity with collagen; *bone sialo-proteins BSP*, having an high content of sialic acid, may mediate cell adhesion such as the osteopontin BSP-I, BSP-II and the bone acid glycoprotein BAG-75; and finally proteins that contain Gamma-Carboxyglutamic Acid (GLA), (i.e. osteocalcin) playing a important role in the inhibition of mineralization, caused by the strong tendency to bind with phosphate ions. The mineral component is mainly represented by calcium phosphate crystals in apatite structure, in which cells unit are formed by flattened hexagonal prism $\text{Ca}_{10}(\text{PO}_4)_6^{++}$, and hydroxyapatite is obtained combining apatite with $(\text{OH})^-$ ions. During the growth, hydroxyapatite precipitates in amorphous aggregates aligned along

INTRODUCTION

the collagen fibers, and then are replaced by thin needle-like apatite crystals. The bone tissue is relatively cell-free, in which four main types of cells can be found, osteoprogenitor, osteoblasts, osteocyte and osteoclast cells. Osteoprogenitor cells, deriving from periosteum, present an high proliferative ability and secrete growth factors for differentiation. Osteoblasts possess a size of about 20 μm and are responsible for the ECM synthesis and mineralization. Osteoblasts tend to form sheets on the bone surface during tissue formation, initially producing matrix only on preexisting bone surface. After the appropriate bone deposition, cells start to form bone in all directions, causing a progressive separation between cells. Afterward, osteoblasts decrease their metabolism and finally differentiate into osteocytes. Osteocytes are the typical cells of mature bone, responsible for tissue maintenance and remodelling. Instead, osteoclast cells are predisposed to bone reabsorption, and derive from hematopoietic stem cells, unlike all the previous which derive from osteoprogenitor cells. Osteoclasts are 100-200 μm plurinucleate giant cells.

1.12 Bone Structure

Trabecular bone is mainly found on the bone extremities (metaphysis, where bone expands its shape and epiphysis at the end, close to the articular cartilage), while the compact bone principally covers the entire external part and it is concentrated along the shaft zone (diaphysis). Both the bone microstructures can be considered very similar with the only difference in the apparent density. Considering the compact bone, the structural unit

INTRODUCTION

consists of cylindrical formation, also called *Osteons* or *Haversian systems*. A blood vessel can be found in the centre of each osteon, and it is contained in the Haversian canal. Bone structure is arranged in concentric cylindrical lamellae around these canals (osteons). The vessels are connected to each other by Volkmann's canal, which cross the section in transversal and oblique way. Lamellae are formed by collagen fibrils on which hydroxylapatite is deposited ($\text{Ca}_{10}(\text{PO}_4)_6(\text{OH})_2$ half of the volume and two thirds of weight). Osteocytes are contained in cavities (lacunae) along the lamella edges, which are connected by several small canals. Osteon is delimited by the cement line (still concentric related to the Volkmann's canal), that is mainly composed by proteoglycans and represents the area with the highest rupture probability caused by osteon delamination under shear stresses.

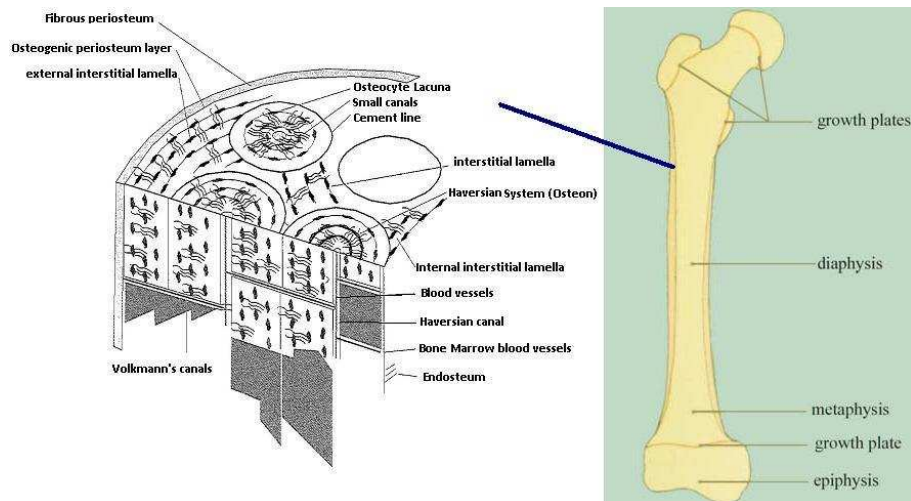


Fig.1.11. Compact bone structure(22).

INTRODUCTION

The gaps between osteons are filled by interstitial lamellae. Figure 1.11 shows the femoral bone structure on different levels. Trabecular bone structure is very similar compare to compact bone, showing concentric lamellae arranged to form a reticular structure oriented along the direction of the greatest stress in which the ratio between mechanical strength and weight is optimized. However, haversian canals are absent and osteoblast layers can be found on the trabecular surface, which make the tissue more suitable for tissue remodelling.

1.13 Structural complexity and mechanical properties

The complex bone substructure is due to several reasons, including:

- modality of bone growth;
- organization of capillary perfusion for cell nutrients;
- structural centrality around the capillary circulation, such as osteons;
- optimum organization of the filling space, considering the total bone weight;
- external stiffening and optimization of bone geometry;
- anisotropy depending on the stress type and amplitude;
- optimization of the mechanical strength.

Bone is characterized by good mechanical and structural properties. The maximum deflection reaches generally low values before fracture, and so tissue can be treated as an anisotropic composite in its linear elastic part.

INTRODUCTION

Compact Bone		Trabecular Bone
<i>Mineral+Collagen</i>	composition	<i>Mineral+Collagen</i>
5-30%	porosity	30-90%
1.8-2.0 g/cm ³	density (ρ)	1.8-2.0 g/cm ³
1.4-2.0 g/cm ³	apparent density (ρ_a)	0.18-1.4 g/cm ³
10-20 GPa	Elastic modulus	$\propto \rho_a^2$
150-200 MPa	Tensile strength (σ_t)	$\propto \rho_a^2$
0.5-30%	Rapture elongation (ϵ_r)	5-10%
Longitudinal σ [MPa]	Tensile	≈ 135
	Compression	≈ 205
Longitudinal ϵ [MPa]	Tensile	≈ 3
	Compression	≈ 1.9
Transversal σ [MPa]	Tensile	≈ 53
	Compression	≈ 130
Transversal ϵ [MPa]	Tensile	≈ 0.7
	Compression	≈ 2.8

Table 1.1. Mechanical properties of cortical and trabecular bone(22).

It is important to underline how bone shows strong viscoelastic behaviours, especially when it is stimulated at different strain rates, changing its stiffness, the maximum deformation and stress before the failure. In table 1.1, the principal mechanical properties are reported. As shown, the compact bone and cancellous bone density is the same, while the apparent density varies due to the porous structure. As a consequence, the mechanical properties are strongly influenced by the ratio of full-empty spaces in the trabecular structure. The complex organization leads to a macroscopic structure with anisotropic properties both in compression and in tension, but also along different stress directions, such as longitudinal and transverse (table 1.1).

1.14 Remodelling

In bone, continuous processes of bone reabsorption and deposition coexist in a dynamic equilibrium, aimed to adapt the bone structure on the different and variables mechanical stresses which normally occur. Currently, it is a general opinion how the evolutionary process has produced an optimal engineering design for all bone types. Considering the bone physiology, several considerations can be formulated on the base of an optimal design, such as *the structural design* in which the material is mainly arranged along the force lines, to ensure a good strength-weight ratio and to distribute homogeneously as well as possible the stress during the maximum load condition (*homogeneous resistance distribution*). These concepts, applied to the geometry of the bone structure, are well known and were firstly formulated by the Wolff's laws in 1982. The first law explains how a bone transformation corresponds to a functional variation, while the second is related to the trabecula directional remodelling as a function of the loading history. Thus, bone remodelling is driven by a dynamic equilibrium between deposition and reabsorption, regulated by mechanotransduction mechanisms in which mechanical signals are converted into biochemical activities by cells. Various models were proposed to explain the mechanisms of cell regulation, in which the most accredited involves the formation of flow, pressure and transport gradients along the canals, causing a cellular response (23-25). In figure 1.12 it is possible to observe the bone remodelling activity depending on the imposed strain, proposed by Frost.

INTRODUCTION

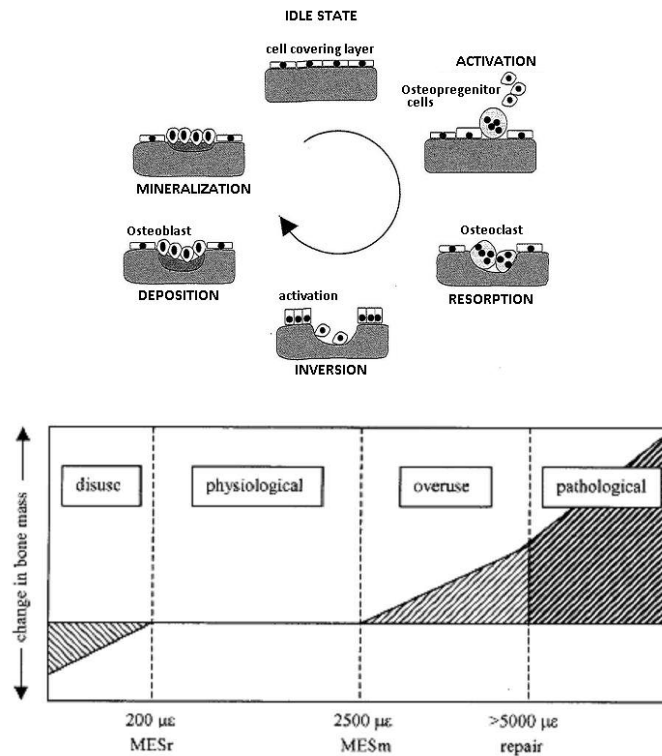


Fig.1.12. Remodelling activities and Frost's theory(26).

1.15. Bone Repair and Regeneration Techniques

In general, bone has a good ability to self-regenerate. However, as any tissue, bone possesses a critical defect size for which spontaneous regeneration cannot be achieved, causing nonunion defect or delayed union defect (regeneration does not occur within a predetermined period, depending on the location). Fractures, which lead to delayed or nonunion defect, are common among the long bone. When the critical size is exceeded, such as 40 mm for tibia, bone transport is needed, for example

INTRODUCTION

using ring fixators, intramedullary nailings, Ilizarov frames or general external fixators. Moreover, in the orthopaedic field, extensive bone reconstruction is needed in case of widespread loss, as resulting by severe congenital malformations, trauma, hypoplasia, ischemic necrosis, primary neoplastic lesions (osteosarcoma, benign bone tumors) or secondary (metastases). Prostheses are also used to provide a replication of the missing bone segment or joint, but poor integration, high probability of infections and rejections can occur, as well as technical problems involving breakage, friction wear and loosening, precluding their general use in orthopaedic field. Currently, bone-grafting plays a predominant role in treatment of delayed or nonunion defects, joint arthrodeses, trauma or tumors; but recently tissue engineering is also considered a very promising technique. A brief description of the common techniques for bone regeneration will be presented.

1.15.1 Bone transfer through fixators(27)

Ring fixators, intramedullary nailings, Ilizarov frames or general external fixator are commonly used to provide bone transfer along the defect, support functions and finally to adjust the bone length and alignment. This procedure is generally preceded by the injury washing through debridement processes, such as lavage or irrigation. Then, bone is internally or externally immobilized with proper fixators. Bone transport presents a high rate 90% of ultimate success. In addition, donor site morbidity generally does not occur, as well as the treated bone can be weightbearing during healing

INTRODUCTION

processes. However, the process rate is relative slow (2 months/cm), leading to complications in prolonged treatment, such as pin site infections, cellulites, contractures and edema.

1.15.2 Distraction osteogenesis(28)

Distraction osteogenesis can be considered a bone transfer technique and it consists in a surgical process used to restore long bone deformities and length. Bone is fractured in two segments (corticotomy), then the relative parts are gradually stretched (distraction rate 1mm/days) during the distraction procedure with an external fixator (Ilizarov external fixator), allowing the stimulation of the biosynthetic activity, new bone formation and the consequent lengthening. If the desired length is achieved, the distraction is followed by a consolidation phase in which the healing process may occur. Distraction osteogenesis can increase both the bone and the surrounding soft tissue length simultaneously. Although this techniques is commonly used to correct long bone deformities caused by congenital diseases and old injuries, distraction is often a long and laborious process and it is reserved only to mentally prepared patients.

1.15.3 Bone-Grafting(28)

The common grafting techniques can be divided in autograft, allograft and vascularized transplants.

Autograft is obviously the most favourable procedure, especially when combining with viable soft-tissue coverage. Autogenous implants, defined

INTRODUCTION

as the “*gold standard*” for regeneration, are commonly considered as a safe solution in terms of compatibility and immune response absence, but also uncomfortable for patient in which a second surgery is needed and an associated morbidity can also occur. The bone trabeculae graft may be reabsorbed either entirely or partially, while new bone formation can be observed. Actually, the regeneration is unpredictable and depends strongly on graft vascularization and nutrient diffusion. Furthermore, the graft availability may limit the application of this technique. In general, cancellous bone grafts are mainly used due to their osteogenic inductive capacity that results higher if compared with compact bone.

When the defect size exceeds the homologous donor possibility, *allografts* may be a good alternative thanks to the existence of bone banks which provide allogeneic bone graft with no size or quantity limitation. Anyway, several studies have demonstrated how allograft transplantation often results in poor and inadequate remodelling, reabsorption, revascularization, and so the implant can be considered as only a mere support. Moreover, it is important to not underestimate the problems concerning the graft rejection and the risk of infections (5-12% of the studied cases). Also in this case cancellous bone is preferred.

The advances in microsurgical techniques have contributed to the application of *vascularized graft*, promoting a continuous circulation and ensuring bone viability. One advantage is given by the possibility of implant bone including muscle and skin. Bone free flaps are generally harvested from both iliac crest, fibula and ribs. During the healing process, tissue

INTRODUCTION

hypertrophy early occurs thus making prolonged immobilization unnecessary. Although vascularized graft leads rapidly to a good healing status, structural support, remodelling and minimal donor site morbidity; this technique requires microsurgical sophisticated procedures (8-12 hours as operation time) including specific infrastructures.

1.15.4 Bone Tissue Engineering(16, 17)

As widely mentioned, a promising alternative to the traditional approaches is constituted by (TE) tissue engineering, which has revealed potential results, causing a significant increase of research works in recent years. Considering tissue engineering for bone regeneration, two alternative are proposed: tissue engineering and *in situ* tissue regeneration. The first involves the seeding and differentiation of autologous osteoprogenitor cells on absorbable and modified three-dimensional scaffolds. Once implanted, the engineered constructs should be gradually reabsorbed and replaced by viable tissue thanks to the vascular and nervous system supports. The clinical applications already in use include cartilage, skin and vascular system. In the second approach, scaffolds are associated to materials in powder form, solution or doped microparticles able to promote a local regeneration. Signalling molecules or growth factors which trigger cell proliferation, such as bone morphogenetic proteins (BMPs), can be chemically conjugated to the scaffold material and released in a controlled rate, by diffusion or material fragmentation. These bioactive materials are

INTRODUCTION

able to induce a local cell response, stimulating the tissue regeneration *in situ*.

From a clinical point of view, bone and cartilage tissue engineering may offer large options and possibilities to improve the current integration, as well as to avoid problems concerning patient rejection, presence of donors and finally the functionality of the substitute, in terms of biomechanical properties(17).

2. TISSUE ENGINEERING

The definition of tissue engineering was coined by the National Science Foundation at Lake Tahoe conference in 1988 when it was stated that "Tissue engineering involves the application of the principles and methods of engineering and life sciences in order to understand the fundamental relationships between the structure and functions in mammalian tissues (both normal and pathological) and to develop biological substitutes to restore, maintain and improve tissue functions". The philosophy of this interdisciplinary field is related on the ability to lead the repair and regeneration of damaged tissues allowing cell growth and thus restoring the original tissue.

Therefore, the main long-term goals of tissue engineering are tissue and organ replacement using cell therapies, in which cell biology, biomaterials science, and surgery are combined. This new discipline uses cells for the production of engineered materials, in which it is crucial to mimic physiological conditions, to guide cell adhesion, proliferation, differentiation as well as synthesis of new extracellular matrix. The trend of recent years was mainly focused on cell culture using supports, also called scaffolds(*16, 18, 29*). In this way, optimal conditions for cell proliferation and matrix synthesis can be created. Scaffolds promote the three-

dimensional organization of cells until tissue synthesis. The paradigm upon tissue engineering fundamentals is the mutual relationship between cells, scaffolds and cellular signals. Cells are the simplest building block units of living organisms and all their characteristic properties can be expressed, such as reproduction, growth, death, assimilation, respiration, motion, ability to synthesize and respond to stimuli. In fact, cells are able to adapt the shape as a function of their activities or as a result of external stimuli. Cells are surrounded by extracellular matrix ECM with different compositions depending on the specific tissue. ECM production can be understood as balance between the anabolic (biosynthesis) and catabolic (lysis of molecules) processes. This equilibrium inevitably changes by introducing foreign materials. One of tissue engineering aims is to successfully replace a tissue, without breaking down this balance. Therefore, the implanted material must reproduce as well as possible the pathway signals, in order to permit the main cellular functions, allowing a correct cell behaviour. The most important cellular functions can be summarized as differentiation, adhesion, migration, proliferation and finally extracellular matrix ECM production. These functions are induced by the presence of specific proteins which govern cell expressions. In cellular differentiation process, a progenitor cell becomes a more specialized cell type through the activation of a particular genome fraction which determines its diversity. This depends on the presence and the interaction between cell receptors and specific molecules on the culture material which act as gene activators. Thus, the process can be strongly influenced by

environmental factors, by the cell-cell and cell-ECM interactions and migration and adhesion play a key role particularly. In the adhesion process, cell attachment provides signals for spreading, migration, survival, and proliferation. As mentioned, cell surface receptors recognize reversibly and specifically ECM components. Therefore adhesion results a fundamental mechanism to induce cellular functions. Migration must also be considered as a mechanism by which cell motions involve the presence of specific signals or pathways on the extracellular matrix. In this way, the important role played by proteins and molecules becomes clear. Another very important process is the proliferation, essential to guarantee life and tissue growth. This process is faster and increase in efficiency when cells are less differentiated. For example, the contact inhibition is an intrinsic property of cells to stop reproducing and in general all the available space is theoretically employed but not exceeded. Finally, the extracellular matrix biosynthesis is crucial to create a biological substitute or to maintain the natural tissue, as a result of the described cellular functions. Many of the mentioned processes are either inhibited or supported by chemical and physical factors, such as the presence of certain molecules (growth factors, adhesion proteins), pH, CO₂, temperature, oxygen, nutrients, metabolite transport and the appropriate medium transfer. All these factors must be considered during a cell culture in order to reproduce the main physiological conditions. Figure 2.1 shows the cell culture progress on a scaffold in term of cellular functions. In fact, cell culture occurs during several stages. In the early hours, the first phase consists in cell adhesion and cell migration as

STATE of ART: tissue engineering

well as the production of the first cellular signals. The second phase includes cell differentiation, proliferation and eventually cell apoptosis (death), which takes place in days or weeks. In the third and final phase, taking months or years depending on the material size, matrix remodelling occurs. Thus, during tissue growth and integration between native and developed tissue, scaffold must provide a mechanical support, encouraging cellular functions. At the same time, scaffold material should also be reabsorbed with a kinetics that is comparable to matrix production.

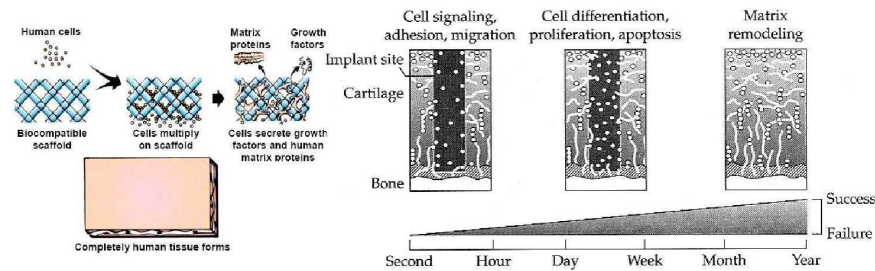


Fig.2.1. Cell culture scheme(193).

The development of 3D scaffolds, support structures or matrices that induce cells to form functional tissues, is one of the main objects of tissue engineering. Tissue engineering scaffolds or matrices are an important component for tissue development and their characteristics are fundamental in forming tissues with a proper cell morphology, orientation, arrangement of intercellular material, and relationship between different cell types. In particular by using scaffolds, transplanted cells can be delivered to a specific place in a tissue driving the growth of cells inside a desired

anatomic site. Therefore scaffolds represent the space available for the tissue to develop and a physical support for cells growth. It is possible to find a lot of commercial scaffolds for tissue engineering, such as cartilage or skin (*Apligraf* is the best known).

Tissue regeneration can be either conducted entirely *in vivo* or assisted by *in vitro* phase. Considering the latter situation, a bioreactor can be defined as any apparatus that attempts to mimic physiological conditions in order to maintain and encourage tissue regeneration in 3D scaffolds and in dynamic conditions. Cell cultures in bioreactors can be considered an intermediate step between the conventional *in vitro* static approach and *in vivo* studies. The aim is thus promoting the formation of cartilage or bone tissue by simulating physiological conditions via the application of specific mechanical and biochemical stimuli(2, 30). Several studies have reported promising results when *in vitro* dynamic conditions were applied before implantation, describing the effect of many variable and how those can influence cell metabolisms(31-33). In several cases, bioreactors can be considered useful tools not only for tissue regeneration, but also to investigate the pathway signals between cells and matrix during biochemical and physical stimulation.

Playing on the system design, functional improvements can be provided through the use of bioreactors in order to engineer cell cultures, making the processes scalable, reproducible and adding substantial advantages to the traditional cultures, such as reducing contamination risk (generally only closed system are proposed), automating a continuous exchange of

nutrients, measuring and controlling cell culture variables (T, pH,% Rh, pCO₂, pO₂,...) and, considering bone and cartilage, also applying specific mechanical stimuli(34-38). To increase the cellular response in these tissues, several mechanical stresses were applied with the intent to mimic physiological conditions: shears induced by fluid (medium)(39-41), tension (unidirectional or biaxial stretching)(42), sometimes shears(43) induced by torsion(44), direct compression(45, 46) and finally the application of hydrostatic pressure(41, 47, 48). Applying appropriate biochemical and mechanical stimuli through a bioreactor, cell culture can be conducted closer to *in vivo* conditions. Many studies have widely emphasized how osteoblasts and chondrocytes respond in different ways(33, 49) depending on the dynamic cell culture conditions, in particular frequency, amplitude and loading time show a strong influence in the culture. Considering cartilage, several mechanical stimuli have been studied and precisely promising results were found using perfusion, intermittent hydrostatic compression and cyclical direct compression. Generally, the increase in chondrogenesis and extracellular matrix synthesis were justified by assuming the parallelism between these types of stimulations and the physiological conditions. In perfusion, chondrocytes were subjected to shear stresses similar to the stresses produced by the natural synovial fluid during normal operation(40). Instead, in direct compression, a triaxial stress state was generated due to the complex scaffold structure and, in particular, compression, tensile, but also shear stresses, which naturally occur in the cartilage extracellular matrix(50-53). Finally, the effect of hydrostatic

pressure was explained considering the external physiological loads, from 0.5-2 MPa up to 10 MPa(54, 55). All three given explanations are consistent, but the assumptions were taken from three different levels, respectively microscopic (cells), macroscopic (matrix structure), and finally on a large scale (human body). Similar stimulations were studied in bone tissue engineering, with the addition of stretching in one or two directions. Again, the conclusions regarding the obtained benefits were focused principally on the parallelism between physiological and applied stresses(39, 49, 56-58). Recent studies have also shown how low pressure, between 10 and 40 kPa, plays an important role in bone regeneration. In fact, the intraosseous pressure calculated for an adult body is about 30 kPa. Subsequently, this pressure results to be the same stress state at which osteoblasts are normally exposed(42, 59).

Now, it is necessary to underline the important role of dynamics for the regeneration process. It was largely proved how a static regime causes a decrease in chondro- and osteogenesis(51, 55), while prolonged stimulations may not result in synthesis increasing when compared with short stimuli. In fact, mechanical stimuli were especially important in cell activation, but long application can lead to cell damage and apoptosis. For this reason, a rest period was often introduced within the same stimulation, and a loading time usually no exceeds one hour(60-64). Finally, the mass transfer plays an important role, not only as a mechanical stimulus but as contribution of new nutrients and waste removal. In fact, spinner flask was the first bioreactor designed for dynamic culture, in which the medium was simply stirred by

promoting the fluid transport. These early studies have demonstrated both the importance of nutrients and waste exchange but the disadvantage caused by a turbulent flow within the culture, in terms of cell damage and apoptosis(65-68).

2.1 Scaffold

An ideal scaffold should be non-toxic, biocompatible, non-immunogenic, porous, easily reproducible and also it must have the mechanical properties as close as possible to the native tissue(69-76). In fact, the proposed scaffold must present an high interconnected porosity and good permeability to allow diffusion of nutrients, waste removal and cellular mobility. In addition, pore size must be included between 50 μm and 500 μm to facilitate cell migration. During the process of matrix remodelling, the scaffold must be designed with a desired degradation and bioreabsorption rate in order to obtain the correct tissue substitution. In skeletal tissues, such as cartilage and bone, scaffold mechanical properties also play a crucial role, providing the adequate strength and stiffness to maintain the assigned space after implant. A list of the main scaffold properties is following reported:

- *Porosity and Morphology*: high and three-dimensional characterized by the presence of an interconnected pore network to allow cell growth, diffusion of nutrients and waste removal(70, 71, 73, 76-78). The pore size must be comparable to the dimension of the seeded cell. For example, osteoblasts size is about 20 microns, thus pore size should be between 100 μm and 500 μm (16, 17, 72). The morphology of the scaffold should be

designed to guide the formation of new tissue in term of size, shape and vascularization.

- *Biocompatibility*: can be defined as the ability of a material to perform with an appropriate host response in a specific application. The definition does not give an absolute concept, but depends on the application. Therefore, the material can be designed and its compatibility can be evaluated(72, 79, 80). For example, a stable implant should not be hydrolysable or a contact lens must prevent cell adhesion as opposed to a scaffold for bone and cartilage tissue engineering. In general, host cells must tolerate the presence of the material without generating immune response. The scaffold must avoid cell damage and apoptosis, enhancing the proper cellular functions.

- *Biodegradability*, for tissue engineered construct, must be controlled in order to ensure the correct degradation rate, showing a kinetics comparable to tissue regeneration(81-86).

- *Bioabsorbability*, for tissue engineered constructs, to allow cell growth *in vitro* and/or *in vivo*, avoiding immune response caused by monomer dissolution.

- *Surface*: chemically appropriate in order to communicate in a proper way with the host cells and to regulate cell expression. Considering cartilage and bone scaffolds, surface must be suitable for initial adhesion, migration and proliferation. If stem cells are seeded, scaffolds must promote differentiation, while in the case of specialized cells, the material must

prevent de-differentiation in other cell types. Finally, the surface must accommodate the ECM synthesis.

- *Mechanical properties* should be similar to the native tissue ones, to guarantee an appropriate response of the material when implanted *in vivo* or mechanically stimulated *in vitro*(87-89). Considering cartilage and bone application, scaffold must show mechanical stability to sustain wound contraction and later forces in the initial part, while maintaining the required three dimensional structure during the degradation.
- *Reproducibility*, focusing on a widespread clinical use and process engineering, both material and its structure must be reproducible, scalable and cost effective by a controlled method, avoiding scaffold mutations or contaminations which may cause culture failure.
- *Sterilization* should be easy, essential to prevent contamination, cellular apoptosis and tissue death. The sterilization process must not modify material structure, e.g. gamma rays significantly reduce the molecular weight of PDLA (racemic blend of Polylactic Acid)

It is important to emphasize how an ideal scaffold does not exist, but a proper scaffold for a certain application can be designed with specific and desired material properties.

Several materials were experimentally studied for scaffold applications in tissue engineering, and they can be grouped into four main categories: synthetic organic materials (i.e. biocompatible polymers), inorganic synthetic materials (i.e. Hydroxylapatite, chalk, Calcium Phosphate, Glass-

ceramic), natural organic materials (i.e. Collagen, fibrin gel, Hyaluronic Acid) and finally inorganic materials natural derived (i.e. Coralline Hydroxylapatite, Calcium Carbonate). For bone and cartilage tissue engineering, the most commonly used materials are natural and synthetic polymers, due to their degradation properties; while in some bone applications, ceramic materials are also used, especially combined with polymers as composites, due to their mechanical properties.

These considerations are focused principally on synthetic and natural polymers for tissue engineering. Synthetic polymers normally used are biodegradable under the aggressive action of the physiological fluids. The material can be decomposed and bio-absorbed through several mechanisms, such as oxidation and hydrolysis. In general, a synthetic material presents reproducibility, stable properties, good workability and high versatility; it can be easily designed and processed if compared with a natural polymer. Otherwise, it is necessary to carefully evaluate the possible toxicity of the released monomers. Polylactic Acid (PLA), the racemic blend of the Polylactic Acid, named Poly-D,L-lactic Acid (PDLLA)(81, 90-95), Poly(ϵ -caprolactone) PCL(83, 96, 97), Polyglycolic Acid (PGA)(98, 99) and their copolymers (i.e. PLGA poly(lactic-co-glycolic acid)(93, 100-102) or PCLLA Poly(ϵ -caprolactone-co-lactide)), but also biodegradable Polyurethanes (PU), Polydioxanone (PDS), Poly(ortho Ester) and Poly(anhydrides) are the most commonly studied and used polymers in tissue engineering field.

Naturally-derived polymers are obtained by extraction from living organisms. In general, a good interaction cell-material can be achieved, increasing cell adhesion and proliferation. In fact, natural polymers are intrinsically able to communicate with cells, offering good biocompatibility, non-toxicity, low chronic inflammatory response and an ideal environment for cell growth. These kind of materials are generally expensive, less processable and less stable in terms of mechanical properties. Collagen, Chitosan, Hyaluronic Acid(103-106), Glycosaminoglycan (GAG)(77, 107), Silk Fibroin(61, 108-111), Starch(112-115), Agarose(116-118) and finally Alginate(119-122) are natural polymers often used in tissue engineering. Thanks to their chemical composition, the organic naturally-derived polymers possess the ability to induce stimuli on the seeded cells during adhesion. However, the main problem is to understand which are the induced stimuli. In fact, cell response may not be what expected or desired.

2.2 Polymer scaffold process techniques(123)

Porous polymeric matrices used in tissue engineering can be produced through several scaffold fabrication techniques, which must provide the correct design for cell support, adhesion, migration, proliferation, differentiation and subsequently ECM biosynthesis. The design of the scaffold, in fact, can significantly alter different cell functions and the geometry can define the adhesion sites for cells. The architecture can influence the cells degree of spreading and the cytoskeleton orientation. It is widely demonstrated that cellular activities depending on scaffold shape and

cells anchorage also control cells gene expression. The desired characteristics, such as porosity, permeability and mechanical properties can be achieved providing a structure mimicking the ECM architecture as much as possible. The commonly used techniques can be divided in two main categories; in the first case, scaffolds are generated with a random structure and unpredictable pore sizes. Generally, the obtained constructs lack in reproducibility, mechanical strength and structural stability. Precisely, Solvent Casting / Particulate Leaching, Freeze-Drying, Phase Inversion, Fiber Bonding, Electrospinning, melt based technologies, have been employed to produce non-ordered scaffolds. Considering also the second category, in recent years, considerable attention has been paid to fabrication methods for producing porous scaffolds with a certain, predetermined design, complex shapes and defined architecture, such as Stereolithography, Selective Laser Sintering, 3D Printing, Shape Deposition Manufacturing, Robotic Microassembly, Fused Deposition Modelling. These techniques are normally based on the use of a computer-assisted device and the material is often deposited layer by layer. High resolution can be achieved depending on the apparatus precision. Following, it is reported a brief explicative list of the mentioned fabrication techniques:

Random structure

- *Solvent casting / Particulate Leaching*; polymer solution is casted on a support until the solvent evaporates. Good film quality, controlled thickness, uniformity and good distribution can be achieved working on process parameters, such as solution viscosity, chemistry of the solvent,

casting substrate but also on process conditions (i.e. temperature, Relative Humidity, pressure). Obviously, the solvent must be volatile. Solvent casting is often combined with particulate leaching to obtain 3D porous scaffolds. Sodium Chloride, Ammonium Bicarbonate and Glucose are generally used as porogen agents with different crystal sizes.

- *Freeze-Drying(124)*; solution sublimation can induce pore formation, under proper pressure and temperature conditions. Adjusting polymer concentration, viscosity, quenching temperature and cooling rate, the desired structure can be obtained in terms of mechanical properties, presence of gradient and structural alignment, pore size and distribution.
- *Phase Inversion(125-127)*; under specific conditions, such as solution viscosity, polymer density, interfacial energy and mechanical stirring, a liquid-liquid dispersion can be inverted by diffusive processes, interchanging mutually the dispersed and continuous phase. After casting, a single phase can be separated using a nonsolvent. In tissue engineering, supercritical carbon dioxide is often used as nonsolvent due to its non-toxic properties.
- *Electrospinning(107, 128-131)*; submicrometric fibers can be produced applying very high voltage on a polymer solution or melt, free to deposit from a needle to a grounded target. The main parameters, which govern this process, can be summarized as solution properties, electric field strength, distance between target and needle, temperature and humidity. In tissue engineering, several applications have been investigated, changing

fiber orientation, morphology, thickness, mesh spacing, but also combining different solutions or melts.

Ordered structure(132, 133)

- *Stereolithography* is based on the use of photopolymerizable liquid polymer. Using a specific light source (generally UV) and proper masks, the scaffold can be fabricated in sheet, layer by layer. The main problem consists of a limited availability of useful and biocompatible photopolymers.
- *Selective Laser Sintering*; sintering of a polymeric powder by local fusion can be achieved using a CO₂ laser beam. Also in this case, scaffolds are built up layer by layer.
- *3D Printing(113, 134, 135)*; scaffolds are produced by stacking different layers in which a binder solution is injected on a polymeric powder, through an inkjet print head. Only the wet powder can adhere and solidify, while the dry powder is removed. This technique is suitable only for simple geometries.
- *Shape Deposition Manufacturing*; a numerical controlled machine is used to cut the scaffold, starting from a clinical image. Cells, specific proteins and molecules can be inoculated during the process.
- *Robotic Microassembly*; a specific precision robotic system is used to connect pre-assembled block units, obtained via lithography.
- *Fused Deposition Modeling(136)*; the most common microfabrication systems are based on the use of a microextruder, which

deposits successive layers of a polymer solution or a melt on a support substrate that a computer-controlled mechanism moves in the x-y-z directions. Scaffolds geometry and properties depend on the dimension of the extrusion die, viscosity of the polymer melt or solution, pressure applied to the extruder, and speed at which the base support moves in each direction.

2.3 Bioreactors, from static 2D to dynamic 3D culture(38)

Tissue engineering takes advantage of life science to produce biological substitutes in which the obtained cellular constructs will be used to repair or regenerate damaged tissues. Therefore, the final product after cell culture must exhibit the proper geometrical dimensions, structure and chemistry as close as possible to the original tissue. For this reason 3D scaffolds from biodegradable and bioabsorbable materials, synthetic or natural, with specific chemistry and interaction properties are widely used in tissue engineering. To achieve tissue remodelling, the desired cell culture differs tangibly from the traditional static 2D culture. In fact, traditional cell cultures are usually carried out on multi-well polystyrene plate, containing a specific treated surface to promote cell adhesion. Cells are seeded with medium and then plates are placed in an humidified incubator where the environmental conditions of 37°C and 5% CO₂ are maintained. The temperature is obviously physiological, while the CO₂ level is needed to stabilize pH in the culture. Culture medium is a buffer solution activated by the presence of carbon dioxide. Generally, a 5% concentration corresponds

to 7.2 pH, depending on the medium type. The waste removal and nutrient transport are performed manually, changing the medium about every two days (or on the base of cell metabolism and activity). Therefore, the *in vivo* conditions are reproduced as close as possible in a static way, considering also all the relative limitations. As previously mentioned, a bioreactor can be defined as any apparatus that attempts to mimic physiological conditions in order to maintain and encourage tissue regeneration, simulating the living organism. In this way, a bioreactor is a suitable device, where cells are cultured in dynamic and reproducible conditions. In fact, tissue culture is a non-steady state process, in which all parameters must be measured and controlled. Precisely, temperature, medium pH, gas exchange, O₂ level, CO₂ level, humidity, nutrient transport, waste removal and finally mechanical-biochemical stimuli are always regulated. Temperature must be constant around 37°C, pH value should remain between 7.2 and 7.4 acting on CO₂ level, humidity should be enough (generally closed to condensation) to avoid medium evaporation, while dissolved O₂ level and nutrient concentrations must be sufficient to guarantee cell functions.

The fundamental part of a bioreactor is the culture chamber, a sterile environment where the cellular constructs are housed. The seeded scaffold can be confined, that means laterally constrained, or unconfined, in which the lateral side is free to move. Growing medium with the necessary nutrients can flow inside the chamber thanks to a predisposed system. The culture medium can diffuse inside the substrate with a proper flow regime, allowing nutrients transport and waste removal. The culture chamber must

also present some general characteristics: each component must be sterilized and manufactured from non toxic materials and should be easy to assemble, still allowing parameter measurements along the medium flow line. It is difficult to carry out a continuous on-line measure, especially considering biochemical signals. So, a bioreactor may be designed taking into account the possibility to introduce custom on-line sensors or, alternatively, an apparatus for sample fast removing for a final external analysis.

A bioreactor is thus developed to cultivate cells under proper dynamic conditions, close to the physiological *in vivo* environment, applying biochemical and mechanical stimuli to improve the tissue-engineered constructs properties. In fact, mechanical stresses can produce changes in cell shape and behaviour, inducing a wide biochemical response which includes the secretion of bioactive molecules such as growth factors, vasodilators, ECM proteins, adhesion proteins and others. In the same way, the local inoculation of biochemical signals on the cell culture can lead to cell gene activation. Consider these factors may be crucial to obtain an engineered construct with adequate properties. Therefore, it is essential to evaluate the normal living tissue conditions to develop a suitable device for driving cell functions and biosynthesis. In fact an ideal bioreactor design, which covers different tissue engineering applications, does not exist, but can be tailored for a specific individual aim.

Finally, the system should also provide high versatility and flexibility, ensuring all the mentioned characteristics. In fact, it is a good practice design to develop an open system allowing the addition of a custom

measurement apparatus, modifications or implementations of new features and the possibility to carry out a scaffold seeding dynamically in the culture chamber increasing the seeding efficiency and cell distribution. Moreover, bioreactors can be used to mechanically characterize the obtained constructs during and after cell culture, providing a wide range of possible tests: DMA to calculate the storage modulus and loss factor, quasi-static ramp to measure the elastic modulus and relaxation-creep test in order to achieve the viscoelastic properties of the material.

2.4 Bioreactor stimuli

Bioreactors are systems capable of applying specific stimuli on cell culture to promote the formation and deposition of extracellular matrix. Currently, the obtained constructs by tissue engineering exhibit low matrix content and low properties compared with the native cartilage and bone. To establish a relationships between culture condition and the resulted composition is crucial to improve the final implant tissue(30).

In vivo, cartilage and bone are subjected to several stresses and through the bioreactor these specific stimuli, both mechanicals and biochemicals, can be applied *in vitro* promoting the chondrocytes or osteoblasts synthesis and matrix deposition. Different variables can be chosen to carry out a cell culture, such as cell type (mesenchymal stem cells, primary cell, immortalized or tumoral cells), seeding concentration and method, medium composition, scaffold type and others. Once the culture protocol is decided, the stimulation can be achieved to optimize the cellular construct and to

create an environment as close as possible to the physiological one. In dynamic cell cultures for cartilage and bone tissue engineering, it is found useful to modulate growth factor concentrations, low/high oxygen partial pressure, mechanical stresses, such as compression, tensile and shear load, as well as pressures and shears induced by fluid.

2.4.1 Low/High oxygen partial pressure(137)

Under normal physiological conditions, articular cartilage exhibits a very low oxygen concentration (hypoxia), thus chondrocytes mainly possess an anaerobic metabolism. In fact, the dissolved oxygen level can reach values below 1%. Some studies have shown an increase in proteoglycan aggregation and cellular synthesis of *in vitro* chondrocyte culture when carried out at low oxygen partial pressures, about 3%(138). Depending on the oxygen level in the tissue, cells can activate aerobic processes, such as respiration, or anaerobic processes, i.e. fermentation, in which a drastic pH drop can be recorded. In general, a combination of both aerobic and anaerobic activities is presented in cartilage. At low O₂ level, cells change their metabolism to produce a series of glycolysis reactions and to satisfy energy needs, reducing pH. In this way, the culture environment may be significantly altered. The dynamic change in oxygen level is an important mechanism for gene expression and signal activation(139).

The biochemical changes, associated to oxygen, are still unclear and the obtained results on the chondrocyte synthesis are often contradictory. However, several studies have demonstrated how the imposition of a low-

oxygen cell culture environment causes an increase in glucose consumption and lactate synthesis, instead of pyruvate production occurring in aerobic conditions. The variation of dissolved oxygen also influences transcription factors such as the HIF-1 α (hypoxia inducible factor)(*140*). HIF-1 α is a biochemical signal linked to the gene expression in anaerobic conditions, which governs the amount of gene transcribed. Among these genes EPO (erythropoietin), endothelial growth factors, glucose transporters and glycolytic enzymes are included. In the absence of HIF-1 α , chondrocytes are unable to maintain sufficiently high levels of ATP, highlighting its key role. HIF-1 α may affect the ECM biosynthesis by chondrocytes, adjusting the synthesis of collagen type II, which decreases under anaerobic conditions. So, the oxygen partial pressure and the relative HIF-1 α expression play a key role in the chondrocyte metabolism and cartilage tissue engineering. However, the required oxygen amount during a cell culture is an open controversial debate, due to the obtained contradictory results(*141-143*).

2.4.2 Mechanical stresses and shear stress induced by fluid(*137*)

Chondrocytes demonstrate a strong sensitivity to a wide range of mechanical loading. This responsiveness have been observed both *in vivo* and *in vitro* studies. Mechanical loads may alter the cellular metabolism, due to stresses, such as compression, stretching, pressure, shear and shear induced by fluid, which are naturally involved in the ECM regulation of articular cartilage, but also *in vitro* engineered constructs.

The principal mechanical stimuli applied in cartilage and bone tissues engineering are direct compression, unidirectional or biaxial stretching, direct shear, direct shear induced by torsion, cyclical or intermittent hydrostatic pressure and finally shear induced by fluid. All the studied stimuli have shown promising results in terms of matrix deposition. Nevertheless, experimental tests were carried out for different purposes and using different characterization techniques, providing an environment as close as possible to the physiological one(38). Some studies have compared static and dynamic mechanical loads, showing how dynamic stimuli generically increase the amount of synthesized ECM(53, 144). Thus, both chondrocytes and osteoblasts seem to prefer a dynamic culture. Frequency, amplitude and loading time may strongly influence cellular metabolism when cells are dynamically cultured.

It is necessary to emphasize how the functionality of an obtained construct for cartilage or bone tissue regeneration is highly dependent on its mechanical properties. For example, in a perfusion bioreactor, the culture medium flow can perfuse inside the scaffold, and a shear state induced by medium can be achieved. The balance between the ECM synthesis and cell damage caused by the flow during the dynamic regime can be regulated and biosynthesis can be induced adjusting the cell culture parameters. For example, cell culture medium flow rate, indicating the shear stresses acting on the construct, should not be exceeded. The liquid flow also plays an important role on the alignment assumed by collagen type II fibers and proteoglycans, although the mechanism is not yet clearly explained. The

kinetic of the reactions is influenced by the shear stresses imposed on the construct. The mentioned effect is usually associated with the presence of calcium-based signalling molecules which can modify cell proliferation and biosynthesis.(137) Therefore, in cartilage tissue engineering, it is possible to optimize the final product properties, defining a flow regime along the radial and axial scaffold directions. In conclusion, these studies have demonstrated how the applied stresses should increase significantly the construct properties, compared with a non-controlled state, such as a turbulent flow(66, 68, 145, 146). In this way, a controlled loading regime can enhance the ECM deposition, improving the culture reproducibility.

2.4.3 Growth factors(137)

The main growth factors used in tissue engineering for cartilage regeneration are the TGF- β (transforming growth factors), insulin I (IGF) and bone morphogenetic proteins (BMPs), supplied in a cell culture to improve the main cellular functions. Indeed, *in vitro* experiments have shown how TGF- β can increase proteoglycans synthesis, also inducing phenotypic dedifferentiation when chondrocytes of articular cartilage osteoarthritis were cultured. Using a concentration of 30 ng/mL an increase in collagen content is obtained, maintaining a high fraction of type II collagen(147). IGF was also combined with cyclic mechanical strain, increasing the ECM synthesis. The BMP factors (2.12 or 13) are employed in a ranging concentrations up to 100 ng/mL, to enhance matrix deposition and collagen content in the engineered construct. Studies have also

demonstrated(148) how the combination of IGF and TGF- β can also increase GAG and collagen contents, if compared with a traditional cell culture. These growth factors, when combined with cyclic loading regimes, can be a powerful tool for the regulation of the main synthesis mechanisms in cartilage tissue.

The aim of bioreactors is providing these described stimuli, to rapidly increase cartilage synthesis for implanting, but at the same time improving the properties of the construct. One of the main tissue engineering objectives is to combine these stimuli with an appropriate choice of cells, a good seeding concentration and a proper scaffold, in terms of material, shape, morphology and structure in order to optimize the future construct, which will subsequently be implanted.

2.5 Bioreactors used in tissue engineering

Several types of bioreactors are commercially available for different purposes, such as tissue engineering, chemical industry, pharmaceuticals, food industry, agriculture and waste processing. For cartilage and bone tissue engineering, there are several suitable bioreactor configurations, depending on the application, the type of stimulation and the established flow profile. Following, a bioreactor list is reported in which the common bone and cartilage bioreactors are described.

Spinner Flask(137)

Spinner flasks are common bioreactors in which a turbulent flow is imposed in order to increase nutrient, waste removal and oxygen diffusion. Spinner flask was the first bioreactor designed for dynamic *in vitro* culture for bone and articular cartilage tissue engineering; combining a simple geometry with a high cell growth efficiency. The seeded scaffolds are typically immersed in the medium and suspended using needles. The culture medium is constantly stirred to ensure the correct diffusion. In fact, cell cultures are carried out in glass containers with a relatively high volume of medium, which is maintained in a constant motion by a magnetic motor. A frequent medium replacement is needed due to the accumulation of cellular metabolites during cell culture.

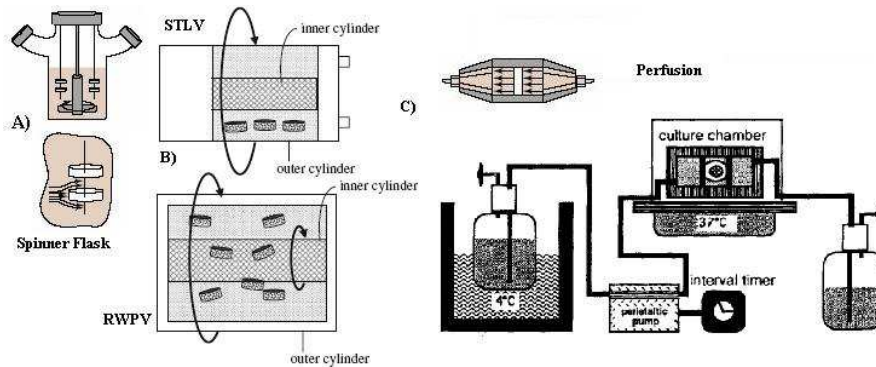


Fig 2.2. Bioreactor layout: (A) Spinner flask, (B) STLV and RWPV, (C) Perfusion(2, 36, 149).

The continuously medium change can be considered one of the main limitation of this technique. In addition, to ensure a constant oxygen and

carbon dioxide supply respectively for cell metabolism and pH stabilization, the chamber is open or not sealed. Gas permeation may be guaranteed by introducing 0.22 μm -filter to avoid bacterial contamination. However, the system must be placed in a sterile humidified incubator at 37 °C and CO₂-controlled(66, 68, 145, 146).

The main defect of spinner flask bioreactor still remains the non-homogeneous flow, which it is difficult to define, analyze and model. Moreover, mass transfer is often inadequate and can cause cell damage and apoptosis. The cartilage construct formed in spinner flask is generally characterized by a more dense area in the outer part, and shows an increase of dissolved GAG in the medium, probably due to the turbulent flow and the associated shear stresses. Thus, compared to other bioreactors, the GAG level in the scaffolds appears to be lower. The results obtained with spinner flask have led to the new system development in order to eliminate non-homogeneous, turbulent and not-controlled flows in the cell culture.(137) In the figure 2.2(a), it is possible to observe a spinner flask bioreactor.

Rotating Wall Vessel(137)

RVW (Rotating Wall Vessel) is a rotating bioreactor. RWV is composed by a cylindrical chamber with an empty space for medium filling and where the scaffold is cultured. The chamber bottom is fixed by two plates to a rotative motor, and the scaffold is subjected to a continuous rotative motion, which generates a microgravitational-like environment. Gas exchange is guaranteed by the presence of a silicone membrane or a bacterial filter.

These systems generally contain an high quantity of medium (about 100-110 mL) and up to 12 constructs can be cultured. The RWV was firstly introduced by NASA and it is currently on commerce. There are several variations of this system, including STLV (slow turning lateral vessel), HARV (high aspect ratio vessel) and RWPV. Through these special configurations, it is possible to modify the nutrient gradient inside the chamber, changing the flow state from a non-homogeneous to a constant profile. Figure 2.2(b) shows the STLV and RWPV layouts(36).

Rotating Wall Perfusion Vessel Bioreactors (RWPV)

The rotating bioreactors, which induce perfusion on scaffold, were widely used in cartilage tissue engineering. Cultures in RWPV were carried out up to seven months experiments in order to evaluate the biological properties of the obtained construct. In principle, RWPV bioreactors were designed to ensure an adequate environment for mammalian cells, which are sensitive to shear. Mammalian cell-based tissues are successfully cultured using RWPV both on Earth and in the absence of gravity. In fact, studies carried out in the Space(150) have tested several bioreactors (rotating and spinner flask) and have generally reported an increase in the engineered construct homogeneity, due to the different gravitational state. Only the scaffolds cultured in RWPV on Earth have shown an homogeneous structure comparable to the previous case. The results are justified by assuming how a microgravity-like environment can be simulated. Therefore, in RWPV,

construct uniformity, GAG and collagen contents in the matrix are relatively high compared to a spinner flask culture(150, 151).

The bioreactor developed at NASA's Johnson Space Center is composed by a cylindrical medium container (110 mL as maximum volume) with the space for 12 scaffolds. The cylinder can rotate on its horizontal axis. The scaffold may be radially suspended, floating on the cell medium thanks to the balance between two opposite forces: gravity and the shear flow generated by centrifugal force. Adjusting this synchronism, the bioreactor is able to cancel the directional effect of gravity, placing the construct in permanent free fall. The outcome of the applied forces results to be unpredictable and random fluctuations can be achieved on the scaffold, in terms of velocity, pressure, shear and shear induced by flow, enhancing the final homogeneity. Long-term studies on cartilage tissue engineering, about seven months, have demonstrated how scaffold mechanical properties are comparable with articular cartilage. However, *in vivo* studies, firstly conducted *in vitro*, have revealed an incomplete integration between the native and the engineered tissue after implant(144).

Tissue integration is still a problem, only partially solved, for many applications of articular cartilage regeneration. Another problem of RWPV concerns the relatively long times needed to obtain a construct with sufficient biological and mechanical properties.

Perfusion Bioreactor(137)

The perfusion culture is a system developed to allow nutrients transport and waste removal directly through the scaffold bulk, surpassing the limited kinetics of the simple diffusion. In the perfusion bioreactor, a permeable scaffold can be fixed and housed on a impermeable chamber. In this way, the culture medium flow is constrained to pass along the scaffold sections. The most common configuration of a direct and constant steady-state flow, in which secondary flows and stagnation points are eliminated. It is also possible to perform a culture with multiple scaffolds, placed in series, using the same medium flow. The perfusion state influences chondrocyte metabolism during *in vitro* growth, such as cell activation, gene expression and biosynthesis, but, also in this case, the mechanism is not yet well-known. In fact, perfusion increases cell proliferation and the matrix synthesis compared to the traditional static cultures. The axial flow, added to provide a wide gas exchange, media transport and waste removal, also produces a general cell alignment along the flow direction. In this way, the scaffold microstructure analysis generally shows the presence of aligned collagen fibers along the chondrocytes, with a wide zone of aggregated proteoglycans. Also the mechanical properties of the cultured scaffolds may be affected by perfusion showing higher elastic moduli in compression when compared to static or spinner flask cultures. In figure 2.2(c) it is possible to observe a typical perfusion system scheme(36, 39-41).

Concentric Cylinder Bioreactor (CCBR)(137)

A important feature of a bioreactor for cartilage regeneration is to reduce the not-controlled and undesired shear stresses induced by turbulent flows and to improve the efficiency of the dynamic culture, minimizing cell damages and apoptosis. These bioreactors are characterized by a high productivity provided by the large surface area. CCBR is designed to minimize shear stresses with a high culture surface area, while maintaining a simple geometry to ensure the nutrient transport. CCBR is constituted by a cylinder placed vertically and equipped with a motor to rotate at constant speed, presenting a shape similar to a viscometer. The produced flow profile is homogenous due to the bioreactor design, in fact the cylindrical shape provides a controlled medium speed. The production of extracellular matrix is influenced by the speed rate. Specific studies have demonstrated how a high flow speed and related high shear stresses may cause an increase in GAG content in the first days, but later a decrease is recorded. At a low rate, a GAG increase is achieved only after two weeks.

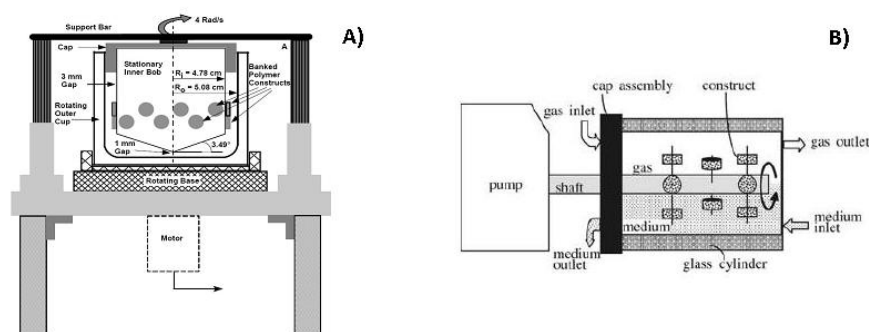


Fig 2.3. (A) CCBR and (B) RSB bioreactor layout

According with the obtained results with CCB $R(152)$, a single constant flow seems to be not sufficient to ensure a proper matrix synthesis; however, after changing the motor speed, the ECM biosynthesis can be modulated by a different hydrodynamic state, suggesting how chondrocyte metabolism may be altered by the speed rate and therefore to the relative shear stresses. Figure 2.3(a) shows the CCB R configuration.

Rotating-Shaft Bioreactor (RSB)(36)

The RSB bioreactor was recently developed for cartilage tissue regeneration and the culture was carried out in two phases. The RSB is composed by a cylindrical container placed horizontally and crossed by a stainless steel shaft. The shaft is linked to a rotative motor which moves the culture chamber, and it is equipped by 22 needles to sustain respectively 22 constructs. The culture chamber is half filled with medium, while the remaining part is occupied by gas, allowing a two phase culture. Fluids are forced through two independent pumps, one for medium perfusion, and the second one for gas exchange. In this way, a continuous mass transfer and a good oxygenation are achieved. During a cell culture, the rotation direction is generally inverted every day. The studies, performed by the RSB bioreactor, have revealed how the generated shear stresses are lower compared with the ones obtained in spinner flask, RWV and CCB R .

In addition, the shear stress level depends on the position of the construct inside the chamber and the slight dynamic microenvironment can be modulated changing the scaffold position. The results, obtained after three

weeks at 10 rpm followed by four weeks at 2 rpm, show a construct with cell morphology, GAG and collagen type II contents similar to natural cartilage, confirming the maintenance of chondrocyte phenotype and the formation of a hyaline cartilage-like tissue. In figure 2.3(b) it is possible to observe the RBS layout.

Biomechanical and Mechanical Indicators(153)

Collagen type II and proteoglycans content can be achieved by means the use of several biochemical techniques, commonly through indirect indicators. The most common method to evaluate the main component contents in tissue engineered cartilage include the radiolabelling, a technique based on the recognition by isotope labelling, to identify the isotope [³⁵S] of sulfate group and [³H] of proline, giving a indirect measure of proteoglycans and other synthesized proteins amount.

Several techniques have been developed to estimate the characteristics of the cultured matrix; among them physical methods are used to assess the weight percentage of both dry and wet construct, or other methods to recognize the specific mRNA involved in the synthesis of specific biochemical signalling molecules. In another very precise technique, *RT-PCR* (Reverse Transcriptase-Polymerase Chain Reaction)(116, 154), the mRNA produced by cells is extracted, multiplied and finally analyzed. Histology is also used to mark certain molecular groups along the section of the sample, for example *Safranin O* assay is carried out to mark the GAG aggregate distributions then viewed by an optical microscope.

Immunohistochemical techniques are also employed to identify more specific molecular markers. For cartilage tissue engineering, the techniques mainly used to assess the quality of the engineered construct and the correct cell activities are generally focused on the measure of GAG, collagen type II contents and the presence of biochemical signalling molecules involved in the matrix synthesis.

In addition to the biochemical assays, mechanical tests are generally carried out to characterize the final cartilage construct. The mechanical parameters, which may be evaluated on the obtained scaffold, are summarized in equilibrium modulus H_A [MPa], dynamic stiffness H_D [MPa] and hydraulic permeability k [$m^4/Ns10^{-15}$]. The equilibrium modulus can be measured with a simple compression test in a confined chamber. When the imposed strain is maintained constant, the recorded stress decreases exponentially due to relaxation. A equilibrium value is finally reached, while the modulus can be calculated by dividing the equilibrium stress to the constant strain(154).

2.6 Mechanical stimulation in tissue engineering cartilage

As widely described, the “*complex organization of articular cartilage is not an intrinsic property of chondrocytes*, but can be considered the result of several physiological stimuli and *in vivo* mechanical loads”.(153) Numerous studies have demonstrated how an unloaded articular joint can be subjected to a mechanical integrity loss, by reducing the proteoglycan and matrix synthesis.

For example, physiologically, a first fluid absorption occurs when the tissue is subjected to a hydrostatic gradient of compression. The fluid is then squeezed out from the matrix, dissipating consequently the energy, while the stress state is mitigated by the matrix structure, avoiding cell damages and apoptosis. Several studies have evaluated the effect both static and dynamic compression to enhance ECM synthesis in articular cartilage tissue engineering. Different load configurations are currently used, such as unconfined or confined compression, and permeable or impermeable configurations in which the chamber walls can or cannot allow the liquid permeation. In unconfined compression, the construct is laterally free to move, enabling the radial expansion during stimulation. In confined compression, the construct is all surrounded on each lateral side. In permeable configuration, scaffolds are housed and cultured between two porous plates which permit the fluid permeation during compression. Actually, the mechanical stress state which takes place in natural articular cartilage, is not yet completely known. However, related studies have emphasized how during unconfined compression an higher ECM deformation occurs if compared to *in vivo* cartilage(153). A brief description is now reported, concerning the results obtained by applying static compression, dynamic compression, tensile stretching, cyclic and intermittent hydrostatic pressure, shear stress, and finally shear stress induced by fluid (precisely by perfusion).

Static Compression(153)

The results obtained using a static compression have showed a decrease of gene expression and matrix biosynthesis of cartilage proteoglycans and proteins if compared with the data achieved applying dynamic forces. These effects are generally attributed to a lower mass transfer, due to the pore reduction which leads to a low nutrient transport, growth factors and metabolite removal from cells to matrix and viceversa. Considering the physiological conditions, matrix shrinkage also induces pH decrease caused by the increase of the negative charge density (FCD) and, accordingly, the amount of ions attracted from medium. In literature, several works show the influence of static stimuli on the cartilage synthesis. Following, these studies are briefly described.

Bushman et al.(116), and Kim and colleagues(155) have conducted experiments in which chondrocytes were seeded and cultured on agarose scaffolds and on devitalized animal cartilage. In these studies uniaxial static compression was applied, using a not confined configuration by two impermeable disks, and a decrease in matrix synthesis was shown. Buschmann and colleagues have obtained a increase in [³⁵S] sulfate and [³H] proline when constructs are not compressed. Static stimuli have induced a small effect on the engineered constructs, entailing a low biosynthesis at early cell culture time points, while inhibiting ECM formation in samples where the compression value were higher or at later time points. On the other hand, Kim et al. have demonstrated how biosynthesis can be resumed and how cells were not damaged due to the mechanical stimulation during

the recovery and after applying a static load for 12 hours at 50% of amplitude. PGA nonwoven fabric constructs with a porosity of 97% were cultured with bovine chondrocytes by Davisson and colleagues(53, 144) and stimulated with static compression tests after three weeks of free-swelling static culture. In this experiment, static compressions were carried out using strains of 10%, 30% and 50%. The obtained results have showed a sufficient amount of deposited matrix, in which 10% and 30% of compression have not reported any effect on biosynthesis and GAG or protein contents, but 50% of compression has reduced the S-GAG and other proteins total content of 57% of 35% respectively when compared to control samples. Other similar experiments were also carried out by Takahashi *et al.*(156) using MSC cells under a static load. These experiments have rather produced an increase in cell activation and matrix synthesis. Biological evaluations were performed with RT-PCR techniques, which have demonstrated how the chondrogenesis increase is due to Sox9 activation, a transcription factor for collagen type II, and due to the relative repressor deactivation, IL-1 β . So, an increment of collagen type II expression was achieved. It is possible to observe the disparity in results obtained using mature chondrocytes or MSCs, which are both cultured in static compression conditions.

Dynamic Compression (153)

Generically, experiments conducted using dynamic compression have always shown an increase of mechanical properties and GAG content in the obtained tissue. In addition, an acceleration of the synthesis process can be

often achieved. However, the dynamic compression always gives better and promising results compared to the static one. During cyclic dynamic stimuli, several physical phenomena can occur, such as mass transfer, signalling molecules transport through the matrix, local hydrostatic pressure or flow gradients, which take place inside the culture chamber and stimulate the engineered constructs. It is difficult to determine the individual effect of each component, since happen simultaneously.

However, it is widely demonstrated how a dynamic cycling compression, may be an useful tool to increase the matrix biosynthesis. Several devices were considered to induce dynamic compression stimuli on constructs, thus the main parameters to take into account during a typical experiment are the following:

- applied load frequency;
- imposed stress or strain amplitude;
- loading time schedule (stimulation duration, number of cycles, rest period between cycles, number of stimulation at day, rest period between stimulation, day number experiment).

Stimulus	Min Value	Max Value
Frequency (Hz)	0.0001	3
Load (MPa)	0.1	24
Strain (%)	0.1	25
Duration	Hours	Weeks

Fig 2.4. Range of frequency, strain and load applied from Darling et al.(153,154).

Table of figure 2.4 shows the common ranges of the previous listed parameters, used in dynamic experiments. Buschmann and colleagues have found a [³⁵S] sulfate increase from 15% to 25% in the obtained tissue, performing a dynamic compression culture on chondrocytes seeded on 3 mm agarose scaffolds. The used culture parameters were 3% cyclic strain at frequencies from 0.01 Hz to 1 Hz with a static offset of about 25% (0.73 mm), using a not confined configuration. The obtained agarose scaffolds seemed to offer similar characteristics and protein content of natural cartilage, thus allowing the maintenance of cell morphology and phenotype. The observed high extracellular matrix content is in agreement with the hypothesis concerning the ECM transport mechanisms which can regulate the signalling molecule behaviour due to the cell-matrix interaction. This experiment also reflects an increase in matrix deposition in the outer part of the scaffold compared to the central zone.

An increase in tissue biosynthesis was discovered by Kim and colleagues as a result of a dynamic load application. Also in this case, the dynamic stimuli have reported a radial inhomogeneity in cellular synthesis, probably influenced by the different stream flow induced by the different applied frequency. Animal derived constructs were analyzed, stimulating cells with frequencies of 0.01 Hz and 0.1 Hz, both revealing an increase in matrix biosynthesis. In the second case, the formed matrix is confined only in the outer part due to the high frequency effect. In fact, radial stresses induced by flow increase with the frequency, while the scaffolds cultured at 0.01 Hz have exhibited a greater homogeneity.

Davisson et al. have cultured chondrocytes on PGA nonwoven fabrics in a confined configuration at 0.001 Hz and 0.1 Hz and 5% in amplitude, modifying the imposed static offset from 10% to 50%. The collected results have showed a significant increase in GAG content if compared with static control culture. The loading regime appears to be more favourable using an offset of 50% at 0.1 Hz, where the increase of protein and GAG contents are higher if compared to the control cell culture, whereas a general increase in protein content was obtained by applying a dynamic regime at 10% of strain offset compared to static compression at the same offset level. The increase of matrix deposition at higher frequencies was probably attributed to a corresponding increase in the flow velocity, while at lower frequency directly to the mechanical deformation.

	0.3Hz	1Hz	3Hz
Superficial Cells	↓ GAG ↑ Proliferation	↓ GAG ↑ Proliferation	↓ GAG ↑ Proliferation
Deep Cells	↓ GAG ↔ Proliferation	↑ 50% GAG ↑ Proliferation	↔ GAG ↔ Proliferation
Full Depth Cells	↓ GAG ↑ Proliferation	↑ 40% GAG ↑ Proliferation	↔ GAG ↑ Proliferation

↑ = increase ↓ = decrease ↔ = no change

Fig 2.5. Experimental results presented by Lee and Co(153,157).

Comparing the results obtained by Kim and Davisson, in both cases it is possible to underline the increase in synthesis obtained through the

application of a dynamic stimuli if compared to static conditions. Nevertheless, Davisson et al. have obtained the best results at 0.1 Hz frequency, while Kim and colleagues have achieved a non-homogeneous tissue at the same frequency. However, it is important to underline the presence of many differences in the experiment setting, and for this reason it is very difficult to compare the results. Figure 2.5 shows the data obtained by Lee et al. using chondrocytes isolated from different parts of articular cartilage. Cells were seeded on 3% agarose scaffolds, in which unconfined dynamic load was applied with a strain of 15% changing the frequency, respectively 0.3 Hz, 1 Hz and 3 Hz. Concluding, several similar studies are reported in literature carried out with few different conditions. Small variations in the experimental setting, stimulation parameters, cultured cell type or biological evaluation techniques can cause a substantial change in the obtained results making the comparison difficult. Depending on the culture parameters and the cyclic compressive stress applied, it is possible to obtain an increase in protein amounts, matrix synthesis, collagen type II and *aggrecan* contents, as well as better mechanical properties of the constructs if compared to the static culture.

	C/C-UN	$\Delta\epsilon\%$	offset $\epsilon\%$	$\nu(\text{Hz})$	$h(\text{mm})$	time	scaffold	type cell
Buschmann et al.	UN-C	3	25	0,01-1	3		Agarose	Chondrocytes
Kim et al.	UN-C	9,77	0,63	0,1-0,01	1-3	23h	Explant	Chondrocytes
Devisson et al.	C	5	10-50	0,001-0,1	2	24h	PGA	Chondrocytes
Torzilli et al.	UN-C	(23,5MPa)	(0,5MPa)	1			Explant	Chondrocytes
Lee et al.	UN-C	15	0	0,3-1-3		48h	Agarose	Chondrocytes
Marín et al.	/	20	25	sin		2-12-24h	HA-derived	Chondrocytes
Dermateau et al.	UN-C	5	5	0,1(2h/12h)		3days	PEGT/PBT	Chondrocytes
Bonassar et al.	UN-C	3	0	0,1			Explant	Chondrocytes
Mauck et al.	UN-C	10	0	1(1h/2h)		(5/7day)x4	Agarose	Chondrocytes

Fig. 2.6. Experimental parameter found in literature, where the analysed parameters are confined or unconfined compression, strain, prestrain, frequency, thickness h , loading time, type of scaffold and finally cell type.

STATE of ART: tissue engineering

Other studies were also performed combining the cyclic load variation and the number of seeded cells. The best properties are obtained by starting with a small seeding concentration, due to the beneficial effect induced by mass transfer and dynamic flow of nutrients, which is inhibited by an excessive presence of cells. Table of the figure 2.6 shows the main parameters used in the principal studies found in literature. Figure 2.7 shows some examples of bioreactors used to apply dynamic stimuli. In general, the motion is ensured by a motor, which can be pneumatic or electric (i.e. stepper motor combined with a screw or a cam system). The load and the deformation are respectively monitored through a load cell and a displacement sensor.

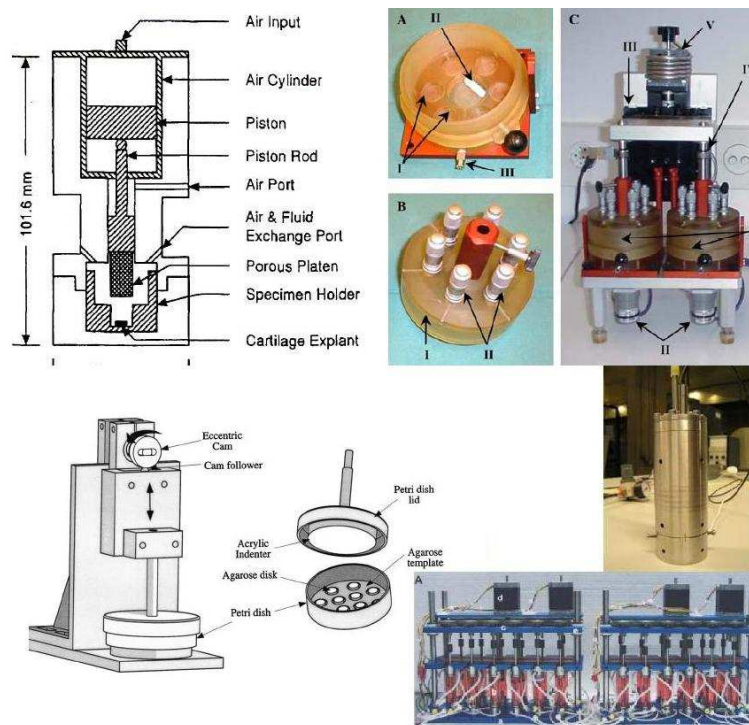


Fig.2.7. Some examples of cartilage bioreactor(31, 46, 158-160).

Tensile Stimuli by Stretching (153)

Some experiments were also carried out using tensile stretching on cartilage. Lee and colleagues(161) have seeded embryonic chondrocytes on elastin membranes. After 5 days of static culture, lamellae were subjected to a 10% of cyclic strain at 1 Hz frequency for 8 hours, or varying the electric fields with a frequency of 60Hz electrical stimulation with current densities up to 1000 nA/mm². Lamellae were fixed using two supports. The results of this *in vitro* experiment have highlighted how chondrocytes not adhered directly to the elastin fibers. Both methods showed an increase in GAG synthesis, respectively two and three times higher compared to controls, while generally lacking in collagen type II and other protein contents.

De Witt et al.(162) have used a different approach, in which chondrocytes were cultured for 14 days. Before applying dynamic conditions, a 5-8 layers of cells were formed to provide a sufficient stiffness. The mechanical stimuli were applied directly to the scaffolds. A stretch of 5.5% at 0.2 Hz frequency was imposed. Results have revealed an increase in gene expression in the early cell culture time point (24h). However, protein and collagen contents result unchanged, thus reporting a GAG increase.

Looking at the literature data, it is possible to observe how, applying a short period of stretching, a change in chondrocyte metabolism and an increase proteoglycan contents can be induced. Other methods used to apply stretching are listed(153):

- Scaffold is stretched after seeding;
- Cells are cultures on a flexible membrane, laterally fixed. The membrane can be stretched through vacuum or pressure.

Hydrostatic pressure - Cyclic and Intermittent (153)

The hydrostatic pressure is a crucial component of articular cartilage. Shear flow or cell deformations cannot be induced by pressure stimuli, but the liquid acts directly on the chondrocytes. Unlike in direct compression, generally the application of hydrostatic pressure does not cause a change in scaffold structure, maintaining its integrity and avoiding shear or tri-axial stress formation. The physiological levels of hydrostatic pressure are estimated in the range between 5 MPa and 15 MPa, where 5 MPa coincides with the stress in a knee during a normal walk.

Parkkinen et al.(163) have cultured chondrocytes on cartilage explants and on simple multi-well plates (without scaffold), applying a cyclic hydrostatic pressure. An increase in proteoglycan synthesis was found as a function of the duration and the amplitude of the used stimulus. A pressure of 5 MPa was imposed, changing the load time and frequency. Short periods of stimulation, about 1.5 hours, have caused significant changes in sulfate incorporation only in the culture carried out on cartilage explants, but not in the simple culture, where it was inhibited. Conversely, long-term stimulations, 20 hours, have showed an increase of sulfate incorporation on both the chondrocyte culture at frequencies of 0.25 Hz and 0.5 Hz, but not at 0.0167 Hz as frequency. Thus the obtained results allow to assert how

chondrocytes-matrix interaction can be modulated by pressure stimuli, involving dynamic culture parameters as frequency and pressure. Simple chondrocyte cultures have produced a more flat and less organized matrix when compared with culture on the cartilage explants. Ikenue and colleagues(**164**) have performed human cartilage chondrocyte cultures, where an intermittent hydrostatic pressure (IHP) was applied at a frequency of 1 Hz. Achieved data demonstrate how pressure duration and magnitude can differentially alter cell expression of matrix protein, in terms of collagen and *aggrecan* contents, thus providing important conditions to increase matrix anabolism and to enhance cartilage repair or regeneration.

In figure 2.8, it is possible to observe the percentage of GAG and collagen contents obtained by Carver and Heath(**165**) in a semi-continuous perfusion system in which pressure was also applied intermittently. Juveniles and adults equine chondrocytes were harvested and then cultured on resorbable PGA meshes, imposing two different pressures 500 psi (~3.5 MPa) and 1000 psi (~ 7 MPa). The loading time was 20 minutes long and was composed by intermittent pressure cycles of 5 seconds ON and 15 seconds OFF. The scheme was repeated every 4 hours for five weeks. Before each loading stimulation, 20 mL of fresh medium was perfused in the scaffold for three minutes. The best results were found obviously in cultures where younger and more active cells were seeded. However, in both cases, the engineered constructs exhibit a small amount of GAGs and collagen when compared with the natural cartilage contents.

Intermittent Pressure	GAG Concentration (mg/g tissue)		Collagen Concentration (mg/g tissue)	
	Foal	Adult	Foal	Adult
Native Cartilage	40 - 120	80 - 120	100 - 150	120 - 180
Control (no pressure)	26.0±24.4	2.0±1.0	6.3±1.6	0.5±0.3
500psi	89.3±31.4	5.7±1.0	6.7±1.9	3.0±0.3
1000psi	133.7±38.5	3.5±1.4	11.9±2.7	7.3±0.5

Fig.2.8. GAG and collagen contents after IHP culture(153,166).

A general increase in protein contents and a better phenotype response by chondrocytes can be obtained applying hydrostatic pressure on the tissue engineered scaffold, nevertheless a drop in cell proliferation may occur.

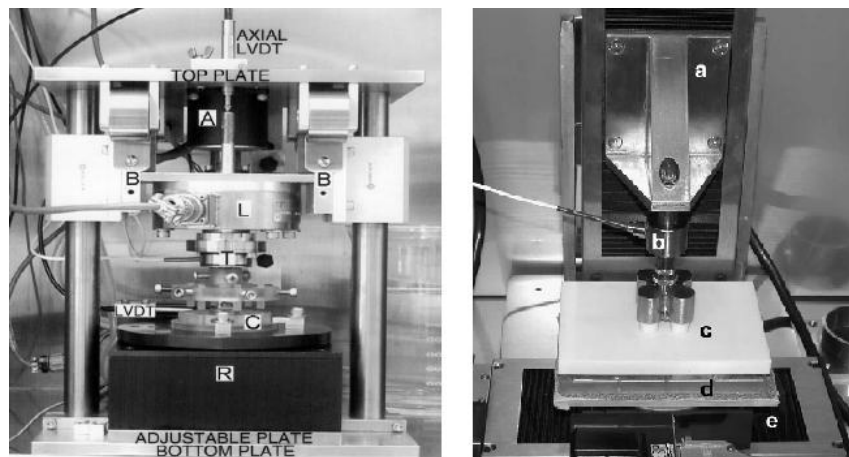


Fig.2.9. Direct shear bioreactor: by torsion (left), direct sliding (right)(44,43).

Direct Shear Stress (153)

The articular cartilage is responsible for the low friction coefficient. A complex tri-axial stress state can be generally achieved during the normal

physiological conditions, including shear stresses on cartilage surface. Recent studies have focused on the correlation between direct shear stress and extracellular matrix biosynthesis. Currently, the beneficial effect induced by dynamic compression was commonly justified as a consequence of flows, structure deformations and pressure gradients which occur within the tissue. Conversely during a dynamic shear stress, only matrix deformation is generated, while flows and pressure gradients can be considered negligible. Therefore, these studies have examined the single effect of shear stimuli, not involving pressure and flow gradients. Frank and colleagues(44) have applied a cyclical dynamic shear strain of 1% at 0.1 Hz as frequency for 12 hours and 24 hours, combined with a static compression. The used scaffolds were bovine cartilage explants. The results show respectively an increase of 25% and 41% in proteoglycan and other protein contents compared to constructs cultured under only a static load. Other studies, Kim et al, have reported similar results in which it is not possible to highlight a significant difference between the outer and the central part of the construct, as achieved in dynamic compression. Figure 2.9 shows two different devices for shear strain application, respectively induced by torsion (on the left) and direct shear (on the right).

Shear Stress Induced by Flow

As mentioned in the previous chapter, the relative motion in articular cartilage can also induce shear stress through the formation of flow and pressure gradients in the tissue. Researchers have tried to simulate this

effect with spinner flasks and perfusion systems, previously already described.

Considerations on the Effect of Mechanical Stimuli (153)

Various devices were developed to apply mechanical stimuli on chondrocyte or MSC cultures to promote their development and improve the characteristics of the obtained construct. The aim of this chapter is to describe the main experiments carried out for tissue engineered cartilage, concerning the use of bioreactors. However, it appears to be clear how, in each examined study, different culture parameters and evaluation techniques were chosen, making difficult a direct comparison. The construct properties results to be lower if compared to the native tissue, in term of composition and functionality. Different type of stimuli were illustrated, and in general dynamic conditions have improved the measured properties if compared to the not-loaded control, with the exception of static compression.

	<i>Dynamic Compression^a</i>	<i>Hydrostatic Pressure^b</i>	<i>Tension^c</i>	<i>Mixed Flask^d</i>	<i>Rotating Wall Vessel^e</i>
Mass transfer	↑	↑ ^α	↑	↑	↑
Proteoglycan /GAG	↑	↑	↑	↑	↑
Total Protein/ Collagen	↑	↑	↔	↑	↑
Cell Proliferation	↑	↓	↑	↑	↑
Other	β	γ		δ	

↑ = increase ↓ = decrease ↔ = no change

α - Via combined perfusion
 β - Radial Biosynthesis
 γ - Acts uniformly on cells, No tissue deformation or fluid flow
 δ - Formation of fibrous capsule

Fig.2.10. Result summary using mechanical stimuli on the cell cultures(153).

In figure 2.10, a summary of the explained stimuli is reported. The engineered constructs which show the best properties are obtained by cyclic compression, low shear, Rotating Wall Vessel with low turbulence and combining IHP and medium perfusion. In these experiments, the GAG content is similar to the native tissue one, while the amount of collagen type II is always less, suggesting how this behaviour could lead to the hypothesis in which *GAG and collagen gene expression are governed by different signalling mechanisms(153)*. Actually, researchers are trying to combine different mechanical stimuli in order to achieve the benefits reported by each stimulus taken separately.

2.7 Bioreactor used in bone tissue engineering

The main purpose of bioreactors is to guarantee the correct oxygen content and mass transfer, increasing the cellular construct properties or at least accelerate the *in vitro* step. Several configurations were designed in order to apply mechanical stimuli on bone cells, trying to mimic the *in vivo* conditions. For example, long bones are both subjected to localized compression and bending due to their curvilinear shape. Shear stress, flow and pressure gradients can be found in Volkmann and haversian canals. Perfusion and pulsatile fluid flow were mostly applied, but also uniaxial stretching, direct compression and pulsatile hydrostatic pressure have reported good results and benefit to cells(38, 42).

Shear Stresses induced by liquid

Several studies have demonstrated how fluid shear occurs in physiological bone environment through the tissue porosity, creating a flow and pressure gradient. Perfusion was both applied on 2D-layer and 3D-scaffold cell culture, showing an increase in mechanotransduction. The commonly proposed experimental settings are very similar to the cartilage perfusion bioreactors. Bone perfusion system differs only for the presence of an oxygen exchanger, in fact osteoblast and osteoclast cultures require a high dissolved oxygen content. GPIa murine stromal cell, cultured on a collagen scaffold for 21 days at 1.3 mL/min by Glowacki et al.(167), have shown an increase in gene expression and DNA content in comparison to the static control. Botchwey and Co. have reported a significant upregulation of ALP (Alkaline phosphatase) and calcium deposition on a 7 days-long culture of SaOS-2 cells seeded on PLGA. McAllister and Frangos have discovered an increase in prostaglandin E₂ (PGE₂) and nitric oxide NO content in rat osteoblastic cells cultured for 3-6 h under shear stress. Finally, Sillon and Co.(168) have obtained an increase in DNA content and a better scaffold distribution and penetration in polyurethane scaffolds seeded with murine preosteoblast and loaded with a flow rate of 1.0 mL/min.

Uniaxial and Biaxial Stretching

Uniaxial stretching seems to reproduce appropriately the stresses found in the mineralized bone, in fact a simple tensile state generates a compressive deformation in the transversal direction, achieving a proper stress state.

Duncan and Turner(*169*) have demonstrated how the stresses naturally transferred to bone cells are principally uniaxial tension and compression forces, while biaxial cannot be considered as an ideal condition to mimic the bone physiological environment. However, biaxial stretching was widely investigated. ALP upregulation compared to static control was found by Yang et al. in primary human osteoblasts seeded on PLLA and uniaxial stretched for 30 min/day at 1 Hz and 1000 μ strain as amplitude. An increase in matrix synthesis and collagen production was achieved in rat osteoblasts cells stretched using a 4-point bending system from 500 to 1500 μ strain for 2-24 h at 0.4 Hz(*170*).

Finally, human osteoblastic precursor cell line (hFOB 1.19) were seeded on matrices and then stretched uniaxially at 1% strain, 1 Hz, 1800 cycles/day (30 minutes) for 21 days. The results obtained by Ignatius et al. show an increase in proliferation and differentiation. In addition, ALP, OCN and OPN were slightly upregulated when compared to unstretched controls, while collagen expression appears to be downregulated(*49*).

Hydrostatic Compression (Pressure)

Considering the large water content, cells can be assumed as virtually incompressible systems. Researchers have justified the application of hydrostatic pressure (HP) asserting the formation of shear stresses and perturbation along the interface cell-substrate, without any clear evidence. Thus, the physiological relevance remains a controversial debate, although HP is commonly and successfully used in both cartilage and bone tissue

engineering. In general, a hydrostatic compression system can apply either intermittent ICP or cyclical CCP pressure, acting on liquid or gas. In the first case, the imposed pressure is transferred as a square wave (pulse), while in the second case the gradient can be considered sinusoidal. In addition, it is important to underline the difference between cell cultures in which liquid or gas were used as vectors to induce a hydrostatic pressure increase. In fact, the dissolved oxygen partial pressure surely increases with the increasing of gas pressure, adding more variables to the system; while this effect is avoided by acting directly on the culture medium. Nagatomi and colleagues(56) have demonstrated how osteoblastic functions are correlated to mechanical load parameters during a cell culture. The impose loading regime, 0.25 - 1 Hz for 20 minutes and 1 h at 10 and 40 kPa, results in ALP upregulation after 5 days, not altering proliferation and OPN expression. Intermittent hydrostatic pressure (ICP) was applied at 0.3 Hz and 13 kPa (rate 32.5 kPas⁻¹) by Roelofsen et al.(57), resulting in ALP, collagen and actin upregulation compared to static control for both mouse OB and OPR cells. ICP at 13 kPa and 0.3 Hz is also used by Klein-Nulend to investigate OPN, ALP and collagen expression in calvarial osteoblast-like bone cells MC3T3-E1.

Direct Compression

The direct compression has been extensively investigated in the field of tissue engineering, although it is mainly used in cartilage tissue engineering. However, a general increase in RNA synthesis was found by Shelton and El Hay under cyclical direct compression(171).

Effect of short-term rest period

Recently, short rest periods were introduced to avoid bone's osteogenic saturation caused by a continuous loading. In fact, mechanical stimuli regulate principally cell activation by mechanotransduction; on the other hand, a prolonged application can lead apoptosis and cell damage.

Batra and colleagues have inserted 5s, 10s and 15s of rest period in oscillatory fluid flow, 1 Pa and 2 Pa as shear stress amplitude at 1 Hz. The rest period insertion causes an increase in intracellular calcium ions and OPN contents compared to continuous loaded controls, while PGE₂ expression reports similar level(60-63).

Bone signaling molecules: cell culture characterization

In order to characterize a bone cell culture, several techniques are commonly used, such as the quantification and identification of certain signaling molecules, growth factors, interleukins, cytokines, gene expressions and specific ions involved in bone remodelling and mineralization. Cell culture can be evaluate analysing the produced proteins, molecules or enzymes, such as using a specific assay for each kind of cellular signals, Wester blotting, gel electrophoresis, or measuring the directly gene expression during the culture, such as using *RT-PCR* or specific kits. Briefly, a description of the principal signaling molecules are reported, to better understand the explained works. *Nitric oxide (NO)*(172) radical can give information about cell activity and bone remodelling, through the inhibition of bone resorption and related *IL-1* (interleukin)

expression. *IL-1* and *IL-6* are also involved in inflammatory response, in fact osteoblasts secrete *IL-6* to stimulate osteoclast formation. Prostaglandin are also important for bone formation, for example *prostaglandin E₂* induces osteoblasts to release bone resorption factors by osteoclasts, while *prostaglandin I₂* is a lipid molecules which drives the ECM synthesis and the angiogenesis decrease, increasing vasodilatation, apoptosis and inflammatory response. *Insulin-like growth factor IGF -1* and *-2* are growth hormone related to eachother, which govern cell proliferation, growth and may act as inhibitor of programmed cell death. Cell viability is also controlled by the cytokine *TGF- β* (*Transforming Growth Factor*). *COX-2* (*CycloOXygenase*) and *c-Fos* are proteins implicated in the regulation of differentiation, proliferation, and apoptosis, encoding the inflammatory response by *AP-1 transcription factor*, in order to counteract cell damage and the invasion of foreign cells or not recognized body (such as tumors). Osteopontin is specifically involved in bone remodeling, playing a crucial role in mineral matrix deposition and osteoclasts adhesion. Osteopontin is encoded by several genes, such as *OPN*, *RunX2* and *Osterix (Osx)* expression by osteoblasts. *RunX2* and *Osx* are entailed in collagen type I upregulation, while *RunX2* and *RunX3* are also associated to osteoblasts differentiation, proliferation (in the first stage of cell culture), and finally they are implicated in mineralization. *Osteocalcin* plays an important role on calcium ion homeostasis and bone mineralization, while osteonectin promotes mineral crystal formation, starting mineralization. *Osteonectin* also presents a strong affinity for collagen type I. *Alkaline phosphatase*

(*ALP* enzyme) removes phosphate groups from several molecules by hydrolyzation and it drives their deposition on the mineral matrix. *ALP* name suggests how it works principally in alkaline environment. Obviously, the *collagen* and *calcium ions* contents play a crucial role in the ECM synthesis and mineral matrix deposition. Depending on their own aims, these signaling molecules may present different trends during the cell culture.

3. MATERIALS AND METHODS

The proposed work is focused on the design and development of bioreactors for bone and cartilage regeneration, in which optimal cell culture conditions are controlled (temperature, nutrients, carbon dioxide levels), and two different mechanical stimuli can be applied on the cell constructs. This section presents technical considerations regarding the developed device and the opportunities in bone and cartilage tissue engineering. In fact, the results of these stimuli must induce the proper activations of cells, naturally accustomed to similar stresses in the joint. The goal of this bioreactor is to reproduce as close as possible the mechanical and biochemical conditions of the physiological environment. The proposed system is designed to work in a completely autonomous way, providing the control of several parameters, even remotely via web. A peculiarity of the proposed system includes the ability of applying two different types of mechanical stimuli, such as direct compression and cyclical hydrodynamic pressure. For this reason, a silicone membrane was introduced as a flexible element of connection between the sterile environment and the mechanical components for stress application, which makes the culture chamber effectively separated and individually manageable, sterilizable and autoclavable, while providing a large gas exchange area close to the cell culture. The system provides a continuous

MATERIALS AND METHODS

medium flow through a peristaltic pump and the ability to set automatically all the timing parameters of stimulation by software, such as the number of cycles, the number of repetitions, eventually the rest periods, offering a wide range of biomechanical stresses.

The proposed work can be divided in three main topics. The first section concerns the bioreactor description, the second describes the production and characterization of the scaffolds used as cell support. Finally, the third paragraph lists the experiments performed in the developed device.

3.1 Materials & Methods part 1: Device description

The device was designed in three main parts. As first, a sterile environment is constituted by the culture chamber and the flow line of nutrients powered through a peristaltic pump. The second part is the support structure that applies mechanical stimulation on the cell culture. Finally, the written software and the computer-controller allow the managing of all parameters, maintaining the required culture conditions.

List of materials:

- Polycarbonate LYX[®] sheet 4 mm and 9.5 mm;
- SYLGARD[®] 184 silicone elastomer;
- four channels peristaltic pump *Rainin RP-1*;
- *Watson & Marlow* platinum-cured silicone tubes;
- DC servo motor *Physik Instrumente (PI) model M230.10*;
- *Honeywell* pressure gauge *model 26PCDFA1G*;

MATERIALS AND METHODS

- button load cell *DsEurope model BC301.3Kg*;
- Pt100 thermoresistors (*Italcoppie cod. RS 621-7383*);
- a real-time embedded controller *National Instruments NI cRIO-9014* with the following chassis : *NI cRIO-9014, NI 9505, NI 9237, NI 9217, NI 9205*;
- CO₂ sensor *GSS model C20-6*;
- filtered power supply 12V(2A) and 24V(2A).

3.1.1 Culture Chambers

Two different culture chambers were prepared to apply direct compression and hydrostatic pressure, respectively. The culture chambers were milled from transparent polycarbonate sheets obtaining a cylindrical section with the following geometrical parameters (Figure 3.1 and 3.2): 23 mm height and 70 mm outside diameter for the direct compression chamber (DCC) and 13.5 mm height and 52 mm outside diameter for the hydrostatic pressure chamber (HPC). The wall and base thicknesses were respectively 10 mm and 3 mm in both chambers. The useful volume resulting from the described geometries was about 40 mL for DCC and 10 mL for HPC. Eight housing holes were obtained on the base to maintain anchored each scaffold during cell culture. The chosen hole dimensions, 0.5 mm depth and 10 mm width, represent also the sample size. The medium inlet and outlet were placed on lateral side of the chamber at the base level, as shown in figure 3.1(c). In both the culture chambers, the medium was supplied by a four channels peristaltic pump *Rainin RP-1* and through *Watson & Marlow* platinum-cured silicone tubes with an inner diameter of 1.6 mm and 1.6 mm wall

MATERIALS AND METHODS

section, allowing the circulation of fresh medium between flask and chamber (Figure 3.3).

Direct Strain Chamber (DCC)

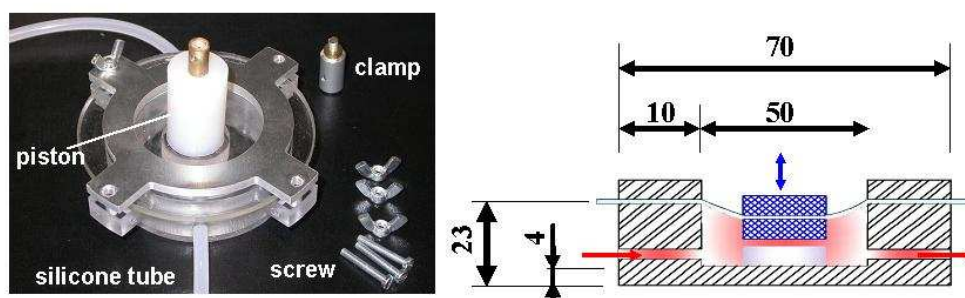


Fig.3.1. Direct compression chamber.

Pressure Chamber (HPC)

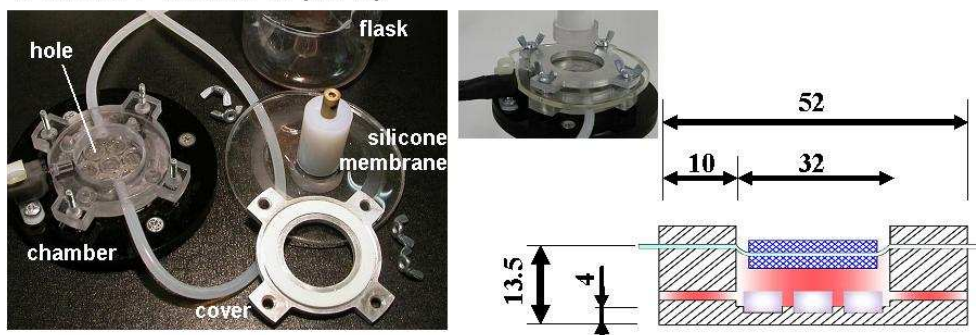


Fig.3.2. Hydrostatic pressure chamber.

Each connection element was isolated from the outside environment to maintain the sterility inside the cell culture area. In fact, the culture chamber was sealed by an elastic silicone membrane with 2 mm thickness (*Sylgard*[®] 184) on the top, which provided also a gas exchange (mainly CO₂ and O₂).

MATERIALS AND METHODS

Mechanical stimuli were transferred to the cell constructs thanks to this connection element: the external displacements can be transposed as biomechanical stresses, precisely compression and hydrostatic pressure. The silicone membrane and the chamber can be closed using an aluminium cover and four screws with wingnuts. The sealing were guaranteed by a PVC o-ring positioned between the cover and the membrane.

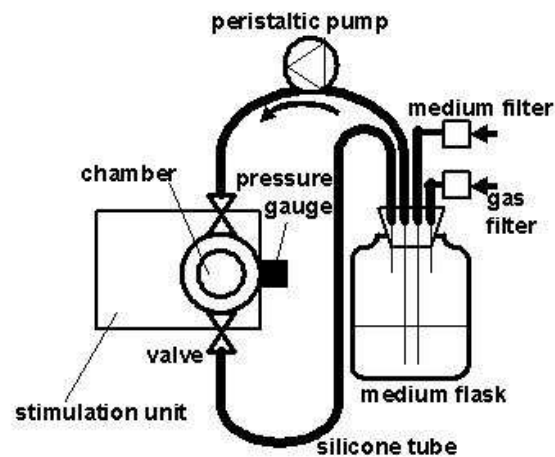


Fig.3.3. Flow line Layout.

In addition, the hydrostatic pressure culture chamber HPC was equipped with a *Honeywell* pressure gauge *model 26PCDFA1G* with $2 \cdot 10^5$ Pa of full scale, positioned on the chamber wall at base level. Two self-assembled valves, to switch on-off the medium flow, were placed outside the chamber on the medium inlet and outlet tube respectively (figure 3.3). The valves simply operate squeezing the silicone tube with an external mechanical

MATERIALS AND METHODS

action. Both chambers can be sterilizable with standard ethylene oxide, and DCC chamber can be also autoclavable.

Silicon elastomer preparation

Sylgard® 184 Silicone Elastomer was prepared by mixing two components, the siloxane base and the curing agent, with a 10:1 ratio respectively. To obtain the silicone membrane, 10 mL of the mixture was cast in a 96 mm petri dish at room temperature for 24h.

Peristaltic pump calibration

Generally, peristaltic pump manufacturers provide calibration curves, representing the flow velocity as a function of the rotational speed and the inner tube diameter. However, the calibrations were carried out using water. Ad hoc calibration curves must be performed, considering the use of a different liquid. Although culture medium is an aqueous solution, it presents a quite different surface tension. In fact, the drop size only depends on the fluid surface tension, liquid density and the nozzle diameter. Thus, simple flow experiments were carried out changing the rotational speed.

Pressure Gauge calibration

The proposed pressure gauge consists in a sealed piezoresistive element, compensated by a Wheatstone bridge which makes possible the measurement. The given conversion factor is 3.33 mV/psi. Equation 6 shows the conversion factor expressed in kPa/V.

MATERIALS AND METHODS

$$3.33 \frac{mV}{psi} \rightarrow 0.00333 \frac{V}{psi} \cdot \frac{psi}{6.89414 kPa} = 4.8302 \cdot 10^{-4} \frac{V}{kPa} \xrightarrow{(\dots)^{-1}} 2070.312 \frac{kPa}{V} \quad (6)$$

Calibration curves were performed in order to make a more accurate pressure measure. In fact a systematic voltage deviation may occur during the installation (biasing method). The pressure chamber (HPC) was connected to a gas cylinder equipped with a commercial pressure gauge (1 kPa resolution) and the calibration curves were obtained from 0 kPa (manometric pressure) to the sensor full scale (200 kPa).

Therefore, the culture chambers were finally tested to verify the sealing. The system was filled with ethanol 70% and maintained at 200 kPa for 1h. Then, ethanol was continuously flowed for a week, measuring the level of the remained fluid inside the flask.

3.1.2 Mechanical components

The device includes a linear actuator to impose a certain displacement, a linear encoder and a load cell to measure deformation and load respectively. The system must guarantee a constant temperature and carbon dioxide level as well as chamber sterility where cells are cultured. The device was also designed to characterize the mechanical properties of the obtained constructs by cyclic compression tests (DMA dynamic mechanical analysis), quasi static ramps, creep and relaxation tests. The device was designed to control four independent single units of stimulation, working in parallel. Every single unit was equipped with a linear actuator *Physik*

MATERIALS AND METHODS

Instrumente (PI) model M230.10 provided with a $0.0046\ \mu\text{m}$ resolution encoder, a maximum thrust force of 70 N and a button load cell *DsEurope model BC301.3Kg* with 30 N of full scale and an accuracy of 0.025 N, as shown in figure 3.4. Figure 3.5 reports the structure layout, built up in aluminium alloy, describing briefly the working principle of the manual positioner and the piston clamp.

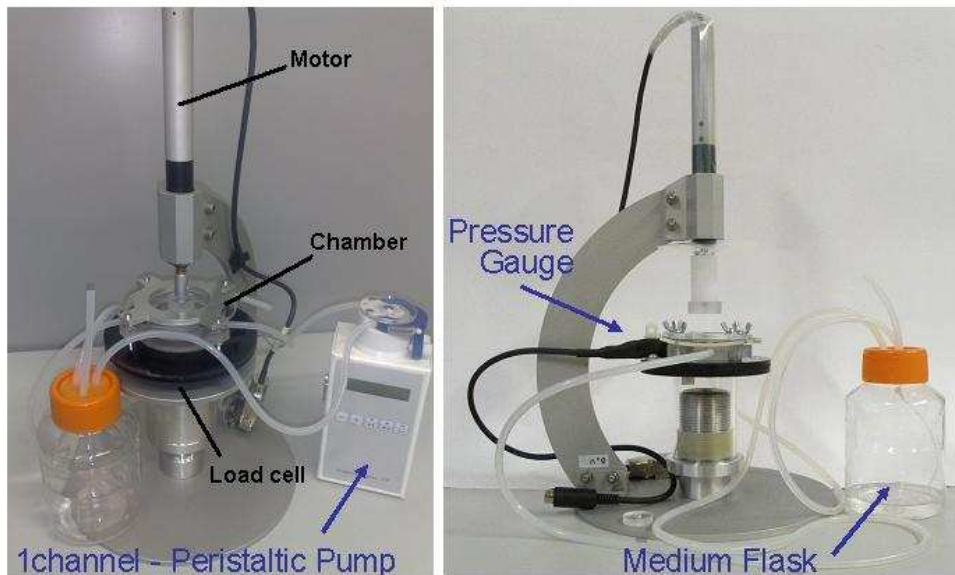


Fig.3.4. Device structure: Direct compression (left) and hydrostatic pressure (right) configuration.

Physik Instrumente (PI) model M230.10

The selected linear encoder is a DC servo motor proceed by Physik Instrument (PI). Model M230.10 provides a linear motion up to 10 mm,

MATERIALS AND METHODS

with a maximum velocity of 1.4 mm/s. The linear actuator is equipped with a sub-micron resolution encoder, while maintaining a compact package.

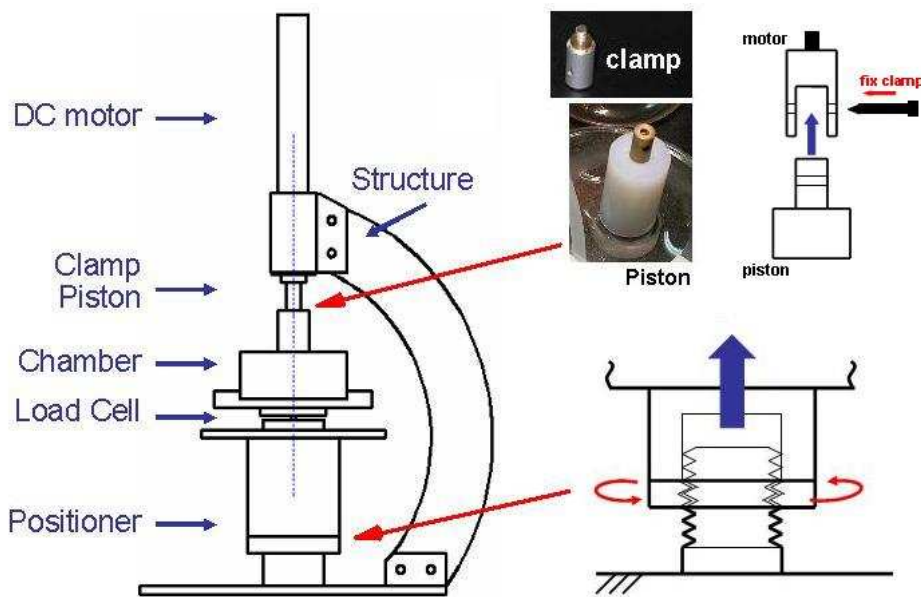


Fig.3.5. Structure Layouts.

Thus, the motor is driven by a closed-loop DC motor, using the encoder as feedback. Linear motion is allowed by a non-rotating tip combined to the gearhead rotative DC motor. In table 3.1 the motor technical data are summarized. In Figure 3.6 it is possible to observe the actuator layout.

In the proposed system, motors are driven by a microcontroller. The chosen signal type is a pulse-width modulation (PWM), in which a high-frequency square wave is generated at 20 kHz with at 12 V amplitude (maximum voltage). The voltage applied to the motor can be varied by changing the

MATERIALS AND METHODS

duty cycle (time ON over a wave period). PWM method is a typical technique to control the device power supply used in several applications and it combines low cost with high precision, working in a digital way. Motor calibrations were also performed, representing the speed measured by the linear encoder as a function of the imposed duty cycle. In fact, a proportional voltage corresponds to a given d duty cycle (12 V($d=1$), 6 V($d=0.5$), 3 V($d=0.25$), 0 V($d=0$), considering $0 \leq d \leq 1$) which results in a constant speed for a DC motor. Thus, motor speed can be proportionally controlled acting on the duty cycle.

Properties	Value	Unit
Travel Range	10	mm
Sensor Resolution	2048	counts/revolution
Design Encoder Resolution	0.0046	$\mu\text{m}/\text{counts}$
Minimal incremental motion	0.05	μm
Backlash	2	μm
Unidirectional repeatability	0.1	μm
Maximum velocity	1.4	mm/s
Maximum push force	70	N
Operating Voltage	0-12	V

Table 3.1. Motor technical data, which can also be found on PI website (www.pi.ws)

DsEurope model BC301.3Kg

The button load cell is made in aluminium alloy, model BC301.3Kg produced by DsEurope. In Fig.3.7 are shown the dimensions and the layout of the load cell. The sensor is composed by a Wheastone full-bridge (350

MATERIALS AND METHODS

Ohm) with a 30 N Full Scale (FS) and a 2 mV per FS Voltage sensitivity. Applying a voltage in the recommended excitation range, 4.16 V, the FS electrical signal (V_{FS}) corresponds to 8.32 mV, thus full-bridge must be amplified.

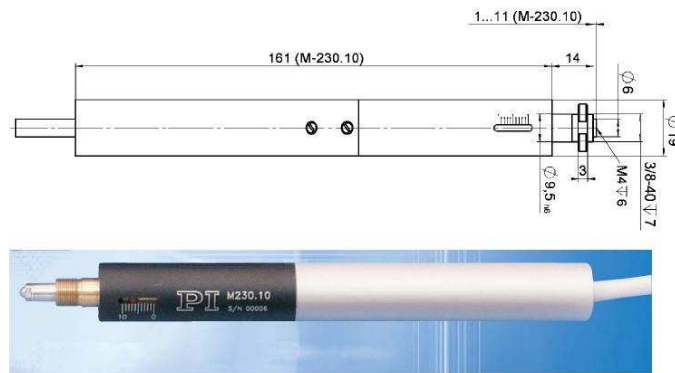


Fig.3.6. Motor layout.

The repeatability error is normally less than 0.1%FS, which corresponds to ± 0.03 N. All the data described are reassumed in table 3.2. Calibration curves were carried out using laboratory standard weights and recording the related voltage measures.

Properties	Value	Unit	
Full Scale (FS)	30	N	
Sensitivity	2	mV/V FS	(10 mV)
Repeatability error	$\leq \pm 0.1$	%FS	(0.03 N)
Total Error	$\leq \pm 0.5$	%FS	
Thermic shift of zero	$\leq \pm 0.08$	%FS/°C	(0.024 N/°C)
Operating Voltage	4-6	V	

Table 3.2. Load cell technical data (www.dseurope.it).

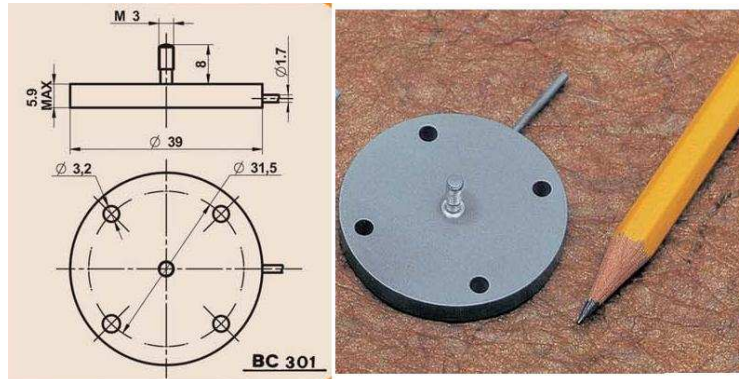


Fig.3.7. Load cell layout.

3.1.3 Controller and Software

The layout of the third part is reported in figure 3.8: a real-time embedded controller (*National Instruments NI cRIO-9014*) is connected to a *NI cRIO-9014 chassis*, containing an FPGA (*Field Programmable Gate Array Spartan2* of 3 Mgate reconfigurable I / O with a clock frequency of 40 MHz). The DC motors, their encoder and the peristaltic pump are controlled by five of *NI 9505 chassis*, the load cells and the pressure sensors are acquired by a *NI 9237 chassis* with 24 bit resolution, while the temperature is measured by Pt100 thermoresistors (*Italcoppie cod. RS 621-7383*) measured by a *NI 9217 chassis*.

The software was developed in NI Labview 8.5.1 environment. The software architecture is expanded over three main levels (figure 3.8). The lowest level concerns the FPGA programming where all I/O signals are acquired, analyzed, managed or generated from the controller to the stimulation unit, which include motor signals to impose the displacement

MATERIALS AND METHODS

and measure signals from encoders, load cells, pressure gauges and thermal probes Pt100 as feedback.

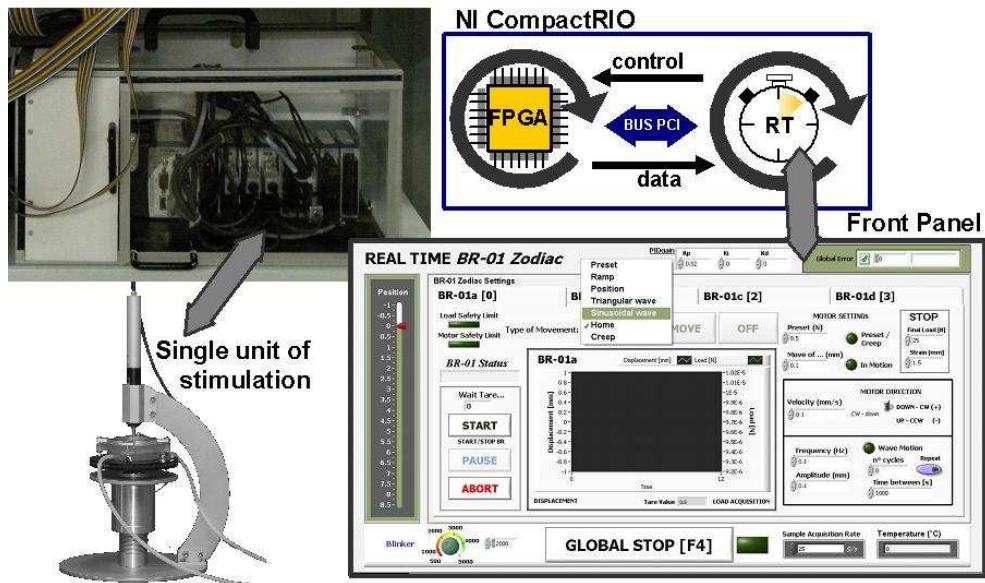


Fig.3.8. Controller and software architecture.

The real-time microprocessor and the FPGA are synchronized in a deterministic way by the second programming level, which is permanently downloaded in the controller. Thus a completely autonomous control of the stimulation units can be achieved, providing a high reliability, the possibility to manage all the working parameters and finally enabling the operator access to the front panel, directly or remotely via Internet network. The measured data are then published on the local network via TCP/IP protocol. The highest programming level was designed to give an user-friendly graphical interface for the experimental parameters settings and data saving (figure 3.8).

3.1.3.1 Hardware description

Real time embedded controller, Technical data

NI *cRIO* 9014 is an embedded real-time controller composed by an industrial 400 MHz Freescale MPC5200 real-time processor for deterministic applications, 128 MB DRAM memory and 2GB nonvolatile storage memory. The NI 9014 is designed to guarantee programmatic communication over the network and built-in Web (HTTP) and file (FTP) servers, allowing remotely data logging. Thus, standalone application can run in an autonomous way. NI 9014 is connected to an FPGA (Field Programmable Gate Array) model NI cRIO-9104 through a PCI high speed bus. NI 9104 is an eight-slot, 3M gate reconfigurable embedded chassis providing custom hardware design using NI LabVIEW software. The cRIO-9104 can contain up to eight different chassis, while maintaining a high frequency reliable communication up to 80 MHz. The used chassis are five NI 9505, for four motors and peristaltic pump respectively, NI 9237 for load cell measuring, NI 9217 for Pt100 reading and finally NI 9205 to acquire general analog signals.


NI 9505 (motor controlling)

The NI 9505 module is a full H-bridge servo motor drive for direct connectivity to actuators such as DC servo motor. This chassis allows PWM generation at high frequency 40 kHz, current consumption and encoder reading (*TTL logic*). In table 3.3 it is possible to observe the wire connection


MATERIALS AND METHODS

scheme relative to the connection between NI 9505 chassis and motor M230.10.

NI 9505	Signal	M 230.10 (Serial Port DB15)
M+	Motor Supply (+)	2
M-	Motor Supply (-)	9
C	COM (Ground Supply)	10
V	External Power Supply (12 V)	//
5	Encoder Power supply +5 V	4
1	Encoder A+	14
6	Encoder A-	7
2	Encoder B+	15
7	Encoder B-	8
3	Encoder Index + ↔ Reference Sens.	13
8	Encoder Index - ↔ Limit Ground	6
9	Encoder Grd ↔ Limit Ground	6
4	Stop ↔ Limit (+), Limit (-)	5-12 (with diode: OR gate)



Shielded wire



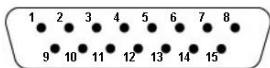


Table 3.3. Wire connection between NI9505 to motor M230.10 (www.ni.com).

NI 9237 (load cell measuring)

NI 9237 is a four-channel analog input device designed to measure bridge sensors. This chassis can perform the needed signal conditioning operations, such as amplification, isolation, filtering and excitation, while acquiring four channels simultaneously. NI 9237 can acquire up to 50 kSamples/s, with a range of ± 25 mV/V and a resolution of 24bit ($25 \text{ mV} \cdot V_{FS} / 2^{24}$). This module can provide excitation voltage, but it is also equipped with a

MATERIALS AND METHODS

connection for external power source when the total sensor consumption exceeds 150 mW. Total bridge consumption is expressed by equation 7, an external voltage source is thus needed. In figure 3.9 the connection scheme is reported, in fact, load cell BC301.3Kg presents only four wires, one pair for the excitation voltage and the second pair for the analog signal, respectively.

$$TotalBridgeConsumption = n^{\circ}channels \cdot \frac{V_{EX}^2}{R_{BRIDGE}} = 4 \cdot \frac{(4.16)^2 V^2}{350\Omega} = 198mW \rightarrow External \quad (7)$$

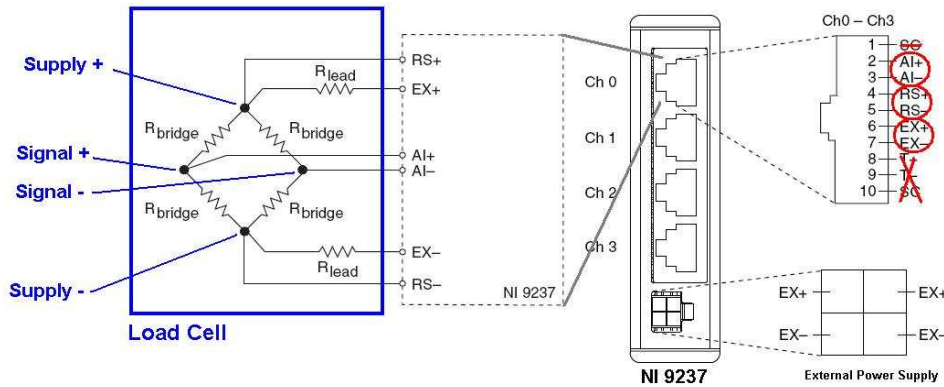


Fig. 3.9. Wire connection between NI9237 to motor Load Cell.

Power Supply, Pt100 and Carbon Dioxide measuring

CompactRIO is powered by a 24 V source, while the total motor consumption does not exceed 12 W, 1 A at 12 V. Resistive thermal devices (RTDs) Pt100 is a platinum 100 Ω resistance, exploiting Ohm's law to measure temperature. In order to obtain a more accurate measurement, the temperature is calculated using equation 8. The thermoresistors are measured by a NI 9217.

$$R = R_0 \cdot (1 + A \cdot T + B \cdot T^2) \rightarrow A = 3.9083 \cdot 10^{-3}; B = -5.775 \cdot 10^{-7}; R_0 = 100\Omega; T(^{\circ}C) \quad (8)$$

MATERIALS AND METHODS

Differently, carbon dioxide level is obtained using a CO₂ sensor *GSS model C20-6*. The measured signal can be directly processed by *cRIO* thanks to a serial driver mounted on the sensor which works with a RS232 protocol. C20-6 sensor gives a full scale of 20% pCO₂, while maintaining a fast resolution of 0.1% (Responsivity \approx few seconds) and a high resolution of 0.01% (Responsivity \approx 30 seconds).

3.1.3.2 Software Description

As previously mentioned, the entire system is managed exclusively into three levels, high frequency low level to guarantee the communication with the devices and sensors, the second level to communicate with the FPGA and the user in a deterministic way and finally the user interface. Each level was developed using LabVIEW 8.5.1.

FPGA

In FPGA software, input and output signals are generated at high frequency, 40MHz, must send the proper signals to motor and the correct power supplies to sensors, while acquiring and amplifying their measurements. FPGA can work in a deterministic way and the operations can be simultaneously performed. Thus, the developed software presents individual cycles which run in parallel.

The first cycle is reported in figure 3.10 and represents the encoder reading. Encoder signals are two out of phase TTL pulse wave (channel A and B). Due to the motor specification, one encoder count is equal to 0.0046 μm ,

MATERIALS AND METHODS

while 2048 counts are a complete revolution. Two channels are needed to understand the shaft direction. When shaft motor is turning clockwise, A occurs before B, otherwise the direction is counterclockwise. The scheme of Fig.3.10 shows the signal reading in which the logic gates add or subtract counts as a function of channel phases. Thus, absolute, relative position (resettable) and velocity can be obtained. Velocity is expressed in tick (clock unit, 40 MHz is equal to 25 ns) per count (0.0046 μm). In this section, the diagrams for a single stimulation unit is reported for an easier understanding.

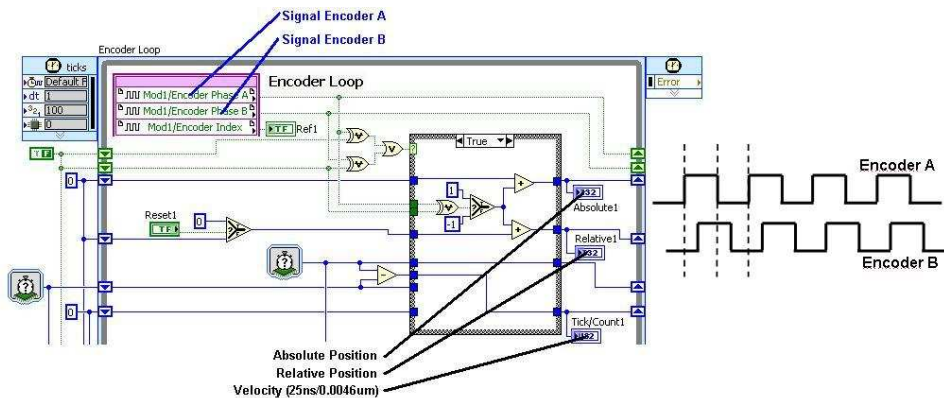


Fig.3.10. Encoder reading and TTL pulse trains.

Velocity and position are read by a second cycle, which filters the velocity with a simple moving average, while setting the stop condition on the imposed position. When relative position is equal to the imposed position, the stop condition is reached. In figure 3.11 the second cycle is shown.

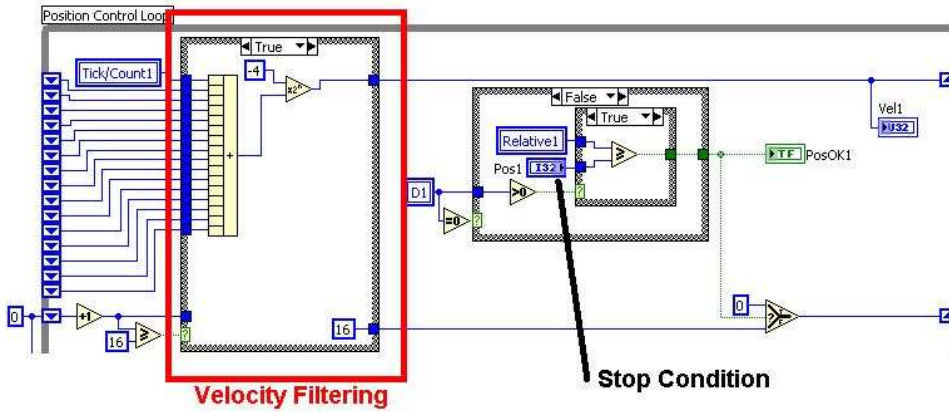


Fig.3.11. Velocity filtering and stop condition.

As previously mentioned, the motor is controlled by changing the duty cycle. The duty cycle can be defined as the time fraction over the period in which the system is in “active” state.

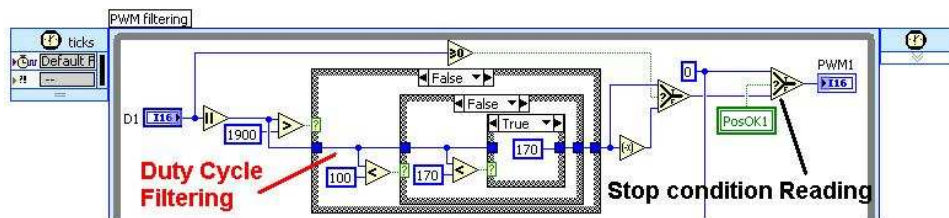


Fig.3.12. Duty filtering and PWM imposing.

Considering the system clock frequency, 40 MHz, and the chosen PWM frequency, 20 kHz, (good compromise between the dynamics required by the motor and provided by the controller), a PWM period is divided in 2000 ticks (40 MHz/20 kHz) in which for a duty cycle “D” of 50% corresponds 1000 ticks in the high state and 1000 ticks in the low state, while for 25% D

MATERIALS AND METHODS

is equal to 500 ON / 1500 OFF and so on. In this way the duty cycle is included between 0-1 to 0-2000 ticks.

In the third cycle, the imposed duty cycle is read, turned in a PWM value and finally filtered to avoid critical situations or unpredictable responses from the controller. In fact the operating range is between 5% and 95%, which corresponds to a minimum active or passive time of about 2 μ s (technical data). A 10% duty filter was also added to overcome the motor friction, and finally the stop condition of the second cycle results in a PWM zeroing.

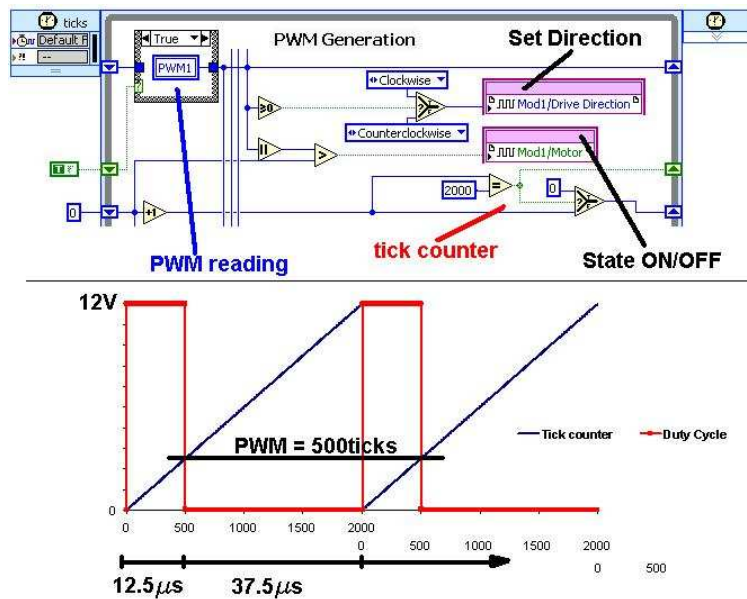


Fig.3.13. PWM writing.

In the fourth cycle, the PWM value is translated in the PWM signal following the graph in figure 3.13, in which an indexing counter drives the motor state ON/OFF. Finally, the direction is detected when duty is less

MATERIALS AND METHODS

than zero, positive values correspond to clockwise, while negative values mean counterclockwise. A fifth cycle enables the motor drivers and detects any errors in the 9505 board. Finally, other three cycles are used to set the load cells (NI 9237), Pt100 probes (NI 9217) and analog inputs (NI 9505); signal scan rates are imposed and signal values are read for each channel, four load cells, four thermoresistors and four analog inputs.

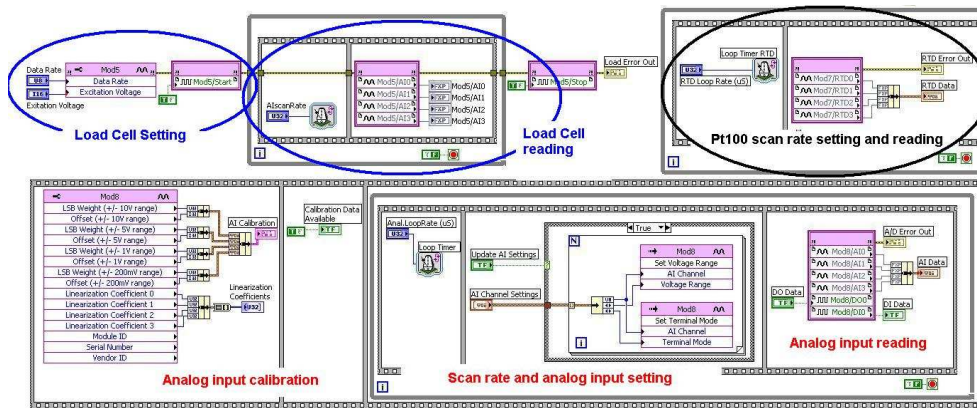


Fig.3.14. Analog input setting.

Each input or output variable used in FPGA software is available in the real-time software, allowing respectively read or write operations.

Real-Time RT Software

The real time part should ensure a stable, reliable and deterministic communication with the FPGA, while allowing the user access to setting parameters. The software architecture can be divided into four parts, FPGA and variable initialization, a cycle in which data are acquired, processed and

MATERIALS AND METHODS

sent via TCP/IP over the network, four parallel cycles to control the motors and finally software closing.

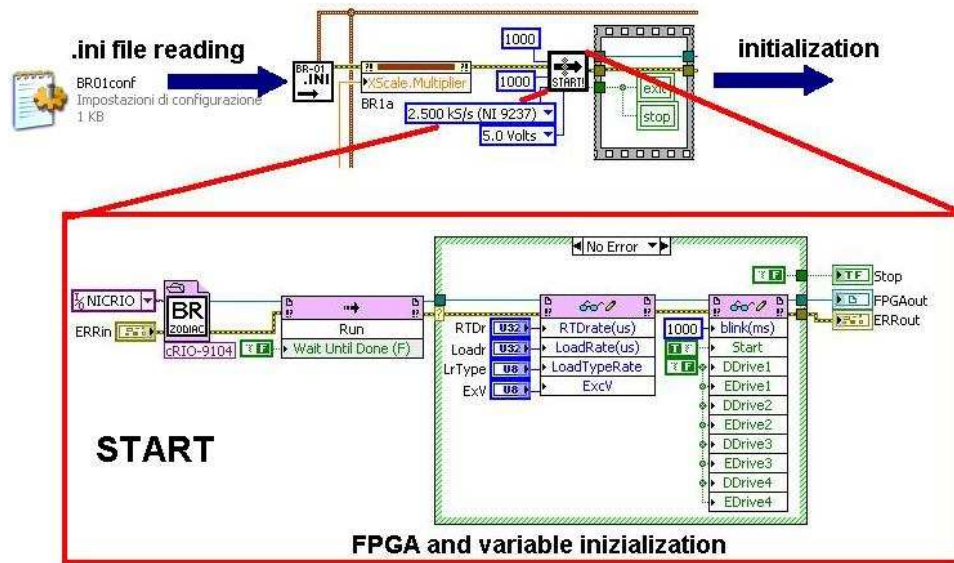


Fig.3.15. Real time initialization.

RT variables are configured by reading an .ini file (initialization file) stored in the controller memory. Motor and load cell calibration parameters and motor absolute positions are read, then FPGA can be initialized writing sensor scan rates. In the second part, a single cycle can acquire, process and convert, plot both displacement and load (or eventually pressure) data and send them over the network to a specific client. This cycle works with an acquisition rate, normally imposed to 25 Hz. Signals are converted for position from *count* to *mm* (in fact FPGA can only work with integers number without division), for load-pressure from *mV* to *N-kPa*, for

MATERIALS AND METHODS

where $u(t)$ is the variable, K_P , K_D and K_I are the proportional, derivative and integral constants respectively and finally $e(t)$ is the error between the real and the measured variable.

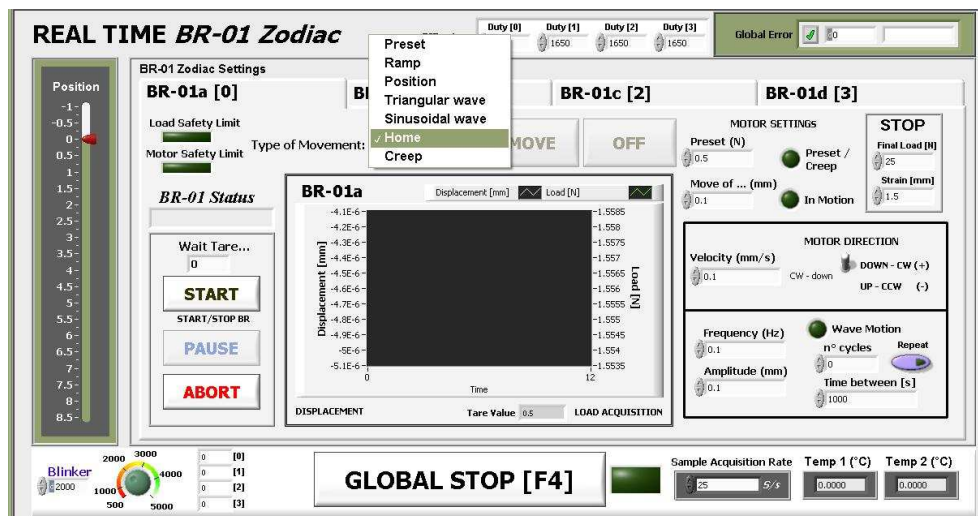


Fig.3.17. Front panel.

The possible events are listed as follows:

- *Tare* load cell (no motion event);
- *Load Preset*, where a certain load is imposed on the sample (once);
- *Ramp*, by which a linear motion is imposed until the imposed stress or strain (quasi static test);
- *Position*, allows to move the piston with a predetermined value;
- *Triangular displacement Wave* (frequency, amplitude, number of cycle);
- *Sinusoidal displacement Wave* (frequency, amplitude, number of cycle);

MATERIALS AND METHODS

- *Sinusoidal Pressure Wave* (frequency, amplitude, number of cycle), which differs from the previous event for few initial cycles of tuning;
- *Home*, through which the motor shaft returns to the initial position. This event should be used as reference;
- *Creep* test, by which a constant load is maintained.

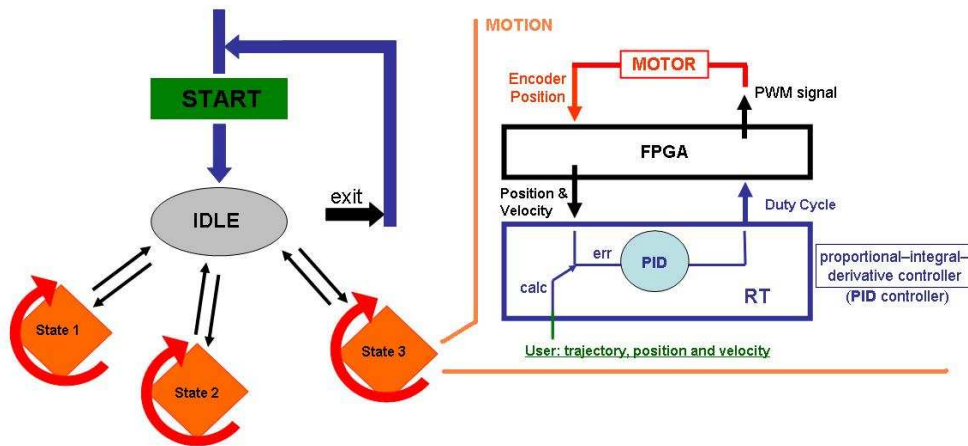


Fig.3.18. State machine diagram and motion PID loop.

The labview wiring relative to the position event state is shown in figure 3.19, in which encoder signals are read and sent from FPGA to the RT software. This event state computes the FPGA information, performs the PID calculation and sends a new duty cycle to FPGA, until the position is reached or the stop button is pressed. The other motion events present a similar philosophy. In the state machine, a continuous errors monitoring is performed, such as the load or motor stroke limit exceeding which leads to an immediate motion stop, or simple warnings occurring when temperature or carbon dioxide presents improper values. An accurate error management

MATERIALS AND METHODS

is also carried out in the presented software in terms of hardware guaranty. Finally in the last part of the real-time software, the motor absolute positions are written in the .ini file in order to be accessible for a future use, motor drivers are disabled and FPGA is correctly closed.

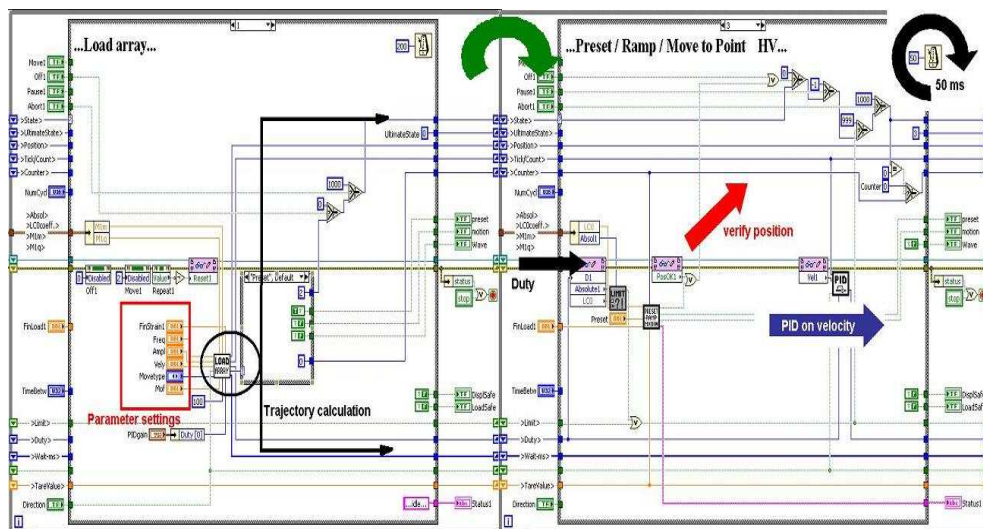


Fig.3.19. Position event state: calculation and running.

User Interface

The user interface resides on the PC in use, differing from the previous described two softwares which are deployed directly on the controller. This client program is used to download the data sent from the RT via TCP/IP protocol. In this programming level, it is possible to set the scan rate, number of scans (file), number of points per scan. Data are saved as .txt ASCII file. Figure 3.20 shows both the front panel and the block diagram for the user interface.

MATERIALS AND METHODS

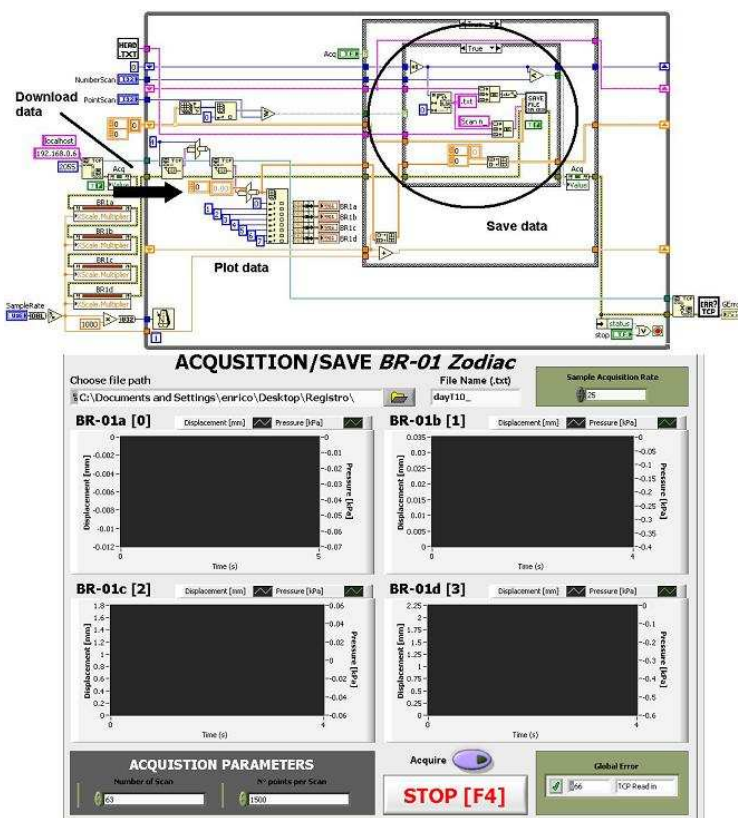


Fig.3.20. Front Panel and back diagram for the user interface.

3.1.4 Stimulation setting description

The silicone membranes, used to close the culture chambers, were equipped with polycarbonate discs (28 mm in diameter and 5 mm thick) placed internally in the centre of each membrane. The disc was joined to an external motor clamp through a stainless steel screw. Working as an insulator, the membrane prevents any contact between medium and the screw.

MATERIALS AND METHODS

Depending on the experimental setting, either direct compression or hydrostatic pressure can be applied on the scaffolds and it is possible to choose the proper type of chamber for cell culture. In the first case, the advantages of using a DCC chamber for direct compression include the ability to be autoclavable with a greater medium volume. During cell culture, the internal polycarbonate disc was placed in contact with the scaffolds through a settable preset by software.

In the second case, with a HPC chamber, it is possible to combine the cell culture to hydrostatic pressure; both the stimulations are also possible. The hydrostatic pressure chamber presents lower geometrical dimensions in order to achieve higher pressure, while maintaining the maximum number of culturable scaffolds. By closing the inlet and outlet valves located outside the chamber, the internal pressure can be increased by compressing the silicone membrane (figure 3.21(b)). After the stimulation, the mass transfer can be restored opening the valves.

Both the chambers were designed to culture simultaneously up to 8 scaffolds, which can be placed in the chamber before the dynamic culture or during the seeding. The mass transfer inside the flow line is obtained by a peristaltic pump. When necessary, the medium contained in the flask may be replaced through a 0.22 μm hydrophilic filter Millex[®] GP PES (polyether sulfone) placed on the cap, while gas exchange is guaranteed by a 0.22 μm air hydrophobic filter Dualex[™] Plus PVDF (Polyvinylidene Fluoride). In fact, the system was designed to work inside a standard humidified incubator at 37 °C and 5% CO₂. Once positioned the scaffolds, the chamber

MATERIALS AND METHODS

can be fixed on the stimulation unit and placed inside the incubator without any contamination risks. The flask medium replacement can be performed directly in the incubator using a syringe and the mentioned filter or under a laminar hood. In figure 3.21(a, b) the operating principles of both the chambers are shown.

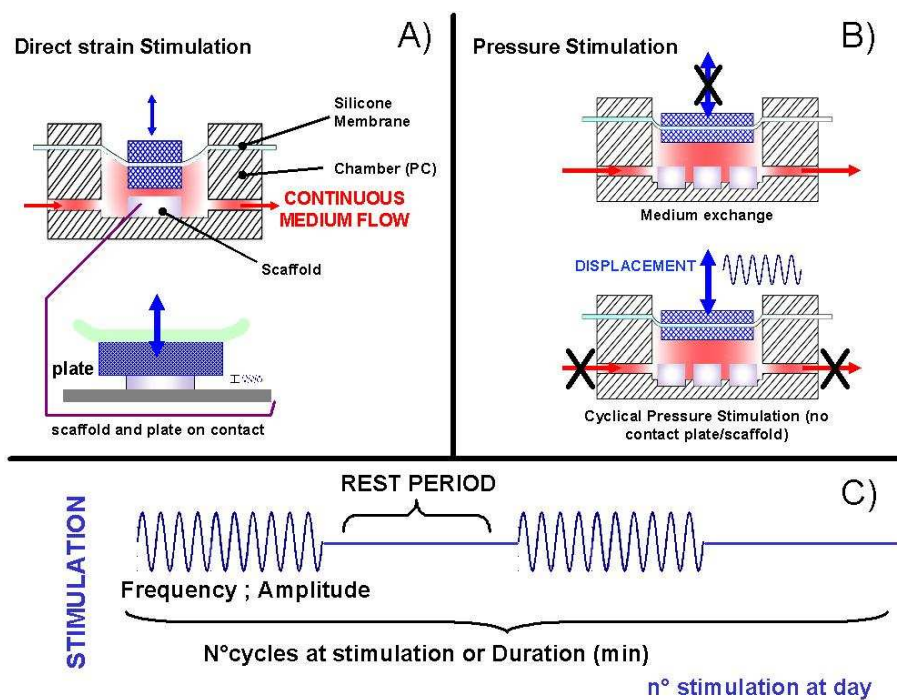


Fig.3.21. Working principles of stimulation in both the configurations, direct compression (A) and dynamic hydrostatic pressure (B) whereas, in the bottom (C) an example of a loading time.

The applicable compression load to stimulate the cell constructs can be modified from 0.05 N to 30 N and the pressure from about 0.1 kPa to 100

MATERIALS AND METHODS

kPa, with triangular or sinusoidal ramps from 0.001 Hz up to 2 Hz of frequency. Several type of stimulations describing the loading time can be imposed: the number of cycles, rest time between two consecutive groups of cycles, the number of groups for each stimulation, the rest period between two consecutive stimulations and the number of stimulations per day, as described by (1) and by figure 3.21 (c).

$$[(n^{\circ}cycles + Rest\ Period\ (s)) \cdot n^{\circ}group/stim + Rest\ between\ Stim\ (s)] \cdot n^{\circ}stim/day \quad (10)$$

The described setting was made possible by the software downloaded on the controller, which works on the motor using a PID feedback on the displacement, load and pressure signals, depending on the test. Furthermore, the software continuously monitors the working values, protecting the system and preserving the cell culture. Moreover, the device was also designed to mechanically test the samples during the cell culture or simply to characterize the material. In fact, mechanical parameters of the sample, such as loss factor, elastic and storage modulus, can be obtained and analysed, even during the cell culture, processing data in real-time, or performing specific tests on the final engineered construct. Thus, working as an universal test machine, it is possible to impose quasi static ramps with constant velocity, frequency tests DMA (dynamic mechanical analysis), relaxation (constant strain) and creep tests (constant stress).

Temperature, Humidity and CO₂ level settings

Temperature, humidity and CO₂ level were guaranteed and maintained constant thanks to the humidified incubator *NAPCO 6500* where the culture was carried out. In general, the incubator maintains constant the temperature at 37°C, the relative humidity at 95-98% with non condensing and the carbon oxide level at 5%. Four Pt100 sensors and a CO₂ sensor *GSS model C20-6* were used to measure locally temperature and CO₂ level, recording their trends and giving any possible warning during the cell culture. The peristaltic pump and the four stimulation units can easily enter inside a standard 170 L incubator.

3.2 Materials & Methods part 2: Scaffold characterization

3.2.1 Cartilage tissue engineering: Silk fibroin sponges

For cartilage tissue engineering it is essential the choice of the best combination between material and production technique to finally obtain a porous structure able to support the applied mechanical stresses and responding in a similar way to the physiological tissue. The porosity is essential to mimic the physiologic environment, where chondrocytes are embedded in a highly dense matrix and isolated in *lacunae*.

Silk fibroin was the chosen material, that is a natural polymer with good mechanical, cellular adhesion and activation properties and a degradation rate similar to the tissue regeneration one(*173-176*). Two different kinds of

MATERIALS AND METHODS

sponges were produced using this material, adding *polyethilen-glycol* (PEG) to the fibroin solution. This addition was necessary to stunt an excessive cellular spreading, favoured by silk fibroin but opposite to the physiologic distribution in the chondral tissue, where cells are roundish and isolate. PEG, indeed, is antiadhesive for cells(173), so limiting their activation. The protocol used for sponges preparation is the following.

Bombyx mori polyhybrid crossbred silkworms cocoons were bred and selected by Centro Sperimentale di Gelsibachicoltura, in Como, Italy. The cocoons were degummed to remove sericins by boiling twice at 98 °C, first in a 1.1 g/l of Na₂CO₃ in distilled water and then in 0.4 g/l of Na₂CO₃ in distilled water, for 1½ h respectively. The degummed silk was water-cooled from 80 °C to room temperature, then rinsed several times in distilled water and dried at room temperature. Degummed fibroin was then dissolved in LiBr 9.3 M solution at 65 °C for 2 h, to generate a 20% w/v solution, and subsequently dialyzed (cellulose membrane, Pierce 3500 Mw *Cut Off* cassettes) against distilled water for 4 days at room temperature. After desalination a second dialysis step against PEG (Mw=10000 Da, 25% w/v) was performed for 5 h, to obtain an aqueous fibroin solution of 7-8% concentration. This solution was finally filtered to eliminate any residual and pH and concentration values were checked. PEG (Mw=4000 Da) was added to the obtained solution to reach a 10% w_{PEG}/w_{fibroin} concentration and then the solution was mixed for 15 minutes. Starting from this solution, sponges were produced using two different techniques, freeze-drying and salt-leaching. The first type sponges were obtained pouring 3 mL of

MATERIALS AND METHODS

fibroin/PEG solution in a Petri plate of 3.5 mm in diameter. The plate was closed, freeze at -20 °C for 2 h and then lyophilized at -50 °C for 4 days. Sponges, soluble in water, were finally stabilized in a methanol/water (80:20 v/v) solution for 10 minutes and repeatedly rinsed to eliminate any residual solvent. For the salt-leached sponges preparation, a 2 mL fibroin/PEG solution was poured in a 3.5 mm diameter Petri plate and 4 g of NaCl, of controlled diameter dimension (500-1180 µm), were added as porogen agent. The plate was then closed and left at room temperature for 3 days, to allow fibroin gelification and the formation of a stable structure. Finally, the sponges were removed from the plate and washed in distilled water for several days to completely remove the salt.

3.2.2 Bone tissue engineering: P(d,l)LA sponges

For bone tissue regeneration, 3D spongy scaffolds were realized using a synthetic polymer, Poly(D-lactic acid). Polyesters are very interesting polymers because of their good mechanical properties, tailorability and controlled degradation rate(81, 82, 86, 94). Moreover, for a successful implant, the system itself and its degradation products must be biocompatible and not toxic. This phenomenon was studied for the PLA and its copolymers, and publications report good biocompatibility results, with only some few inflammatory responses(177). Among polyester family, Poly(D-lactic acid) is very interesting because it is soluble in many different solvents(178), it is easy to process in different 2D and 3D structures and, depending on the process story, it degrades in 2 to 12 months(179). For all

MATERIALS AND METHODS

these reasons P(d,l)LA was used to produce sponges, with a structure able to offer the possibility to cells to penetrate inside. Poly(D-lactic acid) (P(d,l)LA, type RESOMER[®] 207, MW= 252 kDa) was purchased from Boehringer Ingelheim, Germany. The polymer was used without further purification. Dichloromethane (DCM) and dimethylformamide (DMF) were obtained from BDH Chemicals (UK) and J.T.Baker (Holland), respectively. The porous, three dimensional scaffolds were prepared using a solvent cast-particulate leaching technique. The polymer was first dissolved in (70:30 v/v) dichloromethane/dimethylformamide solvent, obtaining a 13% w/v concentration. 15 mL of solution were poured into a glass Petri plate containing 20 g of NaCl salt of controlled diameter dimension (224-315 μm). The suspension was then dried under hood overnight and washed into distilled water for 3 days to eliminate both the residual solvent and the salt. The obtained sponges were finally air dried at room temperature.

3.2.3 Characterization techniques

Each scaffold was characterized in terms of mechanical properties (stiffness, storage modulus and loss factor) and porosity (pore size, interconnection and percentage).

3.2.3.1 Mechanical properties

The mechanical properties of the obtained sponges were measured by using a *Bose* universal testing machine model *ElectroForce3200*, equipped with a 225 N load cell. The compressive tests were performed on wet dishes 12

MATERIALS AND METHODS

mm in diameter and a variable height between 2 mm and 4 mm. Elastic moduli were calculated according to ASTM D 1621-04a, under displacement control in uniaxial ramp condition at a strain rate of 1.2 mm/min at room temperature (50% Relative Humidity). Scaffolds were preconditioned in PBS (Phosphate Buffered Saline) for 2 hours before being tested. To analyse scaffolds viscoelastic properties and behaviour under conditions as close as possible to dynamic culture ones, DMTA (Dynamic Mechanical Thermal Analysis) tests were carried out at 1 Hz, 64 μm as displacement at both 25°C and 37°C. Tests were performed using a *Polymer Laboratories* testing machine *model MK II*, while storage modulus and loss factor were calculated by the following equation (11).

$$\text{applying} \xrightarrow{\text{strain}} \left\{ \begin{array}{l} \varepsilon = \varepsilon_0 \sin(\omega t) \\ \sigma = \sigma_0 \sin(\omega t + \delta) \end{array} \right\} \xrightarrow{\frac{E = \text{stress}}{\text{strain}}} \begin{array}{l} \text{StorageModulus} \quad E_1 = \frac{\sigma_0}{\varepsilon_0} \cos \delta \\ \text{LossFactor} \quad \tan \delta = \frac{E_1}{E_2} \end{array} \quad (11)$$

where ε is the imposed sinusoidal strain at a ω frequency, σ is the measured stress response with a δ phase lag; while E_1 is the storage modulus, $\tan \delta$ is the loss factor and E_2 is the loss modulus proportional to E_1 and $\tan \delta$.

3.2.3.2 SEM and ESEM microscopy

Scanning electron microscopy (SEM *ZEISS Supra 40* – operating mode: high vacuum, secondary electron SE2 detector) was used for observations before and after cell culture, to obtain information both morphological, relating to pore size and interconnection, and biological. Biological samples were previously fixed by a glutaraldehyde solution (2.5% glutaraldehyde in

MATERIALS AND METHODS

cacodylic buffer solution 0.1 M, pH=7.2) for 30 minutes at 4 °C, to preserve the structure of living tissues. Once removed this solution, samples were washed 3 times with a second buffer fixative and then dehydrated by soaking in a series of aqueous ethanol solutions at increasing concentrations (30%, 50%, 70%, 90%, 100%, 100% v/v). Finally, the samples were dried at room temperature under hood. Before imaging, samples were sputter coated with a thin gold layer under argon atmosphere (20 mA at 5x10⁻⁷Pa for 30 sec) by using a sputter-coater (*SEM Coating Unit PS3, Assing S.p.A.*, Rome, Italy). Fibroin scaffolds were also examined by Environmental Scanning Electron Microscopy (*ESEM XL 30, Fei Company*), without performing the metal coating and working with a voltage between 9 and 12 kV.

3.2.3.3 Porosity evaluation

The scaffold porosity was quantitatively evaluated using the principle of liquid displacement. Considering Archimede's principle, the used liquid should be able to permeate the interconnected porosity without interacting or swelling the tested material. Hexane (n-Hexane, *Sigma-Aldrich*, US) was chosen for both fibroin and PDLA sponges. Scaffolds were dipped in a certain hexane V_1 volume in a graduate cylinder (± 0.02 mL) for 10 minutes. After immersion and absorption, the total volume V_2 was measured. Finally, the specimen was quickly removed, recording the residual hexane volume V_3 . The scaffold volume can be calculate subtracting volumes V_2 and V_3 , as follows:

$$V = (V_2 - V_1) + (V_1 - V_3) = V_2 - V_3 \quad (12)$$

MATERIALS AND METHODS

where (V_2-V_1) is the bulk structure volume, while (V_1-V_3) is the hexane volume retained in the scaffold open porosity. The porosity can be achieved starting from the following equation:

$$\mathcal{E}(\%) = \frac{V_1 - V_3}{V_2 - V_3} \cdot 100 \quad (13)$$

This ratio measures the percentage of the free volume on the total volume of the scaffold.

3.2.3.4 Statistical analysis

Porosity and mechanical properties were measured at least on three samples. All results were expressed as the mean \pm its standard deviation calculate using a statistical software (*KaleidaGraph Version 3.5b5*). Unpaired *t*-test was performed to compare the means of each result, previously verifying the equality of the obtained variances with an *F*-test. Significance level was assigned at p-values less than 0.05.

3.3 Materials & Methods part 3: *in vitro* Experiment

3.3.1 *in vitro* experiment description

3.3.1.1 Cartilage tissue engineering: validation experiment

A first preliminary experiment was conducted to validate the developed apparatus and a comparative study, combining static and dynamic cell cultures, using the commercial Rotatory Cell Culture System (*RCCS-4D*, *Cellon, Synthecon Inc.*), was performed.

The described apparatus was tested on fibroin/PEG sponges seeded with primary chondrocytes isolated from goat, 8th passage. After a previous 7 days long pre-static culture, the dynamic cell culture was carried out for other 7 days both under static and dynamic conditions (for both the bioreactors, the commercial and the house made). In the proposed bioreactor, stress and strain were continuously recorded, and the medium flow rate was maintained constant by a peristaltic pump at 0.1 mL/min. Cell culture tests were conducted imposing a sinusoidal compression at 25% strain (0.5 mm) amplitude was superimposed on 0.5 N load offset at 0.1 Hz of frequency. Periodic cycles of 2h-compression followed by 2h-unloaded culture were performed three times a day. The application of sinusoidal displacement resulted in oscillatory stresses on the scaffolds.

Cell adhesion and proliferation were evaluated by means of ESEM imaging, histological analyses and XTT assay, after both the seven days of pre-static (time zero *T0*) and the seven days of dynamic culture (time seven *T7*).

MATERIALS AND METHODS

Scaffolds were prepared from fibroin/PEG blends at 10% w/w of PEG content (PEG MW 4000Da) by both freeze-drying and salt-leaching methods (NaCl as porogen, crystal diameter 500-1180 μm). Three types of sponges were tested, freeze-dried fibroin, freeze-dried fibroin/PEG and salt-leached

fibroin/PEG. Scaffolds were sterilized with Ethanol 70% overnight at 4°C. Chondrocytes were seeded using 200 μL of cellular suspension at a concentration of $2 \cdot 10^5$ cells/mL. Dulbecco's Minimum essential medium 25% (DMEM), 25% HAM'S F12, 10% Fetal Bovine Serum (FBS), 1% Penicillin, 1% Glutamine, 1% Vitamine, 1% non-essential amino acids was used as culture medium composition. Cells were incubated at 37°C in a 5% CO_2 humidified incubator.

3.3.1.2 Cartilage tissue engineering: condition investigations

A second experiment was carried out to assess the effect of dynamic conditions on the seeded chondrocytes; the loading time was reduced to enhance the cellular activation. In fact, this experiment was intended to evaluate both dynamic and static cell cultures for the development of tissue engineered constructs after 14 days in terms of cellular activation and proliferation.

Salt-leached silk fibroin sponges were cultured using primary pig chondrocytes, 6th passage. After three days of static culture (time zero T_0), the experiments were carried out for 14 days both under dynamic and static conditions, analyzing the cultured constructs after seven days (T_7) and

MATERIALS AND METHODS

fourteen days (*T14*) of cell culture. Under dynamic conditions, a sinusoidal compression was imposed at 20% of strain amplitude (0.4 mm) at 0.1 Hz of frequency, superimposing a 0.5 N of load offset; while medium flow rate was maintained constant at 0.1 mL/min. Periodic cycles of 30 min of loaded culture were performed once a day. Cellular activity was evaluated by means of alamarBlue[®] assay, comparing static and dynamic cultures. The seeding parameters and medium composition were the same as described in the previous experiment.

3.3.1.3 Bone tissue engineering: validation experiment

To validate the apparatus, specifically developed for bone tissue engineering application, a preliminary experiment with human osteosarcoma derived osteoblasts (MG63) seeded on PDLA salt-leached sponges was conducted. The obtained results with this house-made device were compared to those obtained by a static culture control and by a dynamic culture carried out in the RCCS commercial rotative bioreactor, previously mentioned. Unloaded conditions were also tested. Dynamic conditions consisted in 30 min of 20% sinusoidal strain (0.4 mm) at 0.1 Hz a day. After three days of static culture (time *T0*), scaffolds were cultured seven days (*T7*) both under static and dynamic conditions. Confocal laser microscopy was used to evaluate cell morphology, distribution, migration and viability; while cell proliferation was assessed through alamarBlue[®] assay.

Salt-leached poly(D,L-lactic acid) (PDLA) porous scaffolds were prepared as previously described. After sterilization with ethanol 70%, scaffolds were

MATERIALS AND METHODS

placed in 48-well plates, washed several times with sterile distilled water and then cultured. MG63 cells were seeded on scaffolds and, considering the scaffold dimensions, the high tendency of cancer cells to grow faster and after previous experimental tests (not reported), a seeding concentration of $5 \cdot 10^4$ cell per sample was chosen. A drop of 100 μ L of cell suspension was put on every sample and left in incubator for 1h; new fresh medium was finally added. All the seeded samples were left for 3 days under static cell culture conditions and subsequently, the samples aimed at the dynamic culture were transferred to the bioreactor chambers. Minimum essential medium (MEM) supplemented with 10% Fetal Bovine Serum (FBS), 1% Penicillin, 1% Glutamine, 1% Vitamine, 1% non-essential amino acids was used as culture medium. Cells were incubated at 37°C in a 5% CO₂ atmosphere incubator.

3.3.1.4 Bone tissue engineering: dynamic hydrostatic pressure, condition investigations

Mechanical stimulation of scaffolds via hydrostatic compression was performed by the developed and produced bioreactor (section 3.1). The biological evaluation was carried out using MG63 cell line using a parallel static culture as control. Visual inspection of cell proliferation and adhesion was performed using confocal laser microscopy after staining cell nuclei and cytoskeleton, while cell viability was evaluated through alamarBlue[®] assay. Cellular metabolism activation and ECM synthesis were also

MATERIALS AND METHODS

characterized in terms of Collagen Type I and ALP gene expression by RT-PCR, while cell morphology was assessed through SEM imaging.

The HPC bioreactor was designed to apply mechanical stimuli to cell constructs. Samples were completely immersed in a sterile chamber, sealed from the external environment. The diffusion of medium and nutrients was guaranteed by a peristaltic pump (0.05 mL/min). Mechanical stresses were applied using an electric motor with displacement control at micrometer precision. Stress were transferred inside the chamber through an elastic membrane, and resulted in a pressure change. The software was designed to control pressure change using a pressure sensor as feedback.

The following conditions were tested for a two week long experiment, applying a sinusoidal wave with the amplitude from 0 to 10 kPa and 20 kPa at 1 Hz and 0.3 Hz. The daily loading stimulation was built with 10 cycles followed by a rest period of 10 s, repeated consecutively for a total amount of 1800 cycles. Two different blank conditions were also analyzed to achieve information about each individual dynamic parameter separately. Cell culture with no stimulation but only medium diffusion was carried out as well as cell culture with stimulation (20 kPa at 1 Hz) but without medium diffusion (changing manually the medium every three days).

After three days of static culture, scaffolds were biologically characterized after 7 days (time *T7*) and after fourteen days (*T14*) of static culture. Scaffold material, preparation and sterilization, cell type, cell seeding method and medium composition were unmodified compared to the experiment described in section 3.3.1.3.

3.3.1.5 Bone tissue engineering: dynamic hydrostatic pressure, long experiment

The influence of dynamic stimuli (dynamic hydrostatic pressure) on PDLLA salt leached sponges seeded with human osteosarcoma derived osteoblasts cell line MG63, over a cell culture period of 28 days was evaluated.

The study aimed to comprehend the effectiveness of dynamic cell culture conditions compared to the standard static ones, in terms of cells proliferation and activity. For this reason, in addition to the normal cell growing and proliferation tests (i.e. calcein confocal analysis and alamarBlue[®] assay) cell activity by expression analysis (RT-PCR) of bone and extracellular matrix-related genes was performed.

The best dynamic conditions, found in the previously described experiment (paragraph 3.3.1.4), were chosen to carry out a 28 day-long test, maintaining the same cell culture conditions. As the previous preliminary experiment (paragraph 3.3.1.4) a 3 days long pre-static culture (*T0*) was chosen, followed by other 5 time points at three (*T3*), seven (*T7*), fourteen (*T14*), twenty-one (*T21*) and twenty-eight (*T28*) days.

3.3.2 Biological evaluation Techniques

The biological evaluation techniques, carried out to characterize the experiments previously described, are following reported.

3.3.2.1 XTT proliferation test

Chondrocyte proliferation on fibroin scaffolds was evaluated by XTT Cell Proliferation Assay (TACSr). XTT technique makes use of tetrazolium salt to obtain information relating to live and active cell concentration in the samples. The involved molecules are reduced by the enzymes belonged to the transport chain of electrons, essential in cell breathing and acting in the mitochondrion of active cells. As a consequence of the XTT reduction, a water-soluble dye absorbing in the orange zone of the visible spectrum is formed. Therefore, when a sample is incubated in culture medium containing the tetrazolium salt, a quantity of dye proportional to live cells is produced. The amount of reagent can be quantified measuring the absorbance of the medium at a specific wave length (450 nm or 492 nm) and it is compared to a reference wave length (620 nm). The XTT Working Solution was prepared mixing 5 mL of XTT activator with 100 μ L of XTT Reagent, protecting from light. Then, the culture medium was removed from the wells and the samples were washed with D-PBS, to remove medium in excess. 150 μ L of medium without red phenol, RPMI, and 50 μ L of Working Solution were add to each well. The well plate was incubated at 37 °C for 6 hours, after which the medium absorbance was measured at 3 different wave lengths (450, 492 and 620 nm) using the microplate *Multiskan EX (Thermo Scientific)*.

MATERIALS AND METHODS

3.3.2.2 Histology

The histological analysis of fibroion/PEG sponges was performed in collaboration with the Pathological Anatomy ward of *S. Chiara* hospital, Trento. At the end of each experimental time, the samples were transferred in a 48 well plate and washed with 1 mL of D-PBS (Dulbecco's modified PBS). Once removed the saline solution, sponges were fixed by 1 mL of 10% buffered formaldehyde. After that, the samples were mounted in paraffin, stained with hematoxylin-eosin and observed with the optical microscope to verify the cell distribution.

3.3.2.3 ESEM & SEM microscopy

Cell behaviour on the samples was examined using both ESEM and SEM apparatus. The procedure and parameters used for biological evaluation follow the same guidelines previously explained in paragraph 3.2.3.2 concerning the scaffold characterization.

3.3.2.4 Confocal laser microscopy (CLM)

Qualitative cell attachment and growth behaviour that is their distribution and migration inside the seeded scaffolds were assessed by confocal laser microscopy (CLM) (*Nikon Eclipse, Ti-E*, Japan) after Phalloidin Rhodamine (PR, Biosource International, Invitrogen) and DAPI (Sigma Aldrich) staining, according to the manufacturers' protocol (Molecular Probes Inc., Oregon, USA). Fixation with a formaldehyde solution (4% formaldehyde in PBS solution) and permeabilization with TritonX (0.2% TritonX in PBS

MATERIALS AND METHODS

solution) were performed before staining the cultured samples. Then, scaffolds were incubated at room temperature for 40 min in RP solution and after for 10 min in DAPI solution, washing the samples three times with PBS after each step.

Cell viability were both examined by alamarBlue[®] and confocal laser microscopy. Considering the latter, qualitative cell viability was further assessed staining the scaffolds with fluorescein diacetate–propidium iodide (FDA–PI) (Molecular Probes Inc., Oregon, USA).

Following the manufacturers' protocol (Molecular Probes Inc., Oregon, USA – Product codes: F1303 and P1304MP respectively), the scaffolds were incubated for 15 min at 37°C in FDA solution and then 2min at room temperature in PI solution, again washing the samples three times with PBS after each step. FDA colours viable cells in green, while PI stains necrotic and secondary apoptotic cells in red.

An alternative method is the calcein. Calcein AM (Biosource International, Invitrogen) is a cell dye that can be used to determine cell viability since the fluorescence intensity of calcein is proportional to the amount of live cells. The nonfluorescent calcein AM, in live cells, is converted to the strongly green fluorescent calcein, when hydrolyzed by intracellular esterases. At specific time points, the 1 µg/ml calcein solution was added to the seeded scaffolds, then incubated at 37°C for 15 minutes. Confocal laser microscopy was subsequently used to excite the dye by a 488 laser wavelength, resulting the live cells in a green color.

MATERIALS AND METHODS

3.3.2.5 alamarBlue[®] Assay

Cells metabolic activity and viability during biological cultures were monitored using the alamarBlue[®] assay (Biosource International Inc., USA), a colorimetric growth indicator based on cellular reducing conditions. The feature of this analysis is that it is not toxic for cells, so it can be used several times on the same samples during a cell culture.

The natural reducing power of living cells is the principle this method is based on to measure cells proliferation. Resazurin, the active constituent of alamarBlue[®] reagent, is a nontoxic, cell permeable compound, dark blue in colour when oxidize and non-fluorescent. Since live cells maintain a reducing environment within their cytosol, once entered in the cells, resazurin is reduced to resorufin, highly red fluorescent. Viable cells continuously convert resazurin in resofurin, varying the optical absorbance of media surrounding cells and so generating a chromatic measure of their viability and proliferation.

During the various experiments the alamarBlue[®] assay was performed according to manufacturer's instructions. Samples, placed in well plates, were seeded with cells and incubated. After proper culturing time points, it was added 10% ready-to-use solution to fresh culture medium, obtaining the so called "alamarMix". This solution was put on the cultured samples in place of the culture medium and a 4 hours incubation at 37°C, protecting from light, followed. This process did not compromise cell health. A total of 3 replicates were used for each sample and each replicate was split into 4 other samples in the final reading. The blank reference was taken from

MATERIALS AND METHODS

unseeded scaffold with the “alamarMix” solution. Finally, other empty wells were filled with only medium. After the incubation period, from each well 4*100 μ l of solution were taken and put in a 96 well plate for the absorbance reading. The resulting absorbance of reduced alamarBlue[®] reagent was read on a spectrophotometer, at 570 nm and 620 nm wave length by the microplate *Multiskan EX (Thermo Scientific)*.

Once extracting the quantities needed for the evaluation, the samples were washed with sterile PBS to remove any “alamarMix” residual and fresh culture medium was then added allowing the cells culture incubation till the successive time point. The absorbance intensity values were analyzed using the following formula (eq. 14):

$$\% reduced = [A_{LW} - (A_{HW} \cdot R_0)] \cdot 100 \quad (14)$$

where A_{LW} and A_{HW} indicate the mean value of absorbance read at 570 nm and 620 nm respectively, while R_0 is a correction factor gives by equation 15:

$$R_0 = \frac{AO_{LW}}{AO_{HW}} \quad (15)$$

which represents the ratio between oxidized alamarBlue[®] at 570 nm (AO_{LW}) and at 620 nm (AO_{HW}), respectively. The oxidized values were obtain subtracting the absorbance of medium from the one of “alamarMix” plus samples. The percentage of reduced alamarBlue[®] error is calculated as follows (eq. 16-17):

MATERIALS AND METHODS

$$Error \text{ (\% Reduced)} = \left[\sigma(A_{LW}) + \left(\frac{\sigma(A_{HW})}{A_{HW}} + \frac{Err(R_0)}{R_0} \right) \cdot A_{HW} \cdot R_0 \right] \cdot 100 \quad (16)$$

$$\text{in which} \quad Err(R_0) = \left(\frac{\sigma(AO_{LW})}{AO_{LW}} + \frac{\sigma(AO_{HW})}{AO_{HW}} \right) \cdot R_0 \quad (17)$$

where $\sigma(x)$ indicates the standard deviation of the variable x . The relative significance level was calculated by unpair t -test using $p < 0.05$, comparing each obtained mean and verifying the equality of variances.

3.3.2.6 Real time-polymerase chain reaction (RT-PCR)

Real-time RT-PCR is a highly sensitive tool for measuring small changes in cellular gene expression and has quickly become the technique of choice to analyze cellular mRNA from various sources. While demonstrating itself as a reliable and accurate method to measure cellular mRNA levels, it also is relatively easy to perform making it an encouraging technique to employ for rapid quantification results(180).

Looking at the progressive development of the osteoblast phenotype, several genes were evaluated in our study related to key cellular events such as proliferation, matrix formation and mineralization. A summary of the genes investigated as well as associated primer sequences are outlined in table 3.4. Each gene was related to a particular stage of the differentiation of the osteoblasts towards the bone tissue formation. Briefly, TGF-B1 was monitored for cell proliferation, Collagen 1 and alkaline phosphatase (ALP) for matrix formation, Osteocalcin (OCN), Osteopontin (OPN) and decorin

MATERIALS AND METHODS

(DCN) for matrix maturity and lastly RUNX2-3 to monitor commitment to the osteoblast lineage.

At different time points (3, 7, 14, 21, and 28 days), static and dynamic culture specimens were quenched in liquid nitrogen and preserved in -80 °C prior to RNA extraction. Following this procedure, total RNA was extracted from cells and the DNA was digested using an RNeasy Mini Kit. In brief, the cells from the scaffolds were lysed with supplied buffer (Qiagen, Hilden, Germany), the lysate was homogenized and ethanol was added before transfer to an RNeasy spin column. The final elute was stored at -80 °C. The integrity of the RNA was proven and documented with Nanodrop®.

According to its availability in each experimental time, a different RNA amount of every sample were reverse transcribed into cDNA Thermoscript (Invitrogen). PCR was performed in a *Rotor Gene 6000* (Corbett Research) in a 77 plate. A 20 µL volume with SYBR Green Mastermix (Kapa Biosystem), cDNA and the primer pairs was used. Primer sequences of selected genes were designed utilizing online software “Universal Probe Library” (<http://qpcr.probefinder.com/organism.jsp>) available from Roche Industries and presented in table 3.4. Target genes were run in triplicate. Light cycling conditions were as follows: activation (95 °C for 2 min), 40 amplification cycles (95 °C for 10 s, 60 °C for 15 s, and 72 °C for 20 s). PCR conditions were optimized for all genes to achieve a PCR efficiency of 2. Melting curve analysis was done to ensure that all transcripts under investigation were represented by a single peak, indicating specificity.

MATERIALS AND METHODS

Gene	Forward Primer	Backward Primer
Housekeeping		
GADPH	agccacatcgctcagacac	gcccaataaccgaaatcc
Proliferation		
TGFB1	gcagcacgtggagctgta	cagccggttgctgaggta
Type I Collagen	caagagtggatcgtggtg	gcctgtctacccttgca
ALP	ccatcctgtatggcaatgg	cgcttgtagttgttgag
ECM Maturation		
Osteopontin (OPN)	gagggcttggttcagc	caattctcatgtagtgagtttcc
Osteocalcin (OCN)	tgagagccctcacactcctc	accttgctggactctgcac
ECM Mineralization		
RUNX2	caccatgtcagcaaaactctt	tcacgtcgctcatttgc
RUNX3	tcagcaccacaagccactt	aatgggttcagttccgaggt
Decorin (DCN)	ggagactttaagaacctgaagaacc	cgtccaacttcaccaaagg

Table 3.4. Select Genes & Associated Primers utilized for RT-PCR

Gene expression was calculated from the PCR efficiency (*181*) and normalized to both a housekeeping gene (GAPDH) and an untreated control sample (culture time = 0). Statistical evaluation of samples was performed using an unpaired t-test of sample specimens versus controls. Values were considered significantly different if $p < 0.05$.

4. RESULTS AND DISCUSSIONS

4.1 Results & Discussions Part1: Device Development

Tissue engineering takes advantage of life science to produce biological substitutes, in which the obtained cellular constructs will be used to repair or regenerate the damaged tissues. Therefore, the final product, after cell culture, must exhibit the proper geometrical dimensions, structure and chemistry as close as possible to the original tissue. For this reason, 3D structures named scaffolds usually biodegradable and bioabsorbable, from synthetic or natural origin polymers, with specific chemistry and interaction properties, are widely used for tissue regeneration.

In this proposal a bioreactor has been designed, in which optimal culture conditions such as temperature, nutrients and carbon dioxide level are controlled and mechanical stimuli are applied on the cell constructs. The results of these stimuli must induce the proper activations of cells, naturally accustomed to similar stresses in the joint. The goal of this bioreactor is to reproduce as close as possible the mechanical and biochemical conditions of the physiological environment. The proposed system is designed to work in a completely autonomous way, providing the control of several parameters, even remotely via web.

RESULTS AND DISCUSSIONS

The device was designed to stimulate cell constructs with different types of mechanical stimulation, direct compression and hydrostatic pressure with different loading time regimes. The stimulation ranges include typical values found in literature, the possibility of applying cyclical deformation (10 mm as maximum stroke) with loads up to 30 N (depending on the material response), with frequency from 0.001 Hz to 2 Hz and finally hydrostatic pressure from 0.1 kPa to 100 kPa.

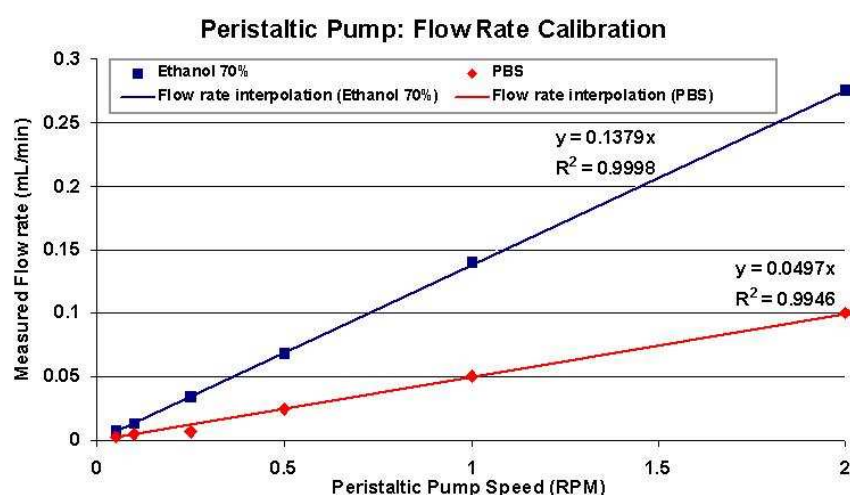


Fig.4.1. Peristaltic pump calibrations

A peculiarity of the proposed system includes the ability of applying two different types of mechanical stimuli, such as direct compression and cyclical hydrodynamic pressure. For this reason, a silicone membrane was introduced as a flexible element of connection between the sterile environment and the mechanical components for stress application, which makes the culture chamber effectively separated and manageable

RESULTS AND DISCUSSIONS

individually, sterilizable and autoclavable, while providing a large gas exchange area close to the cell culture. The system provides a continuous medium flow through a peristaltic pump and finally the ability to set automatically all the timing parameters of stimulation by a dedicated software, such as the number of cycles, the number of repetitions, eventually the rest periods, offering a wide range of biomechanical stresses. To prove the apparatus efficiency, several calibration tests were carried out and reported as follows.

4.1.1 Peristaltic Pump Calibrations

Ad hoc calibration curves were performed testing aqueous solutions. Precisely, ethanol 70% was chosen due to its use as sterilizing liquid, while PBS buffer fluid dynamic behaviour can be assumed similar to culture medium. Culture medium was not tested due to its expensive cost and considering how medium must be used in sterile conditions (biohazard) to avoid bacteria proliferation. The inner tube diameter was maintained constant at 1.6 mm. Data were obtained imposing a constant rotational speed and recording the reached volume after 1 hour. Only flow rates less than 0.1 mL/min were investigated, which corresponds to the range useful for bone and cartilage tissue engineering(68, 145, 146). Figure 4.1 shows the obtained curves in which the measured flow rate [mL/min] is reported as function of rotational speed [rpm]. As expected, ethanol solution flow rate is higher at every rotational speed. In fact, ethanol surface tension ($\sim 22 \text{ mJ/m}^2$) is less than PBS buffer ($\sim 70 \text{ mJ/m}^2$), which can be considered a water-based salt solution. The trends can be well approximated using linear regression,

RESULTS AND DISCUSSIONS

making easier the flow rate calculation, approximating medium flow [mL/min] to $0.0459 [RPM]$.

4.1.2 Pressure Gauge Calibrations

Calibration curves were also carried out to achieve the scaling factor for pressure sensors. In figure 4.2, the trend obtained in the first culture chamber after three repetitions is plotted, showing a good linear interpolation ($R^2 > 0.9998$) with relatively low errors in terms of output signals.

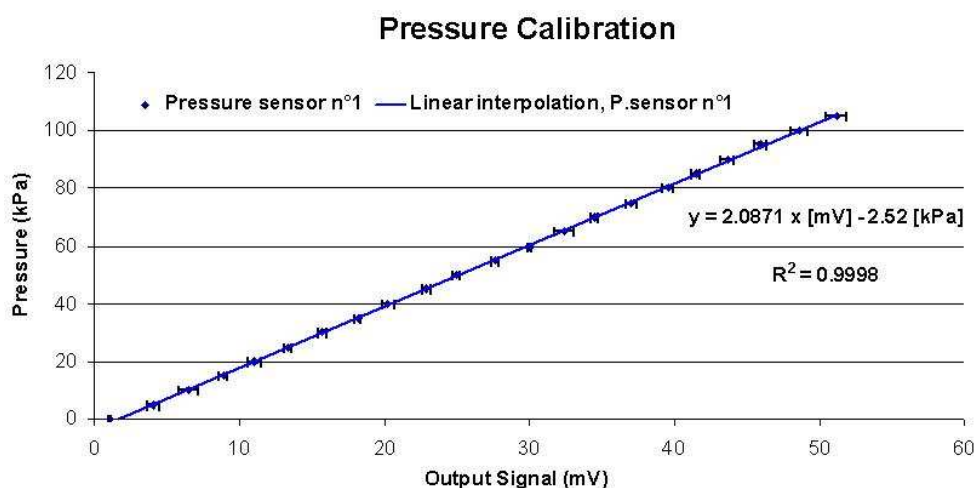


Fig.4.2. Pressure gauge n°1 calibration curve.

Chamber	Scale factor [kPa/mV]	Bias [kPa]	R^2	Max. error [mV]	Max. error [kPa]
1	2.08710	2.52	0.9998	0.309	0.65
2	2.09078	2.334	0.9999	0.175	0.37
3	2.09230	2.53	0.9998	0.212	0.44
4	2.09932	1.73	0.9999	0.132	0.28
	2.07031	0.00	Theoretical values		

Tab.4.1. Pressure sensors, calibration parameters.

RESULTS AND DISCUSSIONS

The maximum measured error is less than 0.7 kPa, as reported in table 4.1. Table 4.1 also shows the calibration parameters calculated for each culture chamber. Each sensor recorded a little pressure bias, probably due to electrical resistance introduced during the device installation (i.e. wire welding). Sensors exhibit good linear output signals, as expected in the measuring range. Considering 100 mV as full scale (200 kPa), the difference between theoretical and measured scaling factor leads to a maximum error of 2.9 kPa at full scale (1.5% relative error).

4.1.3 Load Cell Calibrations

Laboratory standard weights was used to calibrate load cell sensors, recording the measured output signals in a triplicate. Calibration curve for the first load cell is reported in figure 4.3, while the error bar for each measured point is too small to be displayed. In fact, the obtained maximum error for each sensor is less than 0.3 mV (0.65 N), as shown in table 4.2. As expected, the achieved calibration curves exhibit a good linear trend ($R^2 > 0.9998$) in the measured load range (from 0.0 N to 15.0 N). Table 4.2 also reports calibration parameters for all the load cell sensors. The registered gauge factors differ from the ideal one for a maximum of 0.08 N, as calculated by equation 18, which also shows the ideal scale factor conversion.

$$idealGaugeFactor \quad S\left[\frac{N}{mV}\right] = \left(\frac{2mV}{V_{FS}} \cdot \left|\frac{8.32mV}{30N}\right|_{FS}\right)^{-1} = 1.8028 \frac{N}{mV} \quad (18)$$

$$MaximumDeviation = (S_{MEAS.}^{4th} - S_{ideal}) \cdot V_{FS} = (1.7932 - 1.8028) \cdot 8.32 = 0.08N$$

RESULTS AND DISCUSSIONS

where S is the scale factor, S_{ideal} the theoretical value and S^{4th}_{MEAS} the scale factor for the fourth load cell sensor. A little load bias is also reported, but this effect does not cause any problem since a weight tare is performed before the experiment.

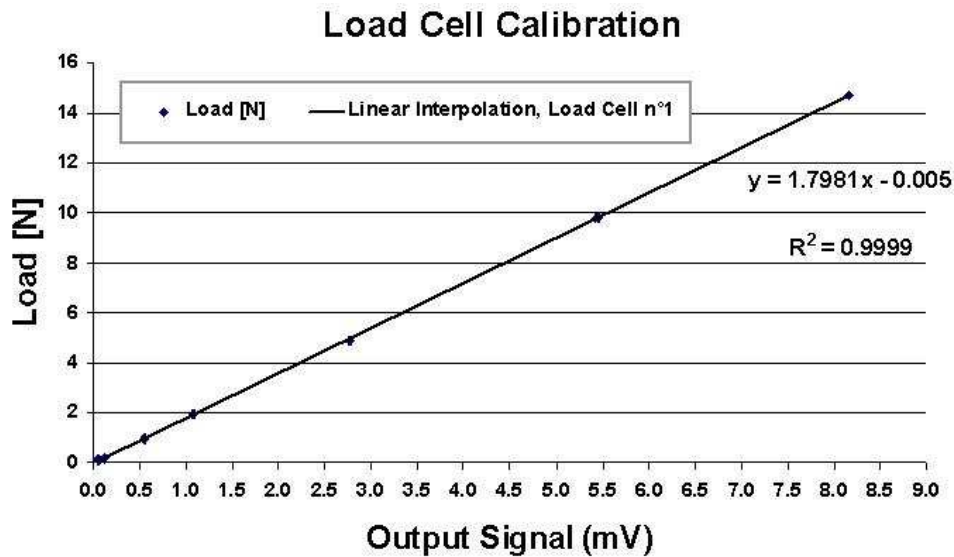


Fig.4.3. Load cell n°1 calibration curve.

Chamber	Scale factor [N/mV]	Bias [N]	R^2	Max. error [mV]	Max. error [N]
1	1.7981	0.005	0.9998	0.309	0.65
2	1.7976	0.002	0.9999	0.175	0.37
3	1.8057	0.006	0.9998	0.212	0.44
4	1.7932	0.003	0.9999	0.132	0.28
	1.8028	0.00	Theoretical values		

Tab.4.2. Load cell sensors, calibration parameters.

RESULTS AND DISCUSSIONS

4.1.4 Motor Calibrations

Motor calibrations were also performed, representing the measured speed on the applied duty cycle. Several imposed duty cycles were analyzed, repeating three times the measures. Concerning the first motor, data are plotted in figure 4.4 in which a good linear trend is obtained ($R^2 > 0.9999$). Also in this case, figure 4.4 does not display error bars due to their small size, making useless their view. In fact, the maximum recorded error was only 6 $\mu\text{m/s}$. In table 4.3, the calibration parameters of each motor are reported, in which the coefficients " m " and " q " correspond to the obtained linear equation, as shown by the report 19:

$$\text{Velocity}\left[\frac{\text{mm}}{\text{s}}\right] = m \cdot \text{Duty}[\%] - q \quad (19)$$

Table 4.3 also shows a maximum motor speed of about 1.46 mm/s. However, it is important to underline how, even if the calculated duty cycle at zero velocity is relatively low (about 5%), motor shaft does not move for duty cycle less than 10%, leading to a real minimum motor speed of about 0.065 mm/s for each motor. This effect is probably attributable to internal friction. The programmed software takes into account the tabulated parameters, also ensuring a motor speed of 0.001 mm/s working as a stepper motor. In fact, considering motor speeds less than 0.07 mm/s, the trajectory will be covered using discontinuous small steps, 0.5 μm . On the basis of the maximum measured speed rate, figure 4.5 shows the region (gray) of the applicable sinusoidal dynamics, plotting the maximum reachable

RESULTS AND DISCUSSIONS

displacement as a function of the frequency. The graph was derived from equation 20.

$$\begin{aligned} \text{Trajectory } s(t) &= \frac{MaxDispl}{2} \cdot \sin(2\pi \cdot \nu \cdot t) \\ \text{Speed } v(t) &= -2\pi \cdot \nu \cdot \frac{MaxDispl}{2} \cdot \cos(2\pi \cdot \nu \cdot t) \end{aligned} \quad (20)$$

$$\text{MaxSpeed } v_{MAX} = \pi \cdot \nu \cdot MaxDispl \rightarrow MaxDispl = \frac{v_{MAX}}{\pi \cdot \nu} = \frac{0.465}{\nu}$$

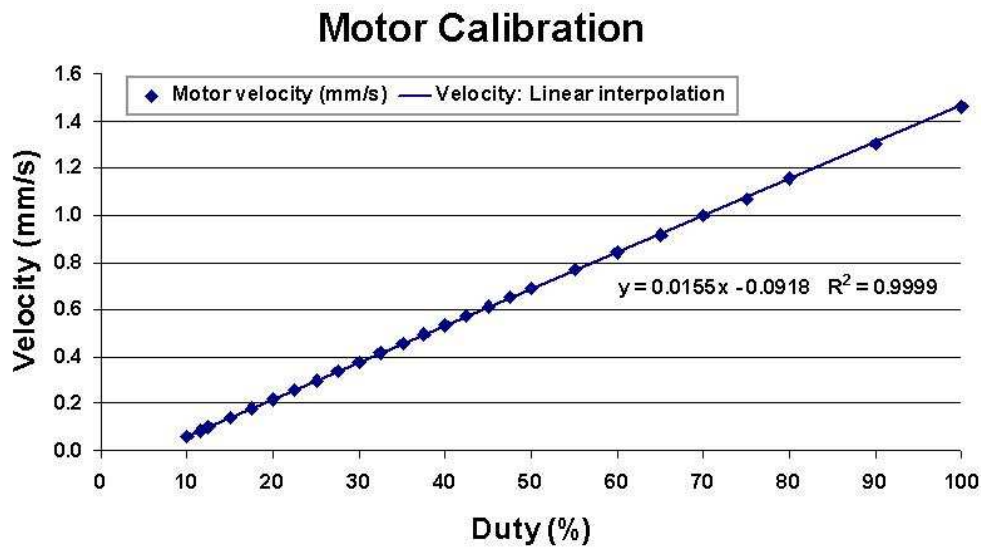


Fig.4.4. Motor n°1 calibration curve.

Motor	m [vel/Duty(%)]	q [vel.mm/s]	R ²	Max. Vel. [mm/s]	Min. Duty [%]
1	0.015548	0.0918	0.9999	1.4595	5.905
2	0.015421	0.0899	0.9999	1.4522	5.830
3	0.015592	0.0954	0.9999	1.4638	6.120
4	0.015498	0.0928	0.9999	1.4570	5.990

Tab.4.3. Motor calibration parameters.

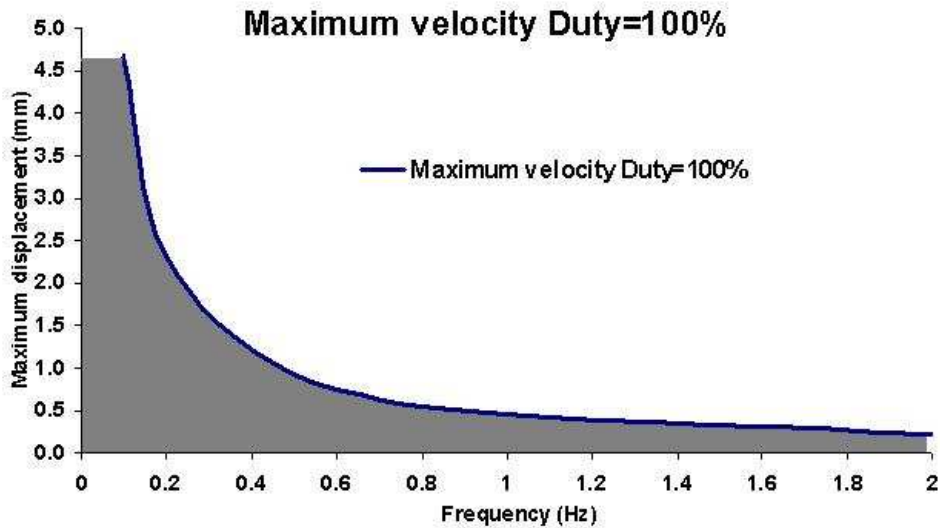


Fig.4.5. Motor applicable sinusoidal dynamics.

4.1.5 Device testing

Figure 4.6 shows some recorded sinusoidal trajectories of displacement, pressure and load. Considering five measures, errors were calculated as the difference between the data and the ideal trajectory: (A) 200 μm in displacement at 0.1 Hz with an error of $\pm 0.2 \mu\text{m}$, (B) 400 μm in displacement at 1 Hz with an error of $\pm 2.5 \mu\text{m}$, (C) 20 kPa in pressure at 1 Hz with an error of $\pm 0.35 \text{ kPa}$, and finally (D) 1.9 N of measured load at 1 Hz with an error of $\pm 0.05 \text{ N}$ (figure 4.6). The graphs show smooth trends without sharp peaks. The obtained profiles were well approximated by sinusoidal trajectories, while maintaining in both cases a relatively low error (less than 2.5%). At low frequencies, the measured error was ten times less than 1 Hz. This is probably due to the system dynamics in which motor maximum speed was nearly reached. For pressure and load cases, the

RESULTS AND DISCUSSIONS

recorded errors were comparable to the sensor sensitivities. Therefore, the device appears to respond adequately, providing a correct positioning. Thus, the right stimulation path can be either imposed or achieved as a feedback. Sinusoidal stimuli were proposed due to their wide use as helpful stimuli in a cell culture or during a mechanical analysis. Sinusoidal curves can be also easily processed giving a representative overview of the system potentialities.

As described, the proposed system presents all the characteristics derived from the bioreactor definition, while maintaining a good flexibility which is mostly guaranteed by the silicone membrane. The device components can be separated to each other. In this way, a custom culture chamber can be easily designed, according to the experiment requirements. The high versatility also allows to carry out the scaffold seeding directly in the culture chamber. After positioning, scaffolds can be seeded, covered with medium and placed in the incubator. Finally, a correct mass transfer can be achieved through a peristaltic pump, allowing nutrient exchange and waste removal, but avoiding a turbulent flow within the culture. For this reason, the culture chambers were characterized by a quasi-laminar flow with adjustable speed and by a mass transfer range of 0.0005-5 mL/min. Therefore, this bioreactor can combine cyclic compression and hydrostatic pressure, carrying out up to four conditions simultaneously in four single stimulation units controlled by a single controller, while maintaining optimal culture conditions. The system, completely autonomous and manageable over the network, seems to offer good benefits for bone and cartilage tissues regeneration.

RESULTS AND DISCUSSIONS

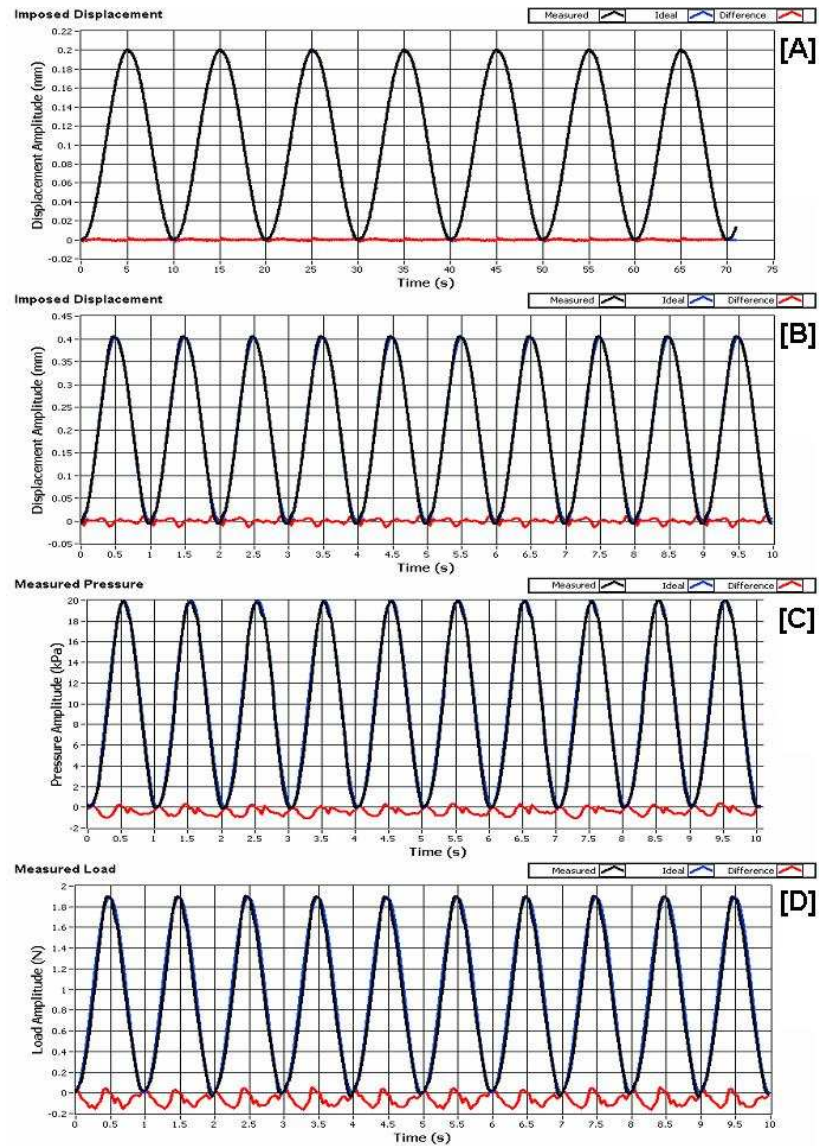


Fig.4.6. The measured displacement, pressure and load are plotted in black, the ideal trajectory in blue, while the differences in red: (A) 200 μm in displacement at 0.1 Hz with an error of $\pm 0.2 \mu\text{m}$, (B) 400 μm in displacement at 1 Hz with an error of $\pm 2.5 \mu\text{m}$, (C) 20 kPa in pressure at 1 Hz with an error of $\pm 0.35 \text{ kPa}$, and finally (D) 1.9 N of measured load at 1 Hz with an error of $\pm 0.05 \text{ N}$.

RESULTS AND DISCUSSIONS

Moreover, the bioreactor can be used to mechanically characterize the obtained constructs both during and after cell culture, providing a wide range of possible tests. In particular, DMA is used to calculate storage modulus and loss factor, quasi-static ramp to measure the elastic modulus in compression and, finally, relaxation-creep test to obtain the viscoelastic properties of the material.

4.2 Results & Discussions part 2: Scaffold characterization

4.2.1 Silk fibroin and PDLA sponges

In this work, silk fibroin and PDLA sponges were used as scaffolding supports for cartilage and bone tissue regeneration applications and their characterization is presented. The different silk fibroin samples are named by a code, depending on the preparation procedure, as follows:

- SpFCP10: freeze-dried silk fibroin sponges, where C is the fibroin concentration and 10 the ratio $w_{\text{PEG}}/w_{\text{fibroin}}$ that is the PEG content;
- SpNaClFCP10: salt-leached silk fibroin sponges, with C fibroin concentration and 10 the ratio $w_{\text{PEG}}/w_{\text{fibroin}}$ that is the PEG content;
- SpFC and SpNaClFC: freeze-dried and salt-leached sponges, respectively, obtained by a C fibroin concentration.

RESULTS AND DISCUSSIONS

4.2.2 Electron Microscopy characterization

Fibroin and fibroin/PEG scaffolds

In this section, ESEM and SEM images of fibroin and fibroin/PEG sponges produced for cartilage tissue engineering are reported and analyzed. Sponges were observed to evaluate pore shape and size, and their possible interconnectivity.

The advantage given by environmental scanning electron microscopy (ESEM) is the possibility to observe wet samples with a relative humidity in the chamber holder up to 100%, under similar conditions to those of their use. The produced fibroin and fibroin/PEG sponges differ, even macroscopically, from dry to wet conditions. For this reason, the morphologies of fibroin and fibroin/PEG scaffolds, produced by both freeze-drying and salt-leaching techniques, were evaluated under wet conditions, which are similar to the cell culture environment. Thus, fibroin and fibroin/PEG scaffold structures were observed by ESEM, to achieve information on the influence of PEG on the obtained sponge morphology.

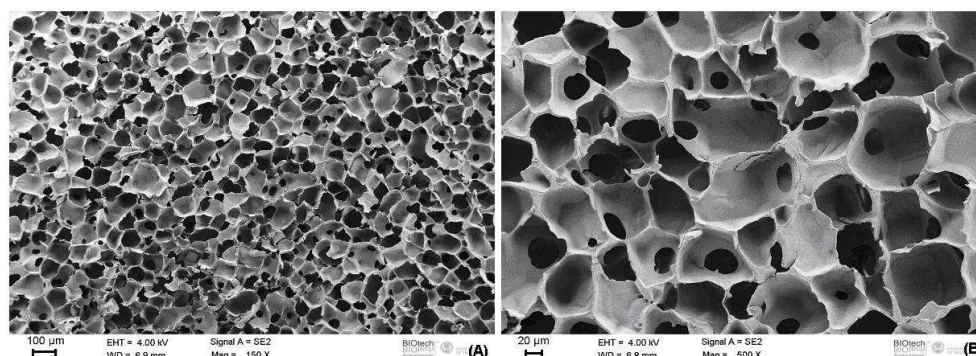


Fig. 4.7. SEM images of freeze-dried fibroin sponges (SpF8). Images show the characteristic high porosity of the structure (A) and the limited interconnection between pores (B). Different magnification are shown.

RESULTS AND DISCUSSIONS

Moreover, SEM observations of the fibroin scaffolds produced by freeze-drying are presented in figure 4.7. Porosity appears very high, round shaped and with well-defined regular pores. Pore size results to be widely distributed about 20 and 140 μm . However, interconnections cannot be assessed accurately, which anyway does not appear very marked. The limited interconnection could be a problem during the *in vitro* cell culture, hindering cell migration within the scaffold. In both cases, the porosity of fibroin and fibroin/PEG freeze-dried sponges appears higher (between 50 and 200 μm) if measured by ESEM compared to SEM, and this is probably due to the swelling effect, in fact water acts as a plasticizer by partially dilating the pores. In addition, a further microporosity is shown on the fibroin/PEG sponge walls (figure 4.8), probably due to the PEG removal during washing.

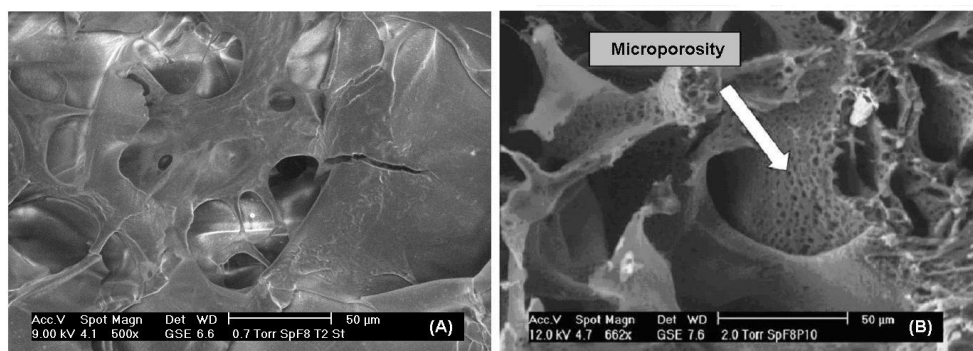


Fig. 4.8. ESEM image of SpF8 (A) and SpF8P10 (B) sponges with 40% RH. Images were acquired during sample drying occurring inside the chamber holder. The PEG/fibroin scaffold wall surfaces exhibit visible micropores with a diameter of few microns (B).

RESULTS AND DISCUSSIONS

This is also confirmed by IR (InfraRed) spectroscopy and DSC (Differential Scanning Calorimetry) analysis performed after washing (data not reported(*182*)), with which residual PEG was not detected. These evidences show how the structure has been influenced by the initial presence of PEG in fibroin aqueous solution. In addition, it is possible to observe the presence of a thin film which covers the surface of PEG/fibroin sponges (figure 4.9). This film must be removed before chondrocyte seeding, thus avoiding possible pore occlusions and promoting cell migration.

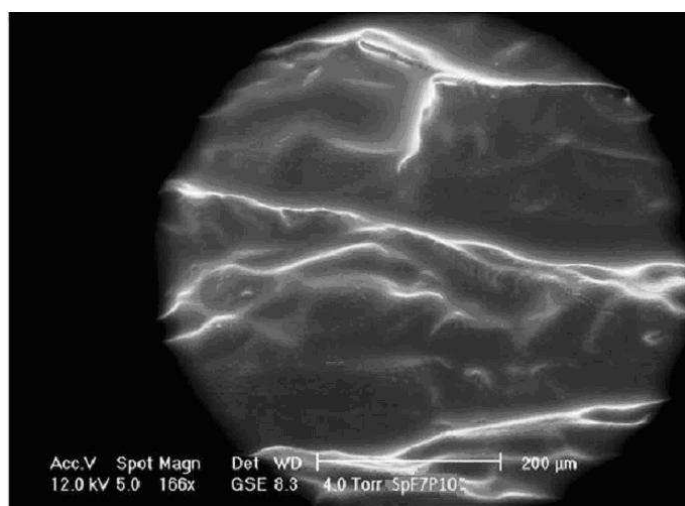


Fig. 4.9. ESEM image of SpF8P10 at 100% RH, the outer surface of sponge is covered by a thin layer and pores are occluded.

Morphology of salt-leached sponges is very different from the morphology of freeze-dried (figure 4.10). The porosity and pore size are very high, surpassing 350 μm .

RESULTS AND DISCUSSIONS

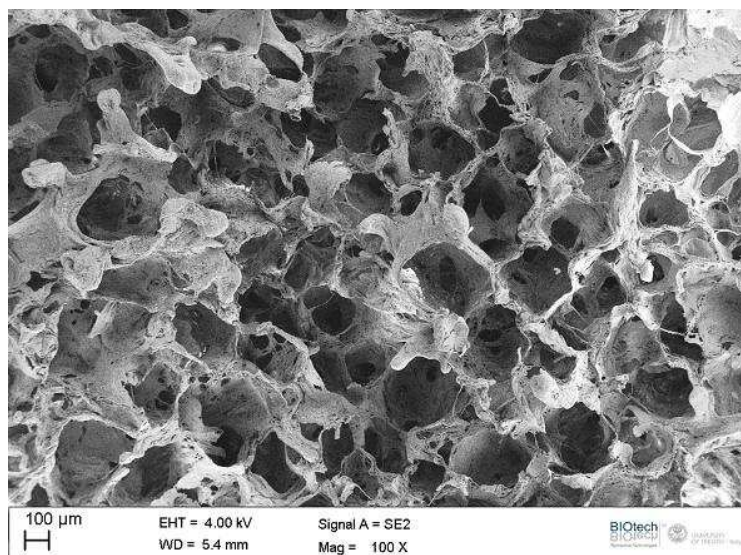


Fig. 4.10. SEM image of SpNaClF8 sponge. Good interconnectivity and high porosity are shown.

ESEM images of salt-leached sponges (figure 4.11) show irregular pores with protrusions if compared to freeze-drying ones. During drying, the structure exhibits the typical roughness of the fibroin scaffold (figure 4.12).

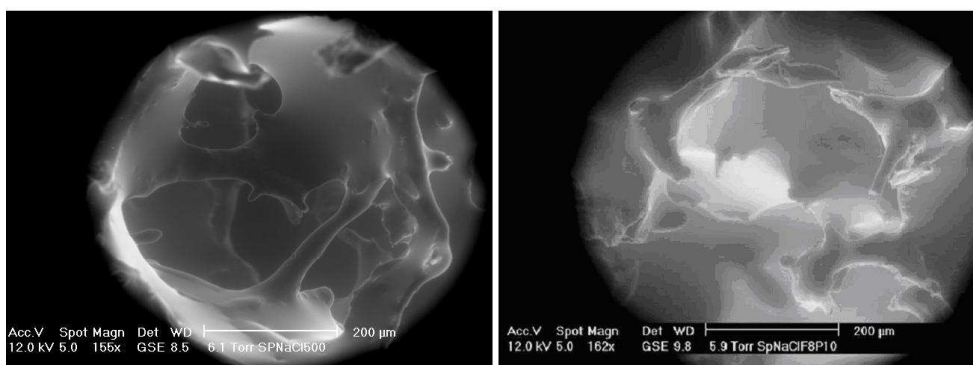


Fig. 4.11. ESEM images of SpNaClF8 (A) and SpNaClF8P10 (B) at 100% RH.

RESULTS AND DISCUSSIONS

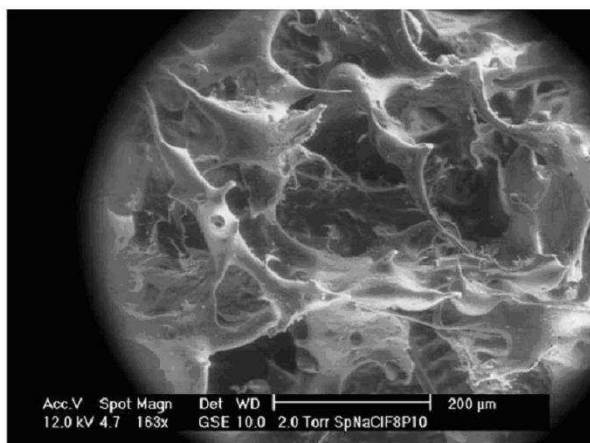


Fig. 4.12. ESEM image of SpNaClF8P10 sponge at 40% RH. The image was acquired during sample drying occurring inside the chamber holder. The irregular structure shows a high roughness and porosity as well as a marked interconnectivity.

In conclusion, two types of scaffolds were produced for cartilage tissue engineering. A high porosity was reached but with different pore size; freeze-drying samples show a pore size between 50 and 200 μm , while salt-leached samples, in wet condition, greater than 300. Addition of PEG seems to have influenced only the microporosity formation during freeze-drying, while the macrostructure, the macroscopic morphology and pore size appear to be similar between the sponges obtained starting from fibroin or fibroin/PEG solution. Finally, considering the salt-leaching technique, a slight mismatch between the formed pores and the salt granulometry can be noted. In fact, pore size is smaller than the used porogen size (500-1180 μm). This effect can be explained considering how the crystal surface should be partially dissolved by the aqueous solution during manufacture processing(175).

RESULTS AND DISCUSSIONS

PDLLA salt-leached scaffolds

For bone regeneration, PDLA scaffolds were prepared by salt-leaching technique using a polymer concentration of 13% (w/v) combined to a NaCl (224-315 μm grain size) content to finally achieve a polymer/salt ratio of 1:10 w/w. PDLA sponge exhibits a completely open and interconnected porosity, ranging from about 20 μm to 400 μm in size, as shown in SEM image (figure 4.13). Even in this case, the obtained structure seems to offer the required characteristics concerning tissue engineering applications.

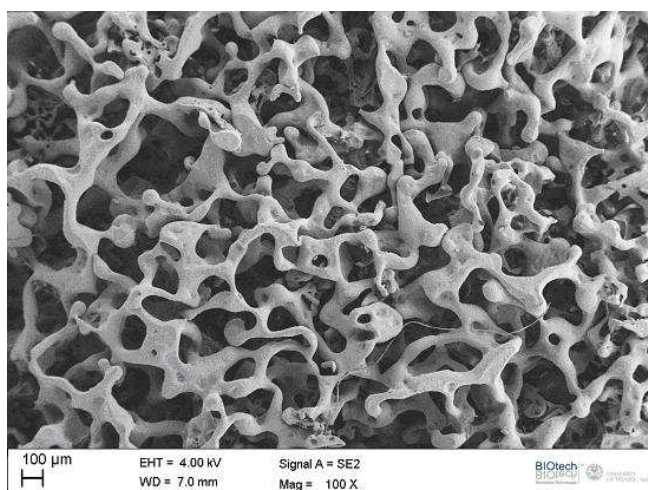


Fig. 4.13. PDLA salt-leached sponge SEM image. Open and high porosity are shown.

4.2.3 Porosity characterization

Fibroin and fibroin/PEG scaffolds

Using the principle of liquid displacement and according to the protocol described in paragraph 3.2.3.3, the scaffold porosity was evaluated in a quantitative way. The results are reported in the table in figure 4.14. Data

RESULTS AND DISCUSSIONS

reflect what has already been observed by SEM/ESEM images. The fibroin sponges produced by salt-leaching possess a higher porosity, 88%, compared to those obtained by freeze-drying, about 72%. In both cases, the addition of PEG (10% $w_{\text{PEG}}/w_{\text{fibroin}}$) leads to an increase of porosity, reaching about 91% in salt-leached sponges and 80% in the freeze-dried ones. This increase seems to confirm the hypothesis asserted after ESEM analysis in which PEG may act as porogen, leading to the formation of additional microporosity (figure 4.8), once removed by washing.

Material	Scaffold	ϵ (%)	$\pm\sigma$ (%)
Silk Fibroin	SpF7	72	2.7
	SpF7P10	80	2
	SpNaClF7	88	1.7
	SpNaClF7P10	91	2.3
P(d,l)LA	SpNaClPDLLA	86	1.6

Fig. 4.14. Porosity values obtained from the produced scaffolds, in fibroin, fibroin/PEG and PDLLA.

Assuming a normal distribution of porosity and considering the calculated standard deviation, no significant difference can be assessed through unpaired *t*-test between the porosity means of fibroin and PEG/fibroin salt-leached sponges, while salt-leaching technique shows a general increase in the obtained porosity when compared with freeze-drying procedures, as also observed by SEM/ESEM imaging. Since means result apparently quite different, the unpaired *t*-test comparison between fibroin and fibroin/PEG produced by freeze-drying also exhibits a significant difference in terms of

RESULTS AND DISCUSSIONS

statistical analysis ($p > 0.05$). Considering the obtained data, it is possible to conclude how the scaffolds present the needed high porosity, about 90 % for the salt-leached scaffolds and between 70% and 80% for the freeze-dried ones.

PDLLA scaffolds

The PDLLA salt-leached scaffold porosity was evaluated in the same way. The obtained value is reported in table of figure 4.14, confirming the high porosity usually generated by the production technique, as already observed by SEM images. The porosity reaches a percentage of 86%, enough to allow cell penetration and migration as needed in scaffolds for bone tissue regeneration. Repeating unpaired *t*-test on each salt-leached scaffold (fibroin, fibroin/PEG and PDLLA), did not give significant differences. Furthermore, the high porosity seems to be a peculiarity of the production technique rather than the sponge material.

4.2.4 Mechanical properties characterization

Mechanical properties of fibroin and fibroin/PEG sponges produced for cartilage tissue engineering were evaluated by five compression tests under wet (PBS) conditions, performed on each scaffold type according to section 3.2.3.1. A limit of the proposed technique is the difficult to obtain a regular and reproducible specimen. Thus, a slight offset load of 0.1 N was previously superimposed. The choice to test scaffolds with a compression test is due to a double reason, the first concerns the difficulty to test sponges

RESULTS AND DISCUSSIONS

under a tensile state (stress triaxiality is easily introduced), the second concerns the necessity to consider a situation as close as possible to the physiological one. The obtained results are reported in table 4.4 and figure 4.15.

Scaffold	Elastic Modulus [kPa]	Error [kPa]
Freeze-Dried Fibroin	97.7	7.86
Freeze-Dried Fibroin/PEG	74.9	7.72
Salt-Leached Fibroin	25.3	4.36
Salt-Leached Fibroin/PEG	25.5	2.89
PDLLA	112.3	5.15

Table 4.4. Compressive properties of produced scaffolds

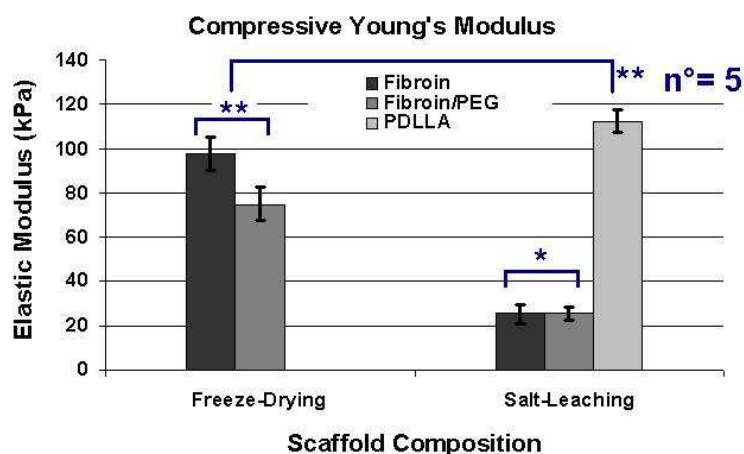


Figure 4.15. Compressive elastic modulus of scaffolds; the properties obtained by the used techniques are compared. (*) indicates no significant differences, while (**) is used when 5%-significance level is exceeded. Each measure is the mean of 5 different samples.

RESULTS AND DISCUSSIONS

According to the porosity data, elastic moduli achieved from salt-leached sponges are less than those obtained from freeze-dried sponges. Figure 4.15 reports how the fibroin and fibroin/PEG scaffolds produced by salt-leaching technique show no significant differences. Compressive elastic moduli are 25.3 ± 4.36 kPa and 25.5 ± 2.89 kPa respectively. Conversely, freeze-dried samples, when compared each other, exceed the 5%-significance level, fibroin 97.7 ± 7.86 kPa and fibroin/PEG 74.9 ± 7.72 kPa. However, compressive elastic modulus of PDLLA appears to be the highest (112.3 ± 5.15 kPa), despite the salt-leached structure, highlighting how the material plays anyway a key role. In Figure 4.16, the stress-strain curve of SpF8 is reported, representing the typical trend of sponges, showing an initial linear elastic region in which compressive elastic moduli are calculated between 2% and 10% (ASTM D 1621-04a).

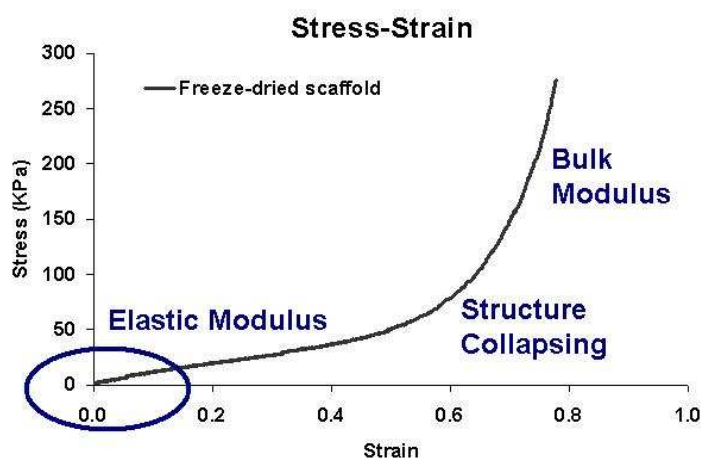


Fig.4.16. A typical stress-strain compressive curve obtained on freeze-dried fibroin. In the first part, the linear elastic part is highlighted, while structure collapsing and bulk compression follow.

RESULTS AND DISCUSSIONS

The structure collapsing follows the first linear elastic part, in which pores are occluded. In some cases, this stage may appear as a plateau without any increase of the recorded load. The last part simply measures the bulk material strength, but the interesting region for tissue engineering applications is for values lower than 30% in strain.

Table 4.5 shows the data achieved from dynamic tests carried out by DMTA analysis (1 Hz, 64 μm at both 25°C and 37°C). Again, the pair or unpair *t*-test statistical analysis performed on the storage modules shows no significative evidences between samples produced by salt-leaching, whereas the 5%-significance level is exceeded in the scaffolds produced by freeze-drying.

Scaffold	25°C			
	$E_1(\text{kPa})$	$\pm E_1(\text{kPa})$	$\tan\delta$	$\pm \tan\delta$
SpF8	142.65	3.53	0.218	0.045
SpF8P10	105.22	3.17	0.192	0.004
SpNaClF8	34.70	1.56	0.160	0.007
SpNaClF8P10	40.00	1.83	0.166	0.006
	37°C			
SpF8	142.55	6.68	0.185	0.028
SpF8P10	97.03	2.20	0.171	0.003
SpNaClF8	34.25	0.92	0.140	0.014
SpNaClF8P10	37.63	2.47	0.154	0.006

Table 4.5. Storage moduli and loss factors of fibroin scaffolds

RESULTS AND DISCUSSIONS

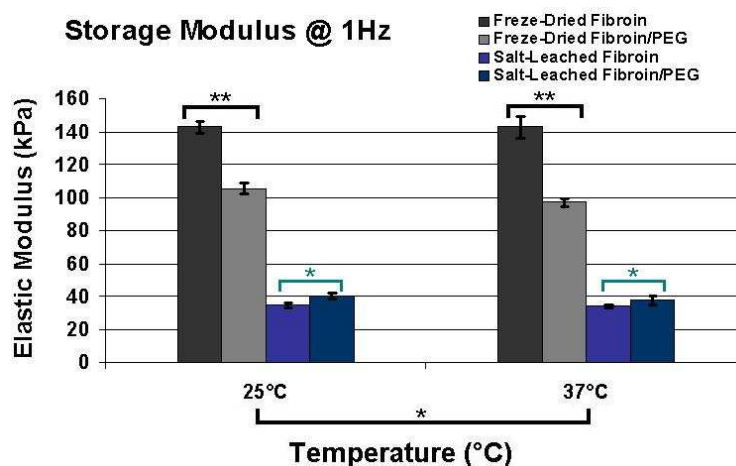


Figure 4.17. Storage moduli of fibroin scaffolds achieved at 1 Hz, 64 μm amplitude and 0.1 N as offset, where the properties at 25°C and 37°C are compared. (*) indicates no significant differences, while (**) is used when 5%-significance level is exceeded. Each measure is the mean of 3 different samples.

Anyway, a comparative analysis between the results obtained at different temperatures does not show any significant differences considering data at 25°C and 37°C, probably due to a slight temperature difference, too low for this kind of material. The recorded storage moduli are comparable with those obtained by quasi-static tests, between about 30 kPa and 140 kPa, although slightly higher, as expected (figure 4.19). In fact, for polymeric materials, the storage modulus generally increases with the applied frequency, reaching a maximum and then decreasing. Table 4.5 and figure 4.18 reported the loss factor $\tan\delta$ at temperatures of 25°C and 37°C. Statistical analysis indicates how any significant changes are found on the scaffolds produced by both salt-leaching and freeze-drying. Excepting for SpF8P10, sponges seem not to show differences in behaviour between 25°C and 37°C, confirming the previous data obtained with the storage moduli.

RESULTS AND DISCUSSIONS

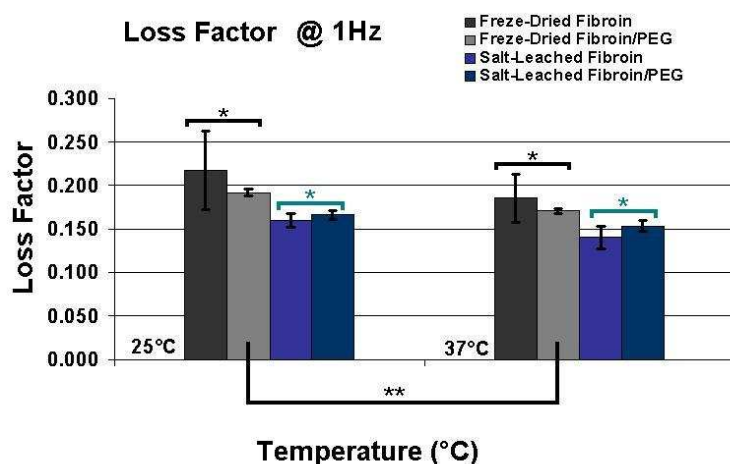


Figure 4.18. Loss factors of fibroin scaffolds achieved at 1 Hz, 64 μm amplitude and 0.1 N offset; the properties at 25°C and 37°C are compared. (*) indicates no significant differences, while (**) is used when 5%-significance level is exceeded. Each measure is the mean of 3 different samples.

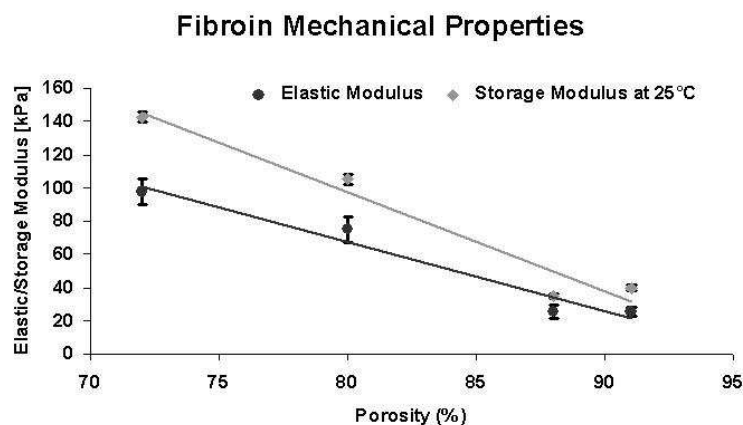


Figure 4.19. Both elastic and storage moduli are plotted as a porosity function.

Furthermore, a crossed comparison was conducted (figure 4.20) between the samples produced by salt-leaching and freeze-drying at the same temperature, showing any defined difference, probably due to the error

RESULTS AND DISCUSSIONS

found in the sample SpF8 0.218 ± 0.045 (20% relative error). This indicates how the accuracy obtained in these measurements is not sufficient to establish a correlation between the measured porosity and the energy dissipated by the materials $\tan\delta$. Figure 4.19 report the calculated moduli as a function of the sponge porosity. A decrease in terms of mechanical properties can be observed (as highlighted) when porosity increases, as obviously expected. In fact, considering the same section, the cross area decreases when porosity increases, reducing the specimen stiffness.

25°C p<0.05 (*) p>0.05 (**)		Freze-Dried Fibroin	Freze-Dried Fibroin/PEG	Salt-Leached Fibroin	Salt-Leached Fibroin/PEG
Freze-Dried Fibroin			*	*	*
Freze-Dried Fibroin/PEG				**	**
Salt-Leached Fibroin					*
Salt-Leached Fibroin/PEG					

Figure 4.20. Crossed comparison between loss factors obtained from fibroin and fibroin/PEG scaffold at 25°C, 1 Hz, 64 μm amplitude, 0.1 N offset. (*) indicates no significant differences, while (**) is used when 5%-significance level is exceeded. Each measure is the mean of 3 different samples.

In conclusion, it is possible to affirm how the mechanical tests performed on sponges confirm the results obtained by both the ESEM/SEM images and porosity tests. Fibroin samples also seem to respond appropriately to the applied stresses, recovering their shapes after load (data not reported). Dynamic tests on PDLA scaffolds were not performed, considering their application. In fact, PDLA scaffolds were principally used for dynamic

RESULTS AND DISCUSSIONS

cell culture under hydrostatic pressure conditions and dynamic compression characterization becomes unnecessary.

4.3 Results and Discussions part 3: *in vitro* Experiment

4.3.1 Cartilage tissue engineering: validation experiment

The aim of this preliminary biological study was the comparison, in terms of cell proliferation, between different cell culturing conditions; dynamic conditions, using a commercial bioreactor and a house-made specifically designed bioreactor, were compared to standard static conditions.

XTT assay

Cell proliferation, measured by XTT assay, was calculated for two different time points, T_0 and T_7 (after 7 days of static culture and 7 days of dynamic culture, respectively) and for the three selected scaffolds, the lyophilized fibroin/PEG sponge SpF8P10, the fibroin/PEG sponge SpNaClF8P10 produced by salt leaching and finally the freeze-dried fibroin scaffold SPF8. The results are reported in figure 4.21. Significant differences can be found among the constructs after static and dynamic cell culture conditions. In fact, cell proliferation is substantially lower in the scaffolds cultured under dynamic conditions, however, no substantial differences between the dynamic conditions conducted in the commercial and the house-made bioreactors are shown. A physiological decrease of cell proliferation after

RESULTS AND DISCUSSIONS

two weeks occurs, even in static culture, affecting also the dynamic conditions.

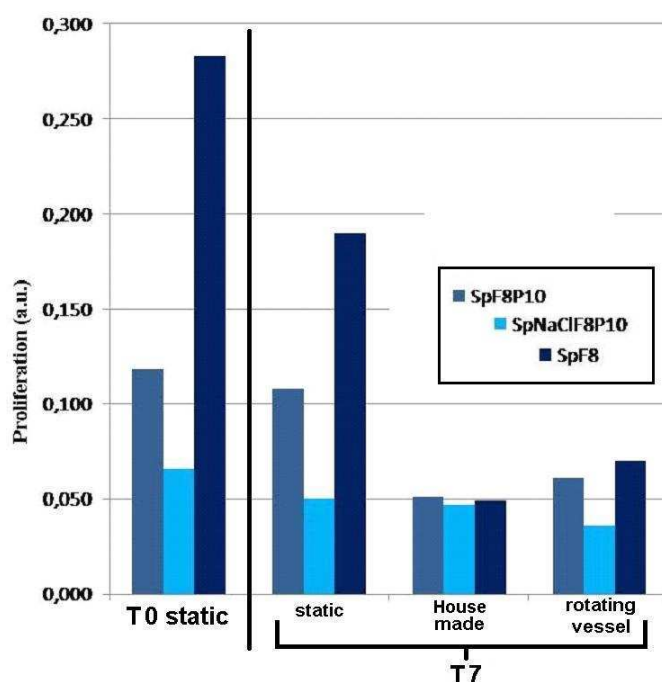


Fig. 4.21. XTT proliferation results for each experimental time point and seeded scaffold, the lyophilized fibroin/PEG sponge SpF8P10, the fibroin/PEG sponge SpNaClF8P10 produced by salt leaching and finally the freeze-dried fibroin scaffold SPF8. The proliferation, measured on three samples, is indicated in arbitrary units (a.u.), while error bars are not reported.

In fact, dynamic cell cultures were conducted starting from scaffolds previously cultured under the same conditions of the static ones. Besides, the physical applied stimuli, such as perfusion in the rotating vessel bioreactor and compression in the house-made one, can induce a greater cell loss in the early stage of dynamic culture, reducing the cell population on scaffolds, probably due to detachment induced by the mechanical stimuli or

RESULTS AND DISCUSSIONS

related to the sample handling during the passage from static to dynamic. Anyway, further experimental evaluations would be necessary to confirm the previous assessments. Furthermore, fibroin sponges produced by freeze-drying show a proliferation behaviour very different to the sponges produced by salt leaching. At each experimental time point, the salt-leached scaffolds possess the lowest number of active cells. Only in the house made bioreactor, this difference seems to be no significant. However, the obtained results show, although qualitatively, how only under static conditions a certain difference in proliferation between scaffolds may be observed, while under dynamic conditions cell proliferation appears very similar. This evidence leads to assume how the effect induced by the different scaffold was hidden by the dynamic conditions which strongly influence the culture by reducing proliferation. This preliminary experiment anyway confirms the effectiveness of the developed apparatus, which reports results very similar to the commercial one. Future works will be focused on the optimization of stimulation parameters to improve the cell culture.

Histology and ESEM microscopy

The histological analysis of fibroin/PEG sponges was performed in collaboration with the Pathological Anatomy ward of *S. Chiara* hospital, Trento. Scaffolds were mounted in paraffin, stained with hematoxylin-eosin and observed with the optical microscope to verify the cell distribution.

RESULTS AND DISCUSSIONS

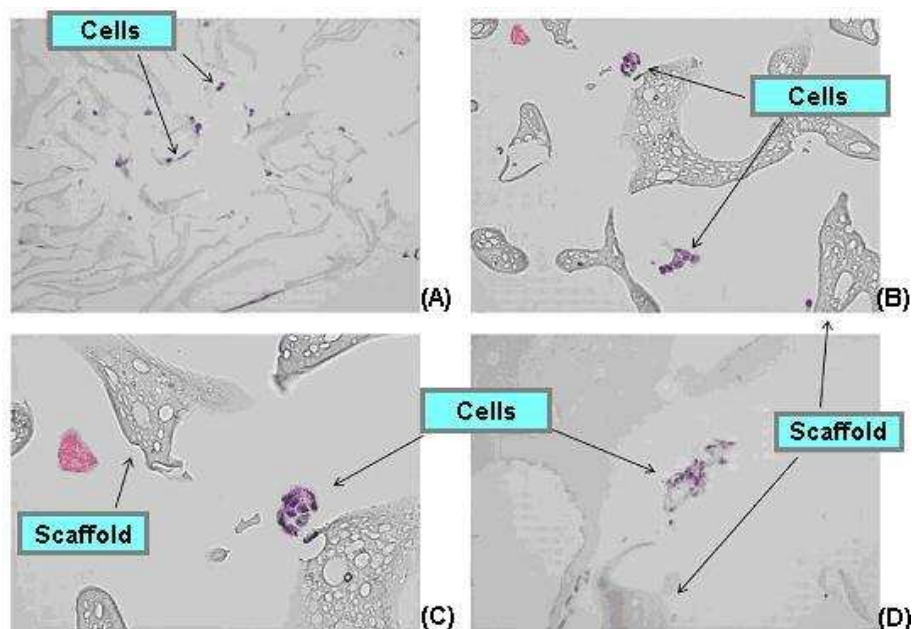


Fig. 4.22. Images after histological staining with hematoxylin-eosin. Cell nuclei are visible in blue-purple; A) Sponge SpF8P10 cultured under static conditions at $T7$; B) Sponge SpF8P10 cultured in house-made bioreactor at $T7$; C) Sponge SpF8P10 cultured in rotating vessel bioreactor at $T7$; D) Sponge SpNaClF8P10 cultured under static conditions after seven days, $T0$.

In most of the histological samples, chondrocytes were not found. This evidence is in contradiction on what observed in the previous XTT evaluation. Each seeded scaffold, even those supported by XTT analysis with a high cell proliferation, was completely free of cellular components. Figure 4.22 reports some histological images. The presence of chondrocytes is very limited. Small clusters are mostly formed and seem not to adhere to the protein matrix. It also is important to notice how the positive or negative cell distribution (samples with or without cells respectively) seem not to follow a clear criterion. In fact, the fibroin SpF8 sponges at time $T0$ (having

RESULTS AND DISCUSSIONS

a maximum absolute XTT value of proliferation) were negative; the fibroin/PEG sponges produced by freeze-drying were negative at time T_0 while showing a slight presence of chondrocytes at T_7 in all the culture conditions. Finally, fibroin/PEG sponges, produced by salt leaching, were positive at time T_1 when the measured proliferation value was the lowest in that experimental time. In light of these observations, it seems reasonable to conclude that problems during sample fixation probably occurred. The chondrocyte adhesive force to fibroin matrix was probably too weak to withstand the action of formaldehyde, considering the applied fixation protocol (section 3.3.2.2). This hypothesis seems to be confirmed by the cellular distribution observed in positive samples, focusing on cluster formation, in which cells appear to be *ripped* from the fibroin matrix.

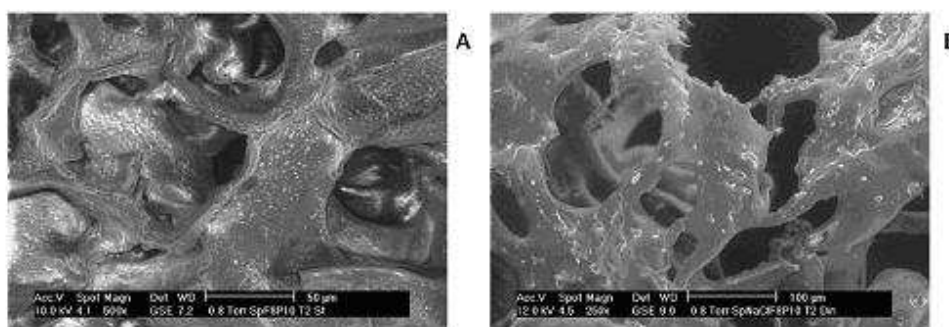


Fig. 4.23. ESEM images related to A) lyophilized fibroin/PEG sponge at T2 cultured under static condition; B) fibroin sponge/PEG produced by salt leaching at T2 cultured in house-made bioreactor. The images were acquired in low vacuum mode.

Similar problems of cells fixation also happened for ESEM analysis. In fact, cells were not detected in any samples. Some representative images are shown in figure 4.23. In conclusion, the experiment must be re-performed,

RESULTS AND DISCUSSIONS

after changing dynamic stimulation parameters and the fixation protocols for imaging.

4.3.2 Cartilage tissue engineering: condition investigations

To assess the effect of dynamic conditions on cultured chondrocytes, a second experiment was carried out, after reducing the loading time to enhance cellular activation. In fact, this experiment is intended to evaluate both dynamic and static cell culture conditions for the development of tissue engineered constructs, in terms of cellular activation and proliferation, after a 14 days long experiment. In this experiment, the load condition was thus reduced, passing from 25% to 20% in strain and decreasing the stimulation time to 30 minutes per day. In fact, prolonged stimulations may not necessarily result in a higher matrix formation if compared with short stimuli. In fact, mechanical stimuli were especially important in cell activation, but long application can lead to cell damage and apoptosis. For this reason, a rest period was often introduced within the same stimulation, and a loading time usually no exceeds an hour. Salt-leached silk fibroin sponges were used as scaffold. This kind of scaffold was chosen for its high and interconnected porosity. In addition, other cell cultures carried out with these scaffolds have reported promising results (data not shown(*183*)). Finally, a 17-days long experiment was thus carried out, shortening the prestatic culture (three days are enough for cell adhesion(*184*)) and prolonging the dynamic one to fourteen days in order to reduce the negative effect on data associated to the passage from static to dynamic. Cell

RESULTS AND DISCUSSIONS

proliferation results, obtained by AlamarBlue[®] assay, are reported in figure 4.24. The obtained results show no statistical differences between static and dynamic cultures after seven days T7. At the fourteenth day T14, a slight increase in proliferation in dynamics can be observed, but no less than 5%-significance level ($p < 0.1$). Furthermore, performing a statistical analysis on the trend of cell population, no defined differences can be assessed in static ($p < 0.2$), while in dynamic a p-value less than 0.05 can be calculated.

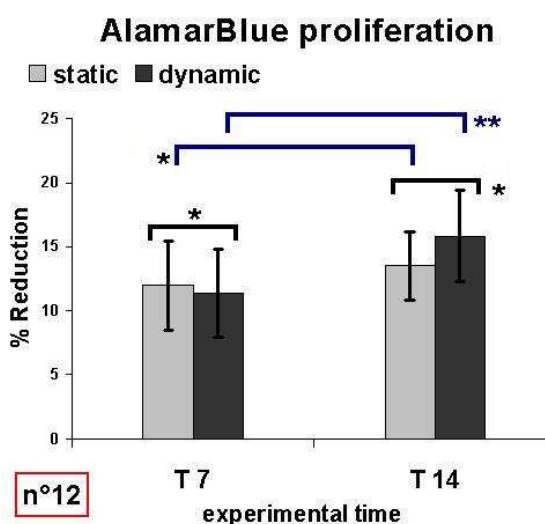


Figure 4.24. alamarBlue[®] results, the proliferation values expressed by % of reduction are compared. (*) indicates no significant differences, while (**) is used when 5%-significance level is exceeded. The tested samples were 3, for 4 measures on each scaffold, resulting in 12 d.o.f..

This evidence leads to conclude how the imposed dynamic conditions, in this experiment, were enough to significantly increase cell proliferation after fourteen days, without cell damage. However, the slight increase in proliferation seems to be in agreement with the general cell type behaviour,

RESULTS AND DISCUSSIONS

characterized by a general slow metabolism and cell growth(158, 185). Future experiments should be performed for a longer period (56-60 days) to assess the matrix synthesis or specific genes expression, maybe starting from a more proper cell concentration (10^6 - 10^7 seeded cells).

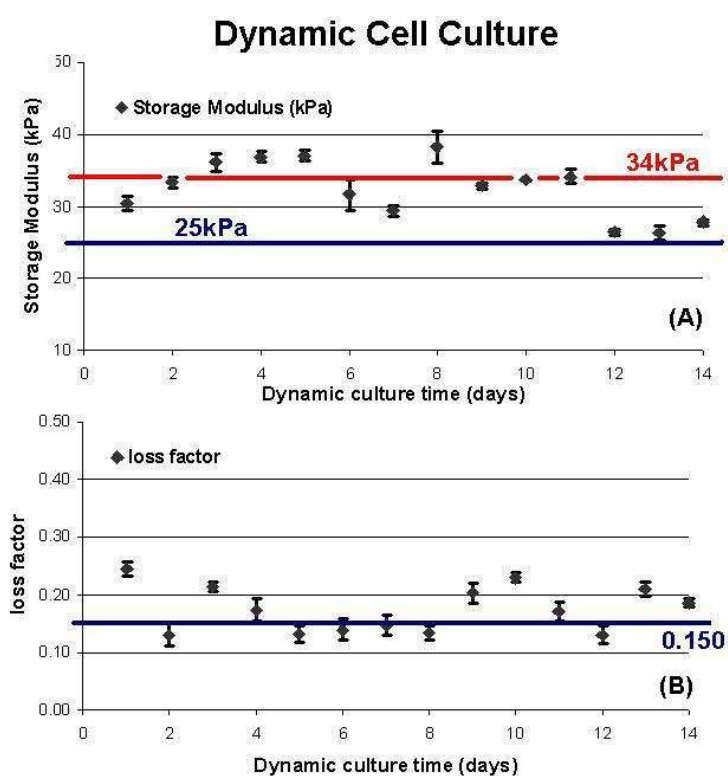


Figure 4.25. Storage Moduli and loss factors obtained daily on the cultured scaffold.

Extracellular matrix deposition was also analyzed during the first two weeks of dynamic cell culture by monitoring daily, during the culture, the storage modulus and loss factor. The trends reported in figure 4.25 does not show an

RESULTS AND DISCUSSIONS

increase during the analyzed period, therefore no measurable deposition of extracellular matrix was found (fibroin scaffolds does not degrade in such as short time), according to literature data(158). However, the obtained values, storage modulus 32.4 ± 3.9 kPa and loss factor 0.175 ± 0.04 , are comparable to those measured in the previous session 4.2, confirming how this device can properly work as a testing machine apparatus for mechanical measuring. Concluding, it is possible to assume that the imposed dynamic conditions seem not to lead cell damage, but cell proliferation is encored after 2 weeks. No matrix deposition was found. Further studies, also including gene activation analysis, are thus needed to better understand the optimum dynamic conditions and their effects on cell culture.

4.3.3 Bone tissue engineering: validation experiment

To validate the bioreactor system developed for bone tissue engineering, another preliminary experiment with human osteosarcoma derived osteoblasts (MG63) seeded on PDLLA salt-leached sponges was conducted, comparing the achieved results with those obtained by the static culture, used as control, and by the dynamic cell culture carried out in the previously used RCCS commercial rotative bioreactor (12 rpm). The unloaded condition was also tested. The imposed dynamic condition was 30 min / day of 20% sinusoidal strain (0.4 mm) at 0.1Hz. After three days of static culture (time T_0), scaffolds were cultured for other seven days (T_7) some of them continuing a standard static culture, others following a dynamic culture.

RESULTS AND DISCUSSIONS

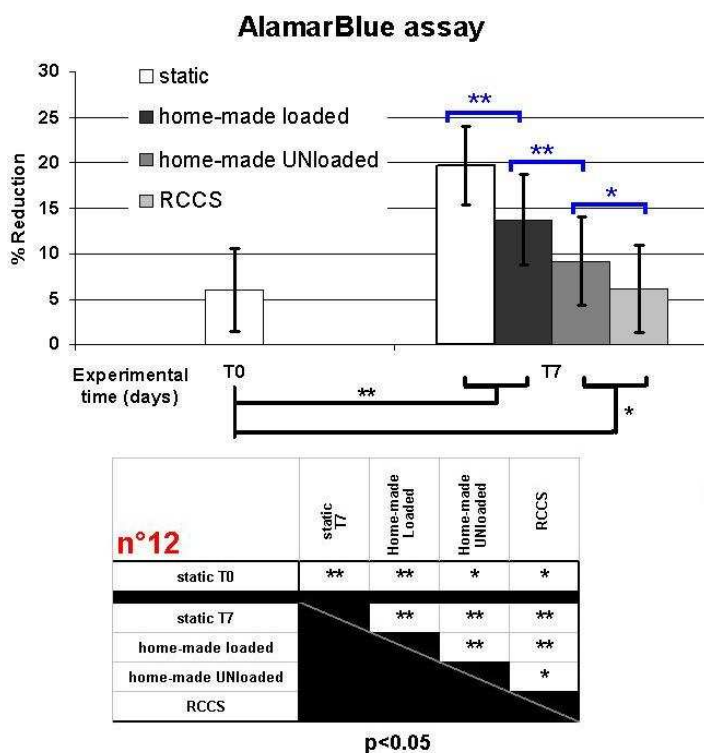


Figure 4.26. alamarBlue® results for T_0 and T_7 . The proliferation value expressed by % of reduction are compared. A crossed comparison is also performed. (*) indicates no significant differences, while (**) is used when 5%-significance level is exceeded. Each measure is the mean of three different samples, carried out 4 times, resulting in 12 d.o.f..

AlamarBlue® proliferation results are reported in figure 4.26. The statistical analysis performed on proliferation data shows a greater number of active cells in the static culture compared to the dynamic, considering the first culture week (after 3 days of pre-static), as already seen in the previous first two experiments. In this case, it is possible to observe a significant differences ($p < 0.05$) between scaffolds cultured in static and dynamic.

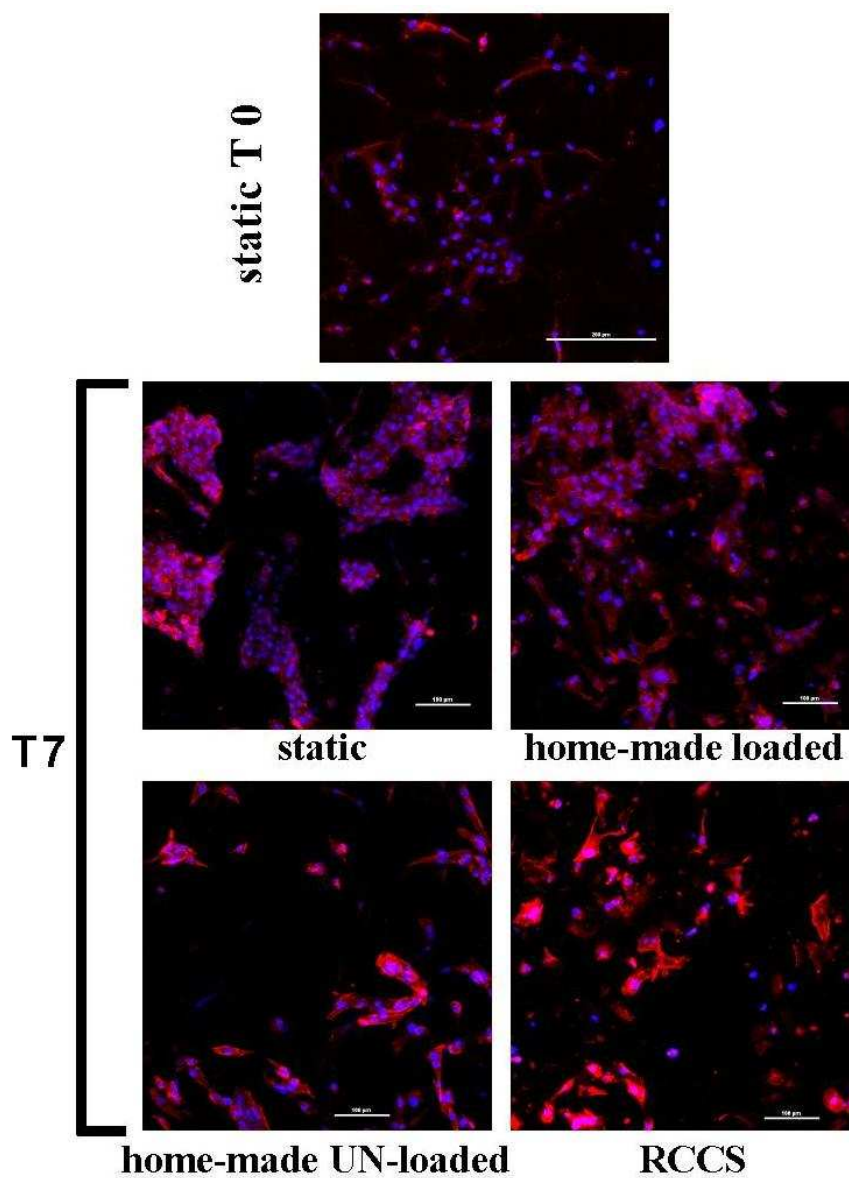


Fig.4.27. Confocal images of cultured scaffolds, after Phalloidin Rhodamine (resulting in red color for cytoskeleton) and DAPI (blu, for nuclei) staining.

RESULTS AND DISCUSSIONS

Moreover, among the samples cultured under dynamic conditions, only those loaded in the house-made bioreactor show a significative increase in proliferation. Furthermore, only the samples cultured under static and the “loaded” scaffolds report a significative proliferation increase over the selected time points, T_0 to T_7 . Thus, also in this case, the imposed conditions in the rotary bioreactor resulted in cell damage during the culture. Scaffolds cultured in the house-made bioreactor also seem to report cell damage, suggesting that a first negative effect found in dynamic was slightly compensated by the compression-induced cell activation. However, this evidence is only a hypothesis to be better verified using other more specific methods for gene expression quantification, such as RT-PCR.

Visual inspection of cell proliferation and adhesion was performed using confocal laser microscopy, after specific staining for cell nuclei and cytoskeleton. Figure 4.27 shows the confocal images acquired on the cultured samples; after staining, cell cytoskeleton resulted in red color, while cell nuclei in blue. The confocal images appear to be in agreement with the proliferation data; only the scaffolds cultured under static conditions and loaded in dynamic seem to be well populated. In fact, a good distribution and cellular morphology is shown, while scaffolds cultured in the rotary bioreactor and the unloaded ones report a non-optimal distribution, also presenting fewer cells. In fact, osteoblasts should physiologically form a layer covering the scaffold material to subsequently start the extracellular matrix deposition(22). Finally, figure 4.28 shows a qualitative evaluation of cell migration, considering the maximum measured

RESULTS AND DISCUSSIONS

depth reached by cells for each different sample. Any statistical analysis was not performed on migration, in fact a single sample for each condition was analyzed. Interestingly, the obtained depth for the house-made bioreactor corresponds to the applied displacement amplitude.

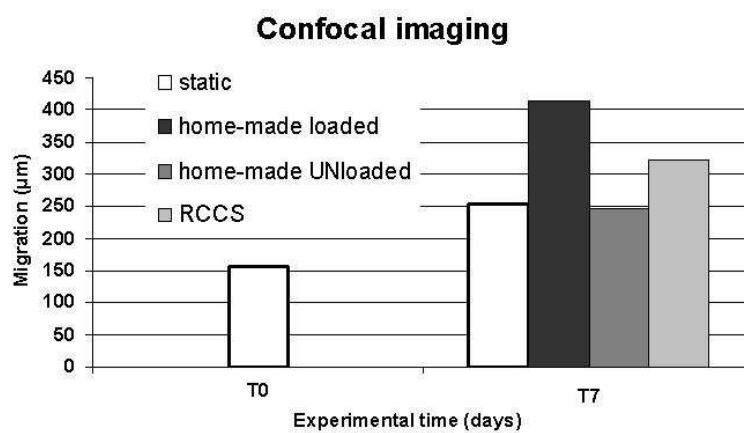


Fig.4.28. Qualitative migration measured through confocal images.

In conclusion, it is possible to assert that the results obtained by the developed bioreactor are better compared to those achieved by the rotary commercial bioreactor in terms of cell proliferation and migration, although a greater proliferation is shown in static culture.

4.3.3.1 Bone tissue engineering: dynamic hydrostatic pressure, condition investigations

The ability to control and influence cell behavior to produce tissues, both hierarchical and functional in nature, is critical in tissue engineering and regenerative medicine. The ability to mirror both the natural structural

RESULTS AND DISCUSSIONS

morphology as well as cellular micro-environment of the replacement tissue is vital for the success of an engineered tissue(186). Bone tissue is unique in that it has a strong ability to adapt its internal architecture and density in the presence of mechanical stimulation. This fascinating ability of bone to remodel to fit the desired physiological demand is essential in the production of functional bone replacements. Bone architecture is unique in that it has the capacity to adapt to external stresses. First proposed by Wolff in the late 1900's, bone tissue was believed to transform according to the level of physiological stresses encountered. Later, Frost would further speculate that in addition to architecture, bone homeostasis is directly related to the physiological stress environment. Various techniques have been devised to simulate physiological stress *in vitro*(187). Of these techniques fluid shear, compressive strain and uniaxial stretching devices are amongst the most commonly studied systems. Since bone tissue experiences a wide spectrum of stresses, a combination of techniques is often employed such as combining fluid shear with substrate deformation.

Bioreactors are often employed in cell cultures to enhance cell growth and tissue formations through the application of mechanical stimuli. Consequently, it has been shown that the application of various dynamic stresses, such as shear and strain, can influence osteoblasts genotype as well as matrix production(188, 189). Undoubtedly, a combination of such mechanisms *in vitro* plays a vital, if not synergistic, role in guided tissue formation. However, the exact mechanisms of how these factors influence cellular development and tissue organization are still elusive. In an effort to

RESULTS AND DISCUSSIONS

elucidate these mechanisms, we developed a dynamic culturing method that utilizes hydrostatic compression to stimulate cell substrates. By controlling the frequency, magnitude and even cycle of applied stress, cell behavior can be influenced. The aim of this work was to apply a systematic study of the dynamic culture parameters and investigate the response on osteoblasts proliferation, migration and genotypic expression.

Cell proliferation of both dynamic and static cultures at different pressures (10 and 20 kPa) and frequencies (1 and 0.3 Hz) was evaluated by alamarBlue[®] assay. At day 7 under 1 Hz frequency, a significant deviation between 10 and 20 KPa can be observed indicating more favorable culture conditions under higher pressures. However, when the cultures were extended to 14 days this trend began to diminish and the gap began to narrow (anyway the hypothesis of equal mean was statistically rejected with a p-value of 0.05 and 24 d.o.f.). In comparison, when applying 0.3 Hz frequency, no appreciable difference between pressure magnitudes could be distinguished. From the data it is clear that both pressure magnitude and frequency can play a role, albeit synergistic, in cell proliferation. Only 20 kPa/1Hz dynamic condition seem to provide an higher proliferation in dynamic compared to static in the first seven day. Cell attachment and morphology was quantified using Confocal Laser Microscopy (CLSM) after Rhodamine Phalloidin and Dapi staining. The presence of cells was observed at all time points and culture conditions. At 7 days cultures, cell attachment and migration phenomena could be observed. By 14 days substantial cell populations could be seen throughout the thickness of the

RESULTS AND DISCUSSIONS

scaffolds. Unlike the alamarBlue assay, images did not indicate a substantial deviation between applied mechanical stimulation. However, there is some indication that cell attachment and spreading was less active at a pressure of 20 KPa.

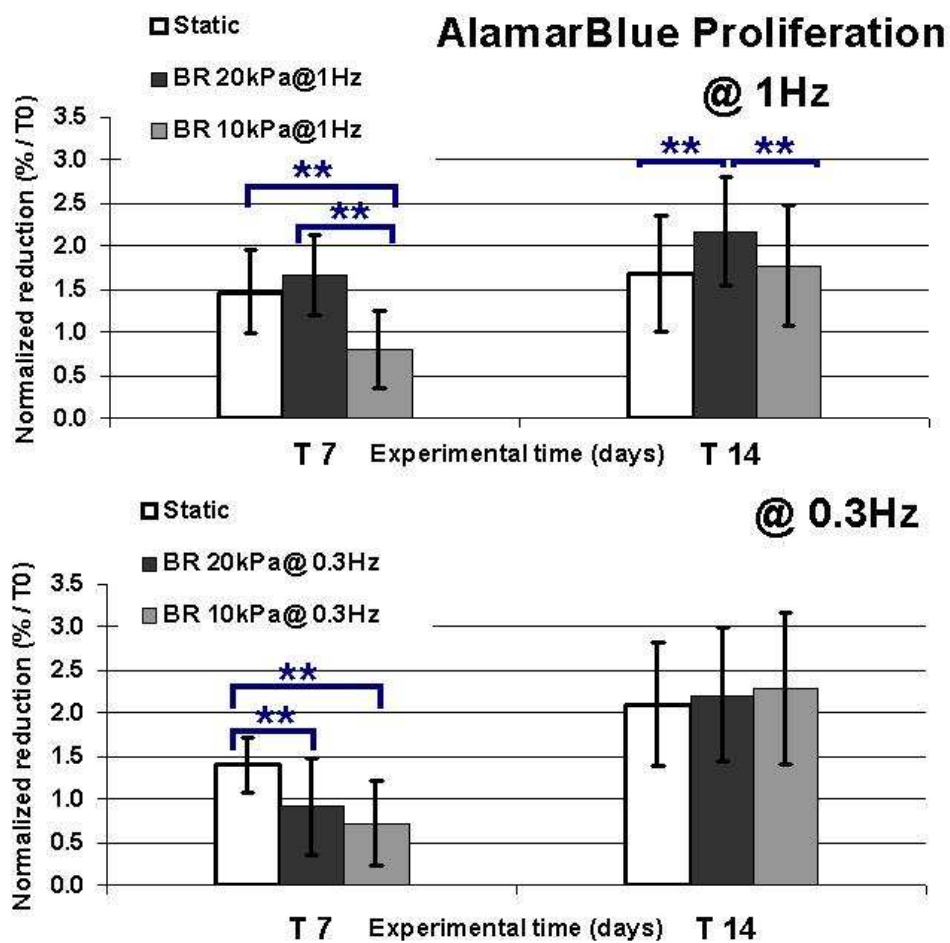


Fig.4.29. Reports alamarBlue® proliferation results normalized on the static T0 percentage of reduction. (**) indicates a p-value less than 0.05, considering 24 measures (eight measure for 3 samples).

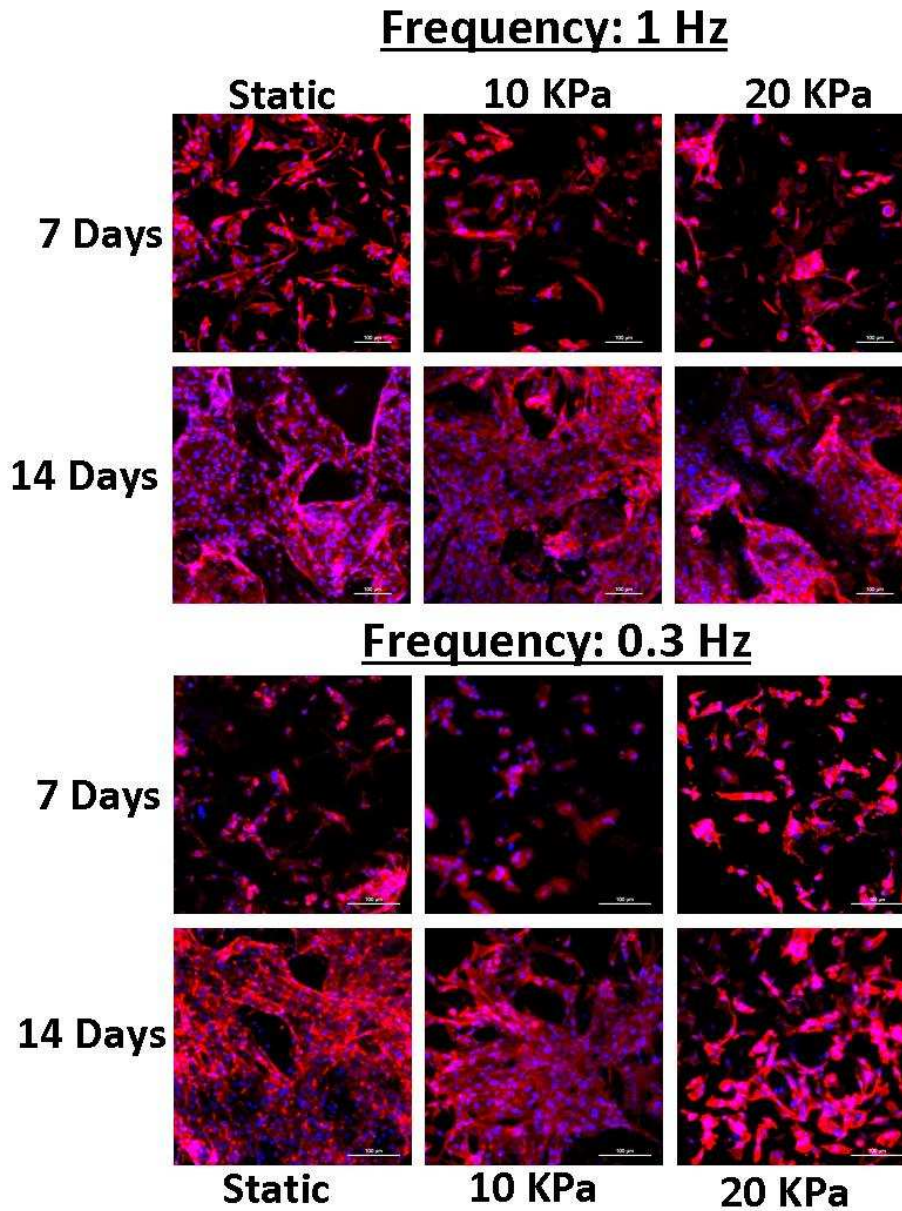


Fig.4.30. DAPI/Phalloidina staining: confocal images acquired on cultured scaffold, blue dot indicates the cell nucleus, while the cytoskeleton in red.

RESULTS AND DISCUSSIONS

Cell viability was further assessed with confocal laser microscopy (CLSM) after staining with fluorescein diacetate–propidium iodide (FDA–PI) FDA stains viable cells green, while PI stains necrotic and secondary apoptotic cells red. Images confirmed the presence of viable cells in all samples minus 10 KPa, 1 Hz at 7 days. The lack of active cells for the 10 KPa, 1 Hz condition reiterates the alamarBlue[®] data presented above with results low cell proliferation. However, active cells are observed once the culture is extended to 14 days indicating a regulation of the cell activity.

This experiment presented here is a preliminary evaluation of cell kinetics under mechanical stimuli. To further evaluate biological activity, future experiments will include RT-PCR to map the cell gene expression during dynamic conditions. RT-PCR is a powerful biological assessment technique that can provide information on matrix production and mineralization, both of which are critically important in the formation of tissues. In addition, many parameters in dynamic culture can influence cell activity and proliferation. Future experiments will focus on investigating more of the dynamic culture parameters such as applied cycle number and rest period between cycle session. Thus, it was decided to conduct a 28 days-long experiment with the best found conditions, in terms of cell proliferation, that is 20 kPa/1 Hz.

Note: In the blank experiment carried out under dynamic conditions with only diffusion of nutrient, a decrease in proliferation occurs also after 14 days, while a trend similar to those previously explained was reported in the test performed at 20 kPa and 1 Hz, but without a continuous diffusion of

RESULTS AND DISCUSSIONS

nutrient (data not shown). Considering this last evidence, the nutrient flow rate was reduced from 0.05 mL/min to 0.01 mL/min.

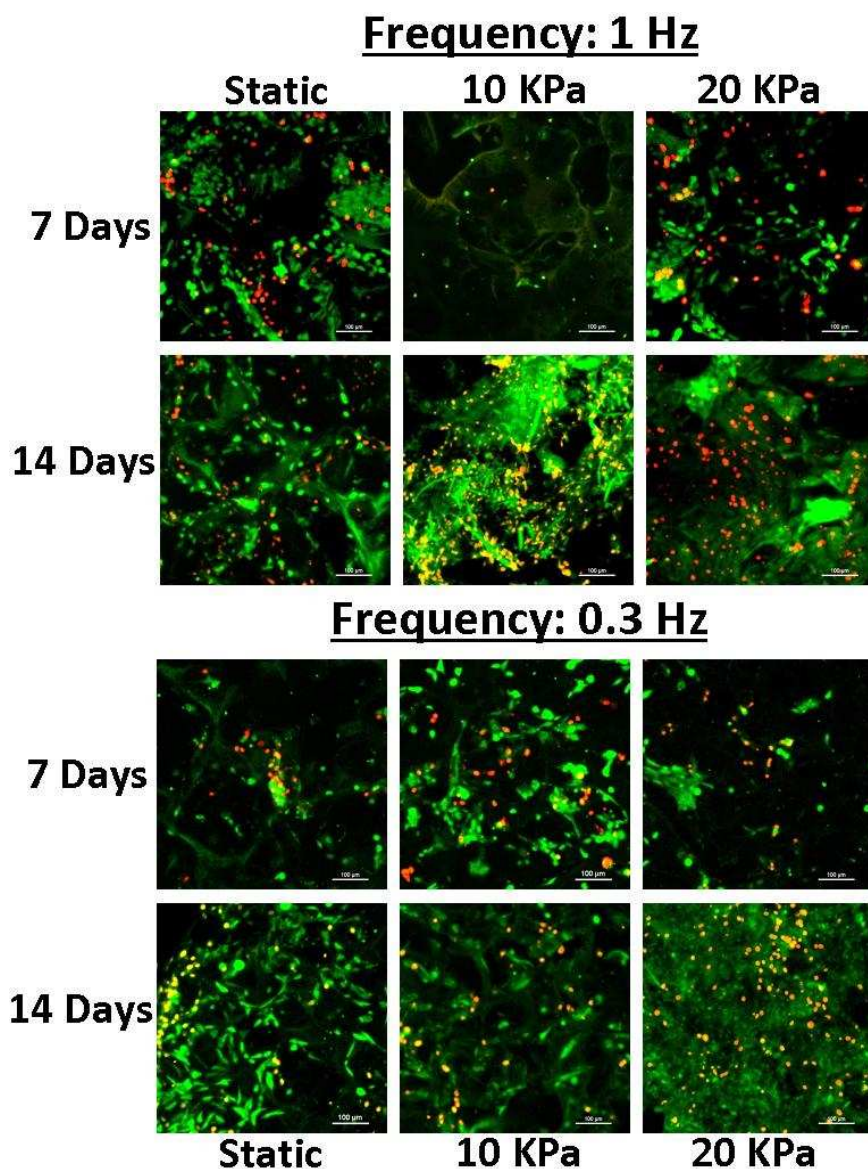


Fig.4.31. FPA/PI staining: confocal images acquired on cultured scaffold, green dot indicates alive cells, while red one indicates death cells.

RESULTS AND DISCUSSIONS

4.3.3.2 Bone tissue engineering: dynamic hydrostatic pressure, long experiment

The influence of dynamic stimuli (dynamic hydrostatic pressure) on PDLLA salt leached sponges seeded with human osteosarcoma derived osteoblasts cell line MG63, over a cell culture period of 28 days was observed. The study was focused on the evaluation of dynamic cell culture conditions compared to the standard static ones, in terms of cells proliferation and activity. Figure 4.32 shows the proliferation trend measured by alamar Blue assay. Cell proliferation trends after both static and dynamic culturing conditions seem not to differ to each other. A general increase of proliferation during the first days of cell culture (14 days) is shown, followed by a plateau.

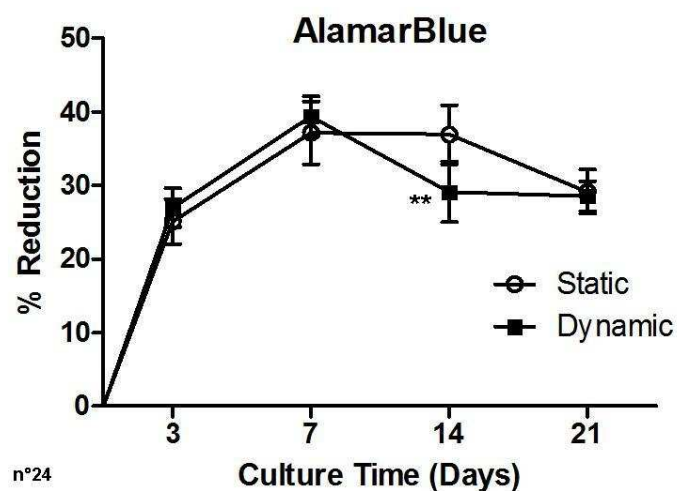


Fig.4.32. alamarBlue[®] cell proliferation measured on cultured scaffolds. (**)
indicates a significant difference p-value less than 0.05 (n=24).

RESULTS AND DISCUSSIONS

Cell viability (figure 4.33) was analyzed by confocal laser microscopy after staining viable cells with Calcein AM, resulting in a green color. Live cells increase with culturing time, as expected. Furthermore, the confocal images are the result of a stack of different layers for a depth of about 250 μm and by looking inside the sample (different viewing modes are possible but no further images are reported) it is possible to assess that live cells are homogeneously distributed inside the examined volume. Cell structure, spreading behavior and distribution inside the considered volume was analyzed by confocal laser microscopy (CLM) after Rhodamine Phalloidin and Dapi staining (figure 4.34). In particular, Rhodamine Phalloidin is a high affinity probe for F-actin which is also conjugated to a fluorescent dye; thus the cytoskeleton can be stained resulting in a red color. Besides, Dapi is a fluorescent stain that binds strongly to DNA and, if excited with ultraviolet light, appears in a blue color.

Both the static and dynamic cell cultures, for every chosen time point, were examined by CLM. Cells were able to enter the porous scaffold structures even from the early evaluated time points. Generally, the total cell amount, qualitatively increased with the culturing time till day 14, for both static and dynamic cell culture, as also proved by alamar Blue assay. Conversely, cell distribution and spreading behavior resulted dissimilar in the two cell culture methods. In the dynamic study cells appeared to distribute following a sheet like configuration while in the standard static culture cells appear less connected to each other. This is probably due to the higher cellular

RESULTS AND DISCUSSIONS

activity, corresponding to a higher matrix production of cells dynamically cultured, as confirmed by PCR analyses.

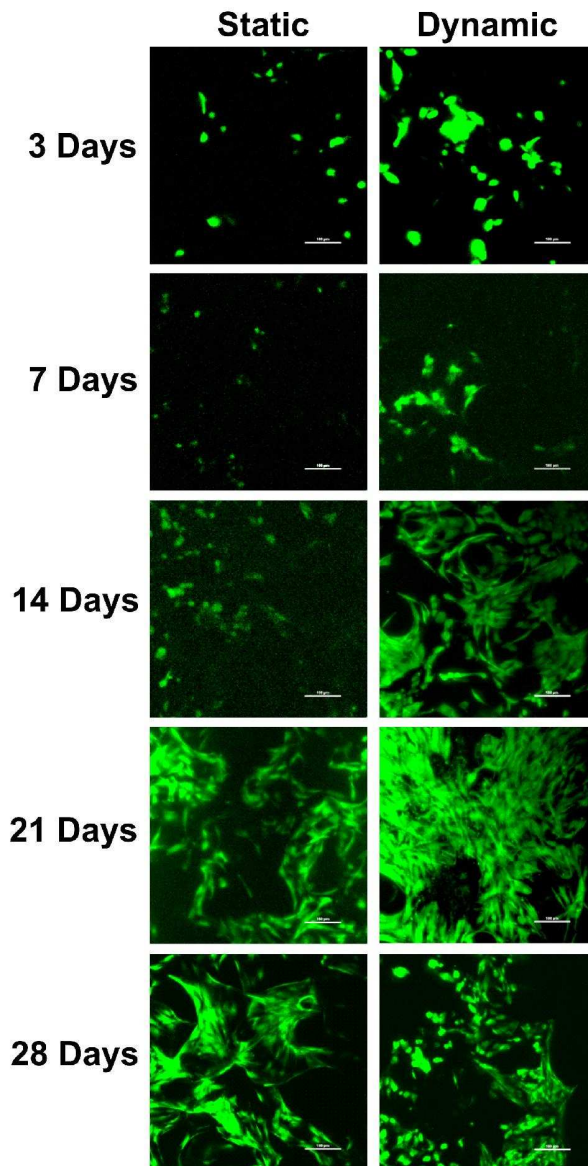


Fig.4.33. FPA/PI staining: confocal images acquired on cultured scaffold.

RESULTS AND DISCUSSIONS

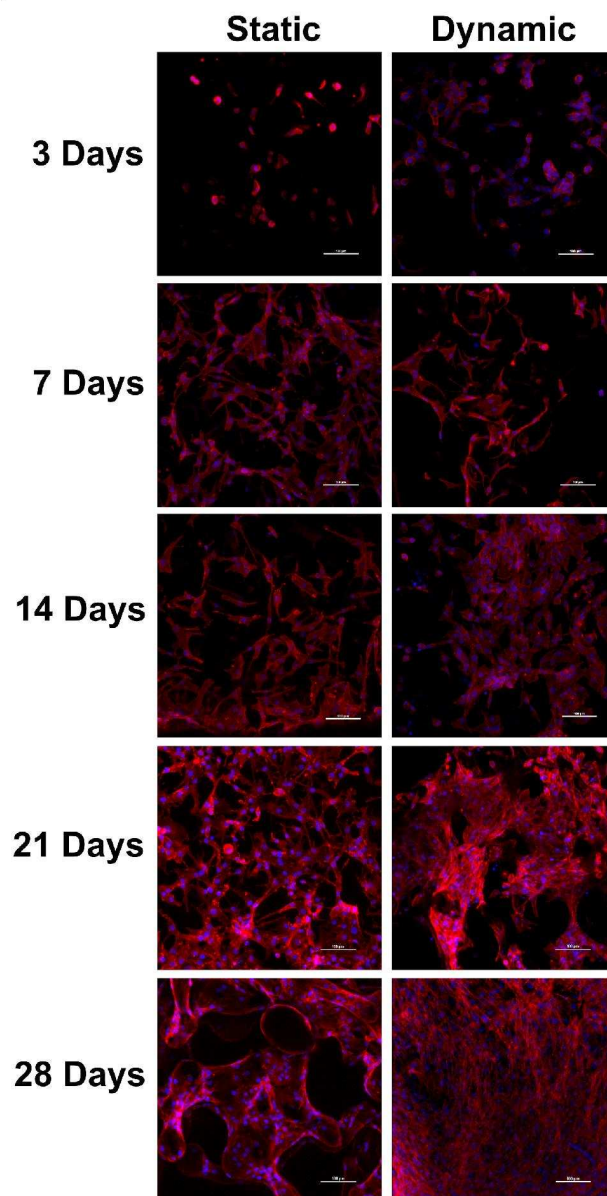


Fig.4.34. DAPI/Phalloidina staining: confocal images acquired on cultured scaffold.

RESULTS AND DISCUSSIONS

RT-PCR

In this study cellular gene expression was qualitatively evaluated to reveal the effect of the experimental conditions on the modulation of genes specific to key developmental stages of the osteoblast lineage. During the progressive development of the osteoblast, three key stages can be identified: proliferation followed by matrix deposition and maturity and concluding with matrix mineralization. In this study, the aim was to investigate genes specific to these three stages of osteoblast development to evaluate the effect of the experimental conditions on the modulation of the cellular genotype. A summary of the relative gene expression of select genes of interest in this study are presented in figure 4.35.

Proliferation:

During proliferation, a number of genes are expressed, initiating a cascade of events promoting cell division, migration and expansion. Genes related to the family of transforming growth factor- β (TGF- β) have long been considered to play an important role in cellular proliferation and expansion. When combined in cell culture, TGF- β 1 has a profound role towards increasing cellular proliferation while also exhibiting neotissue formation properties(*190*). Moreover, TGF- β 1 has also been revealed to be an important factor towards cellular commitment to bone cell lineages, thus playing both a role in proliferation and differentiation events. To demonstrate these events in our study, the relative expression of TGF- β 1 between static and dynamic conditions was evaluated, with results presented

RESULTS AND DISCUSSIONS

in figure 4.35. Data evidenced, under static conditions, a steady increase in expression over the culture period. In the dynamic series, a bimodal expression sequence with peaks of TGF- β 1 present at days 3 and 21 was observed. Early expression of TGF- β 1 likely correlates to a stronger commitment to bone cell lineage as there was not a significant difference in proliferation measured between the static and dynamic series. Furthermore, the gradual increase of expression up to day 21 supported the continued commitment to the osteoblast activity.

Matrix Deposition & Maturity

A number of events occurs during the formation of extracellular matrix, which leads to the deposition of matrix specific proteins and molecules. In bone tissue, collagen I is the most prevalent matrix protein comprising the majority of the total protein content of bone ECM. Concomitant to matrix collagen deposition is the requirement for increased cellular activity, most commonly observed through ALP activity. Hence, in our study we observed both collagen and ALP activity, as presented in figure 4.35. Dynamic conditions clearly enhanced the collagen expression throughout the study with a distinct peak at 21 days. While it is not clear the specific nature of the increased expression at day 21, one possible explanation is that prior to this period of culture the cells were becoming adjusted to the dynamic conditions; only after a set period of time collagen is produced pronouncedly. In additions, with regard to ALP, a significant increase in activity was apparent in dynamic conditions versus static controls.

RESULTS AND DISCUSSIONS

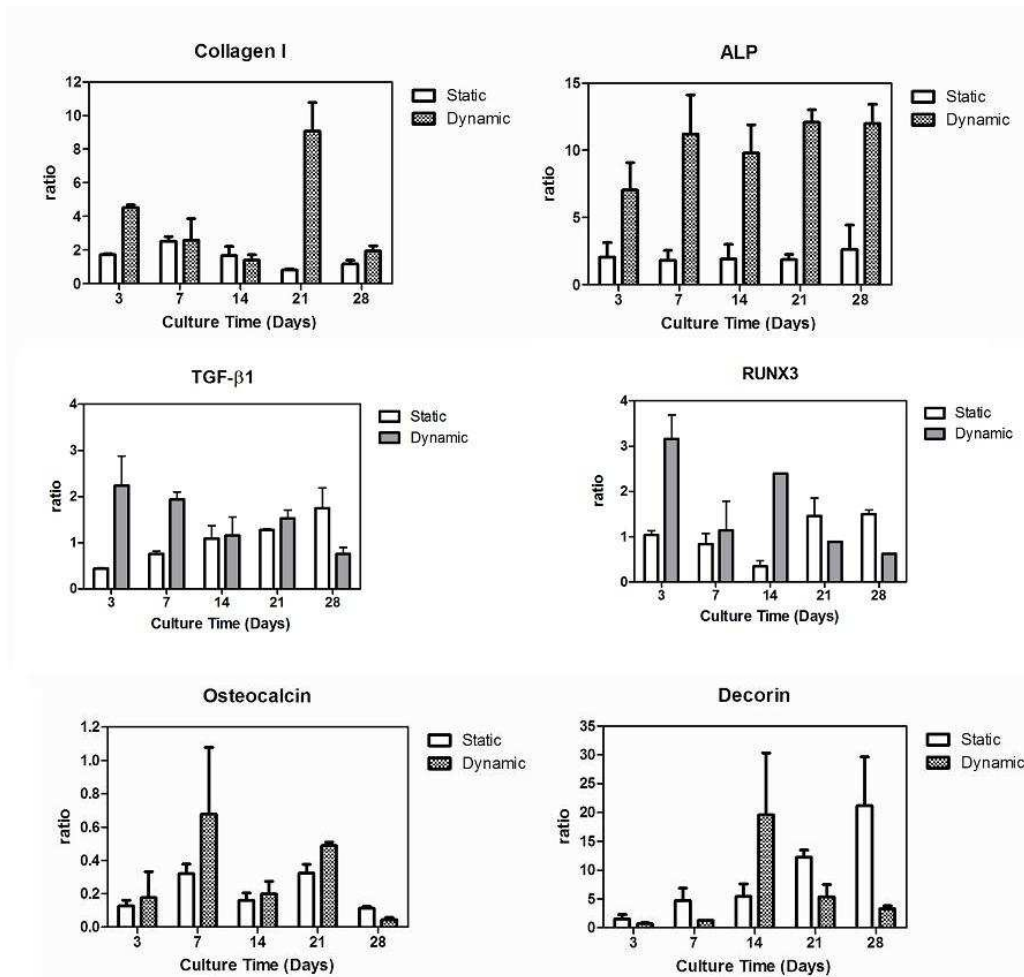


Fig. 4.35. Summary of the relative gene expression measured by RT-PCR.

RESULTS AND DISCUSSIONS

This is not unexpected as increased ALP activity is correlated to enhanced ECM production which can be verified by the increased levels of collagen production. Thus it can be speculated that the dynamic stimuli improves both cellular activity to produce matrix as well as actual protein production through collagen.

Matrix Mineralization

Once the production of mature matrix has occurred, as apparent through collagen deposition, matrix mineralization commences. There are a number of cellular cues involved in the late stages of osteoblast development, specifically related to the process of matrix mineralization such as osteocalcin and decorin. Osteocalcin is a bone matrix specific protein which is expressed throughout the production of ECM. Data showed a bimodal expression of osteocalcin with peak expressions displayed at days 7 and 21 for both static and dynamic cases. However, interestingly, the expression of osteocalcin in the dynamic series is greater than that of the static.

Thus it may be concluded that the dynamic conditions influenced the production of bone specific matrix proteins but did not affect the modulation of such genes. Decorin is more specifically expressed during the late stages of ECM production and is related to the mineralization stage of the bone matrix. From the data it can be seen that in the static condition there is a gradual increase in expression from early to late in the culture period. This is not unexpected as decorin is usually correlated to the amount of collagen present in the culture. Yet, a different behavior was observed in the dynamic

RESULTS AND DISCUSSIONS

case, in which decorin displayed a peak expression at day 14 and then diminished. Likely, this is a result of the early expression of collagen in the dynamic series and thus resulting in a maximum expression at day 14.

Summarizing, the PCR test performed evidences that dynamic stimulation during cell culture leads to the modification of genes expression connected to matrix production. Application of mechanical stimuli, thus, strongly influences cell activity during the culture in *in-vitro* experiments.

5. FINAL REMARKS

The object of this thesis work was the design and the development of a bioreactor system for tissue engineering applications. These kind of systems are becoming widely studied and exploited because, by using them during cell culture, additional fundamental parameters and external cell stimulation can be introduced, guiding the cell culture method in a more advanced way, more similar to the *in vivo* conditions. Basically, the improvements introduced by bioreactors are related to the reduced times needed for cell migration/proliferation. Furthermore, by adding external stimuli to the seeded scaffolds, cells activation can be stimulated.

The designed bioreactors were optimized, in terms of software development and structural components engineering. Different configurations for specific applications and needs were also considered.

In particular, the produced bioreactors were tested for cartilage and bone tissue engineering applications and different experimental procedures were used after a proper optimization of processing parameters

Therefore, bioreactors resulted promising and potentially powerful systems, able to perform a cell culture under dynamic conditions influencing cell behaviour and proliferation. Both chondrocytes and osteoblasts cell cultured were subjected by this culture method able to mimic the physiological

FINAL REMARKS

conditions; moreover, osteoblasts activity was also heavily affected by the bioreactor stimuli, resulting faster and extremely sensitive to the external environment.

6. REFERENCES

- 1 Langer, R. and Vacanti, J. P. (1993) Tissue Engineering *Science* **260**, 920-6
- 2 Martin, I., Wendt, D. and Heberer, M. (2004) The role of bioreactors in tissue engineering *Trends in Biotechnology* **22**, 80-6
- 3 Griffith, L. G. and Naughton, G. (2002) Tissue Engineering--Current Challenges and Expanding Opportunities *Science* **295**, 1009-14
- 4 Mow, V. C., Kuei, S. C., Lai, W. M. and Armstrong, C. G. (1980) Biphasic Creep and Stress Relaxation of Articular Cartilage in Compression: Theory and Experiments *Journal of Biomechanical Engineering* **102**, 73-84
- 5 Mow, V. C., Ratcliffe, A. and Woo, S. L. (1990) Biomechanics of Diarthrodial Joints **Volume 1**,
- 6 Martin, R. B., Burr, D. B. and Sharkey, N. A. (1998) Skeletal tissue mechanics,
- 7 Bentley, G. and Minas, T. (2000) Treating joint damage in young people *BMJ* **320**, 1585-8
- 8 Mow, V. C., Ratcliffe, A. and Robin Poole, A. (1992) Cartilage and diarthrodial joints as paradigms for hierarchical materials and structures *Biomaterials* **13**, 67-97
- 9 Nordin, D. M. and Frankel, V. H. (2001) Basic biomechanics of the musculoskeletal system,
- 10 Buckwalter, J. A., Mow, V. C. and Ratcliffe, A. (1994) Restoration of Injured or Degenerated Articular Cartilage *J Am Acad Orthop Surg* **2**, 192-201
- 11 Beris, A. E., Lykissas, M. G., Papageorgiou, C. D. and Georgoulis, A. D. (2005) Advances in articular cartilage repair *Injury Proceedings from the 2nd European Symposium on Bone and Tissue Regeneration 25-27 November 2005* **36**, S14-S23
- 12 Curl, W. W., Krome, J., Gordon, E. S., Rushing, J., Smith, B. P. and Poehling, G. G. (1997) Cartilage injuries: A review of 31,516 knee

REFERENCES

- arthroscopies *Arthroscopy: The Journal of Arthroscopic & Related Surgery* **13**, 456-60
- 13 Obradovic, B., Martin, I., Padera, R. F., Treppo, S., Freed, L. E. and Vunjak-Novakovic, G. (2001) Integration of engineered cartilage *Journal of Orthopaedic Research* **19**, 1089-97
- 14 Risbud, M. V. and Sitterling, M. (2002) Tissue engineering: advances in in vitro cartilage generation *Trends in Biotechnology* **20**, 351-6
- 15 Sikavitsas, V. I., N., B. G. and G., M. A. (2002) Formation of three-dimensional cell/polymer constructs for bone tissue engineering in a spinner flask and a rotating wall vessel bioreactor. *Journal of biomedical materials research* **62**, 136-48
- 16 Burg, K. J. L., Porter, S. and Kellam, J. F. (2000) Biomaterial developments for bone tissue engineering *Biomaterials* **21**, 2347-59
- 17 Hutmacher, D. W. (2000) Scaffolds in tissue engineering bone and cartilage *Biomaterials* **21**, 2529-43
- 18 Lubiatuski, P., Kruczynski, J., Gradys, A., Trzeciak, T. and Jaroszewski, J. (2006) Articular Cartilage Repair by Means of Biodegradable Scaffolds *Transplantation Proceedings* **38**, 320-2
- 19 Behravesh, E., Yasko, A. W., Engel, P. S. and Mikos, A. G. (1999) Synthetic biodegradable polymers for orthopaedic applications *Clinical Orthopaedics & Related Research* **367**, 118-29
- 20 Brittberg, M., Lindahl, A., Nilsson, A., Ohlsson, C., Isaksson, O. and Peterson, L. (1994) Treatment of deep cartilage defects in the knee with autologous chondrocyte transplantation *N Engl J Med* **331**, 889-95
- 21 Buckwalter, J. A. (1998) Articular cartilage: injuries and potential for healing *J Orthop Sports Phys Ther* **28**, 192-202
- 22 Redaelli, A. and Montevicchi, F. (2007) Biomeccanica Analisi Multiscala di tessuti Biologici,
- 23 Salzstein, R. A., Pollack, S. R., Mak, A. F. and Petrov, N. (1987) Electromechanical potentials in cortical bone *J Biomech.* **20**, 261-80
- 24 Zeng, Y., Cowin, S. C. and Weinbaum, S. (1994) A fiber matrix model for fluid flow and streaming potentials in the canaliculi of an osteon *Annals of Biomedical Engineering* **22**, 280-92
- 25 You, L., Cowin, S. C., Schaffler, M. B. and Weinbaum, S. (2001) A model for strain amplification in the actin cytoskeleton of osteocytes

REFERENCES

- due to fluid drag on pericellular matrix *Journal of Biomechanics* **34**, 1375-86
- 26 Frost, H. M. (1983) A determinant of bone architecture. The minimum effective strain *Clin Orthop Relat Res* **175**, 286-92
- 27 Farmanullah, Khan, M. S. and Awais, S. M. (2007) Evaluation of management of tibial non-union defect with Ilizarov fixator *J Ayub Med Coll Abbottabad* **19**, 34-6
- 28 Brown, K. L. and Cruess, R. L. (1982) Bone and cartilage transplantation in orthopaedic surgery. A review *J Bone Joint Surg Am* **64**, 270-9
- 29 Hutmacher, D. W. (2000) Polymeric scaffolds in tissue engineering bone and cartilage *Biomaterials* **21**, 2529-43
- 30 Butler, D. L., A., G. S. and F., G. (2000) Functional Tissue Engineering: The Role of Biomechanics *Journal of Biomechanical Engineering* **122**, 570-5
- 31 Altman, G. H., Lu, H. H., Horan, R. L., Calabro, T., Ryder, D. and Kaplan, D., L. (2002) Advanced Bioreactor with Controlled Application of Multi-Dimensional Strain For Tissue Engineering *Journal of Biomechanical Engineering* **124**, 80-6
- 32 Huang, C.-Y. C., Hagar, K. L., Frost, L. E., Sun, Y. and Cheung, H. S. (2004) Effects of Cyclic Compressive loading on Chondrogenesis of Rabbit Bone-Marow Derived Mesenchymal Stem Cells *Stem Cells* **22**, 313-23
- 33 De Croos, J. N. A., Dhaliwal, S. S., Gryn timer, M. D., Pilliar, R. M. and Kandel, R. A. (2006) Cyclic compressive mechanical stimulation induces sequential catabolic and anabolic gene changes in chondrocytes resulting in increased extracellular matrix accumulation *Matrix Biology* **25**, 323-31
- 34 Chang, C.-H., Lin, C.-C., Chou, C.-H., Lin, F.-H. and Liu, H.-C. (2005) Novel Bioreactors for Osteochondral tissue engineering *Biomedical Engineering Applications, Basis & Communications* **17**, 38-43
- 35 Pörtner, R., Nagel-Heyer, S., Goepfert, C., Adamietz, P. and Meenen, N. M. (2005) Bioreactor design for tissue engineering *Journal of Bioscience and Bioengineering* **100**, 235-45

REFERENCES

- 36 Chen, H.-C. and Hu, Y.-C. (2006) Bioreactors for tissue engineering
Biotechnology Letters **28**, 1415-23
- 37 Démarteau, O., Jakob, M., Schäfer, D., Heberer, M. and Martin, I.
(2003) Development and validation of a bioreactor for physical
stimulation of engineered cartilage *Biorheology* **40**, 331-6
- 38 Chaudhuri, J. and Al-Rubeai, M. (2005) Bioreactors for Tissue
Engineering: Principles, Design and Operation *Springer eds.*,
- 39 Bancroft, G. N., Sikavitsas, V. I. and Mikos, A. G. (2003) Design of
a Flow Perfusion Bioreactor System for Bone Tissue-Engineering
Applications *Tissue Engineering* **9**, 549-54
- 40 Pazzano, D., Mercier, K. A., Moran, J. M., Fong, S. S., Dibiasio, D.
D., Rulfs, J. X., et al. (2000) Comparison of Chondrogenesis in Static
and Perfused Bioreactor Culture *Biotechnology Progress* **16**, 893-6
- 41 Watanabe, S., Inagaki, S., Kinouchi, I., Takai, H., Masuda, Y. and
Mizuno, S. (2005) Hydrostatic pressure/perfusion culture system
designed and validated for engineering tissue *Journal of Bioscience
and Bioengineering* **100**, 105-11
- 42 Basso, N. and Heersche, J. N. M. (2002) Characteristics of in vitro
osteoblastic cell loading models *Bone* **30**, 347-51
- 43 Waldman, S. D., Spiteri, C. G., Gryn timer, M. D., Pilliar, R. M. and
Kandel, R. A. (2003) Long-term intermittent shear deformation
improves the quality of cartilaginous tissue formed in vitro *Journal
of Orthopaedic Research* **21**, 590-6
- 44 Frank, E. H., Jin, M., Loening, A. M., Levenston, M. E. and
Grodzinsky, A. J. (2000) A versatile shear and compression
apparatus for mechanical stimulation of tissue culture explants
Journal of Biomechanics **33**, 1523-7
- 45 Fehrenbacher, A., Steck, E., Rickert, M., Roth, W. and Richter, W.
(2003) Rapid regulation of collagen but not metalloproteinase 1, 3,
13, 14 and tissue inhibitor of metalloproteinase 1, 2, 3 expression in
response to mechanical loading of cartilage explants in vitro
Archives of Biochemistry and Biophysics **410**, 39-47
- 46 Torzilli, P. A., Grigienė, R., Huang, C., Friedman, S. M., Doty, S.
B., Boskey, A. L., et al. (1997) Characterization of cartilage
metabolic response to static and dynamic stress using a mechanical
explant test system *Journal of Biomechanics* **30**, 1-9

REFERENCES

- 47 Hansen, U., Schünke, M., Domm, C., Ioannidis, N., Hassenpflug, J., Gehrke, T., et al. (2001) Combination of reduced oxygen tension and intermittent hydrostatic pressure: a useful tool in articular cartilage tissue engineering *Journal of Biomechanics* **34**, 941-9
- 48 Suh, J.-K., Baek, G. H., Arøen, A., Malin, C. M., Niyibizi, C., Evans, C. H., et al. (1999) Intermittent sub-ambient interstitial hydrostatic pressure as a potential mechanical stimulator for chondrocyte metabolism *Osteoarthritis and Cartilage* **7**, 71-80
- 49 Ignatius, A., Blessing, H., Liedert, A., Schmidt, C., Neidlinger-Wilke, C., Kaspar, D., et al. (2005) Tissue engineering of bone: effects of mechanical strain on osteoblastic cells in type I collagen matrices *Biomaterials* **26**, 311-8
- 50 Parkkinen, J. J., Lammi, M. J., Helminen, H. J. and Tammi, M. (1992) Local Stimulation of Proteoglycan Synthesis in Articular Cartilage Explants by Dynamic Compression In Vitro *Journal of Orthopaedic Research* **10**, 610-20
- 51 Kisiday, J. D., Jin, M., Dimicco, M. A., Kurz, B. and Grodzinsky, A. J. (2004) Effects of dynamic compressive loading on chondrocyte biosynthesis in self-assembling peptide scaffolds *Journal of Biomechanics* **37**, 595-604
- 52 Mauck, R. L., Soltz, M. A., Wang, C. C. B., Wong, D. D., Chao, P.-H. G., Valhmu, W. B., et al. (2000) Functional Tissue Engineering of Articular Cartilage Through Dynamic Loading of Chondrocyte-Seeded Agarose Gels *Journal of Biomechanical Engineering* **122**, 252-60
- 53 Davisson, T., Kunig, S., Chen, A., Sah, R. and Ratcliffe, A. (2002) Static and dynamic compression modulate matrix metabolism in tissue engineered cartilage *Journal of Orthopaedic Research* **20**, 842-8
- 54 Gavénis, K., Kremer, A., Vonwaller, M., Hollander, D. A., Schneider, U. and Schmidt-Rohlfing, B. (2007) Effects of Cyclic Hydrostatic Pressure on the Metabolism of Human Osteoarthritic Chondrocytes Cultivated in a Collagen Gel *Artificial Organs* **31**, 91-8

REFERENCES

- 55 Elder, B. D. and Athanasiou, K. A. (2009) Hydrostatic Pressure in Articular Cartilage Tissue Engineering: From Chondrocytes to Tissue Regeneration *Tissue Engineering: Part B* **15**, 43-53
- 56 Nagatomi, J., Arulanandam, B. P., Metzger, D. W., Meunier, A. and Bizios, R. (2001) Frequency- and Duration-Dependent Effects of Cyclic Pressure on Select Bone Cell Functions *Tissue Engineering* **7**, 717-28
- 57 Roelofsen, J., Klein-Nulend, J. and Burger, E. H. (1995) Mechanical stimulation by intermittent hydrostatic compression promotes bone-specific gene expression in vitro *Journal of Biomechanics* **28**, 1493-503
- 58 Macdonald, A. G. and Fraser, P. J. (1999) The transduction of very small hydrostatic pressures *Comparative Biochemistry and Physiology - Part A: Molecular & Integrative Physiology* **122**, 13-36
- 59 Downey, D. J., Simkin, P. A. and Taggart, R. (1988) The effect of compressive loading on intraosseous pressure in the femoral head in vitro *Journal of Bone and Joint Surgery* **70**, 871-7
- 60 Waldman, S. D., Couto, D. C., Grynypas, M. D., Pilliar, R. M. and Kandel, R. A. (2006) A single application of cyclic loading can accelerate matrix deposition and enhance the properties of tissue-engineered cartilage *Osteoarthritis and Cartilage* **14**, 323-30
- 61 Yamamoto, K., Tomita, N., Fukuda, Y., Suzuki, S., Igarashi, N., Suguro, T., et al. (2007) Time-dependent changes in adhesive force between chondrocytes and silk fibroin substrate *Biomaterials* **28**, 1838-46
- 62 Batra, N. N., Li, Y. J., Yellowley, C. E., You, L., Malone, A. M., Kim, C. H., et al. (2005) Effects of short-term recovery periods on fluid-induced signaling in osteoblastic cells *Journal of Biomechanics* **38**, 1909-17
- 63 Robling, A. G., Burr, D. B. and Turner, C. H. (2000) Partitioning a Daily Mechanical Stimulus into Discrete Loading Bouts Improves the Osteogenic Response to Loading *Journal of Bone and Mineral Research* **15**, 1596-602
- 64 Srinivasan, S., Weimer, D. A., Agans, S. C., Bain, S. D. and Gross, T. S. (2002) Low-Magnitude Mechanical Loading Becomes

REFERENCES

- Osteogenic When Rest Is Inserted Between Each Load Cycle
Journal of Bone and Mineral Research **17**, 1613-20
- 65 Vunjak-Novakovic, G., Martin, I., Obradovic, B., Treppo, S., Grodzinsky, A. J., Langer, R., et al. (1999) Bioreactor Cultivation Conditions Modulate the Composition and Mechanical Properties of Tissue-Engineered Cartilage *Journal of Orthopaedic Research* **17**, 130-8
- 66 Papoutsakis, E. T. (1991) Fluid-mechanical damage of animal cells in bioreactors *Trends in Biotechnology* **9**, 427-37
- 67 Vunjak-Novakovic, G., Obradovic, B., Martin, I., Bursac, P. M., Langer, R. and Freed, L. E. (1998) Dynamic Cell Seeding of Polymer Scaffolds for Cartilage Tissue Engineering *Biotechnology Progress* **14**, 193-202
- 68 Vunjak-Novakovic, G., Freed, L. E., Biron, R. J. and Langer, R. (1996) Effects of Mixing on the Composition and Morphology of Tissue-Engineered Cartilage *AIChE Journal* **42**, 850-60
- 69 Hollister, S. J. (2005) Porous scaffold design for tissue engineering **4**, 518-24
- 70 Mikos, A. G. and Temenoff, J. S. (2000) Formation of highly porous biodegradable scaffolds for tissue engineering *Electron. J. Biotechnol.* **3**, 23-4
- 71 Motta, A., Maniglio, D., Merzari, E., Foss, C., Bella, E. and Migliaresi, C. (2008) Multicomponent scaffold for osteochondral defect tissue engineering *TERMIS 2008*,
- 72 Schieker, M., Seitz, H., Drosse, I., Seitz, S. and Mutschler, W. (2006) Biomaterials as Scaffold for Bone Tissue Engineering *European Journal of Trauma* **32**, 114-24
- 73 Tateishi, T., Chen, G. and Ushida, T. (2002) Biodegradable porous scaffolds for tissue engineering *Journal of Artificial Organs* **5**, 77-83
- 74 Thomson, R. C., Yaszemski, M. J., Powers, J. M. and Mikos, A. G. (1996) Fabrication of biodegradable polymer scaffolds to engineer trabecular bone *Journal of Biomaterials Science, Polymer Edition* **7**, 23-38
- 75 Vacanti, J. P. and Langer, R. (1997) Synthetic Biodegradable Polymer Scaffolds,

REFERENCES

- 76 Vats, A., Tolley, N. S., Polak, J. M. and Gough, J. E. (2002) Scaffolds and biomaterials for tissue engineering: a review of clinical applications *Clinical Otolaryngology & Allied Sciences* **28**, 165-72
- 77 O'Brien, F. J., Harley, B. A., Yannas, I. V. and Gibson, L. J. (2005) The effect of pore size on cell adhesion in collagen-GAG scaffolds *Biomaterials* **26**, 433-41
- 78 Shin, M., Abukawa, H., Troulis, M. J. and Vacanti, J. P. (2008) Development of a biodegradable scaffold with interconnected pores by heat fusion and its application to bone tissue engineering *Journal of Biomedical Materials Research Part A* **84A**, 702-9
- 79 Athanasiou, K. A., Niederauer, G. G. and Agrawal, C. M. (1996) Sterilization, toxicity, biocompatibility and clinical applications of polylactic acid/ polyglycolic acid copolymers *Biomaterials* **17**, 93-102
- 80 Chun, H. J., Kim, G. W. and Kim, C. H. (2008) Fabrication of porous chitosan scaffold in order to improve biocompatibility *Journal of Physics and Chemistry of Solids* **69**, 1573-6
- 81 Grizzi, I., Garreau, H., Li, S. and Vert, M. (1995) Hydrolytic degradation of devices based on poly(DL-lactic acid) size-dependence *Biomaterials* **16**, 305-11
- 82 Ho, K. G., Pometto, A. L. and N, H. P. (1999) Effects of Temperature and Relative Humidity on Polylactic Acid Plastic Degradation *Journal of Environmental Polymer Degradation* **7**, 83-92
- 83 Hongfan, S., Lin, M., Cunxian, S., Xiumin, C. and Pengyan, W. (2006) The in vivo degradation, absorption and excretion of PCL-based implant *Biomaterials* **27**, 1735-40
- 84 Jenkins, M. J. and Harrison, K. L. (2008) The effect of crystalline morphology on the degradation of polycaprolactone in a solution of phosphate buffer and lipase *Polymers for Advanced Technologies* **19**, 1901-6
- 85 Williams, D. F. and Zhong, S. P. (1994) Biodeterioration/biodegradation of polymeric medical devices in situ *Int. Biodeter. Biodegrad.* **95**,

REFERENCES

- 86 Zhang, X., Espiritu, M., Bilyk, A. and Kurniawan, L. (2008) Morphological behaviour of poly(lactic acid) during hydrolytic degradation *Polymer Degradation and Stability* **93**, 1964-70
- 87 Giordano, C., Russell, A., Wu, B. M., Borlanda, S. W., Cima, L. G., Sachs, E. M., et al. (1997) Mechanical properties of dense polylactic acid structures fabricated by three dimensional printing *Biomaterials Science* **8**, 63-75
- 88 Martin, I., Obradovic, B., Treppo, S., Grodzinsky, A. J., Langer, R., Freed, L. E., et al. (2000) Modulation of the mechanical properties of tissue engineered cartilage *Biorheology* **37**, 141-7
- 89 Schlichting, K., Schell, H., Kleemann, R. U., Schill, A., Weiler, A., Duda, G. N., et al. (2008) Influence of Scaffold Stiffness on Subchondral Bone and Subsequent Cartilage Regeneration in an Ovine Model of Osteochondral Defect Healing *The American Journal of Sports Medicine* **36**, 2379-91
- 90 Garlotta, D. (2002) A Literature Review of Poly(Lactic Acid) *Journal of Polymers and the Environment* **9**, 63-84
- 91 Ghosh, S., Viana, J. C., Reis, R. L. and Mano, J. F. (2008) Development of porous lamellar poly(l-lactic acid) scaffolds by conventional injection molding process *Acta Biomaterialia* **4**, 887-96
- 92 Hong, Z., Reis, R. L. and Mano, J. F. (2008) Preparation and in vitro characterization of scaffolds of poly(l-lactic acid) containing bioactive glass ceramic nanoparticles *Acta Biomaterialia* **4**, 1297-306
- 93 Kim, S. Y., Kanamori, T., Noumi, Y., Wang, P. C. and Shinbo, T. (2004) Preparation of porous poly(D,L-lactide) and poly(D,L-lactide-co-glycolide) membranes by a phase inversion process and investigation of their morphological changes as cell culture scaffolds *Journal of Applied Polymer Science* **92**, 2082-92
- 94 Li, S. and Mccarthy, S. (1999) Further investigations on the hydrolytic degradation of poly(DL-lactide) *Biomaterials* **20**, 35-44
- 95 Pluta, M. and Galeski, A. (2007) Plastic Deformation of Amorphous Poly(l/dl-lactide): Structure Evolution and Physical Properties *Biomacromolecules* **8**, 1836-43

REFERENCES

- 96 Yilgor, P., Sousa, R. A., Reis, R. L., Hasirci, N. and Hasirci, V. (2008) 3D Plotted PCL Scaffolds for Stem Cell Based Bone Tissue Engineering *Macromolecular Symposia* **269**, 92-9
- 97 Zhang, Y. Z., Huang, Z. M., Xu, X., Lim, C. T. and Ramakrishna, S. (2004) Preparation of Core-Shell Structured PCL-r-Gelatin Bi-Component Nanofibers by Coaxial Electrospinning *Chemistry of Materials* **16**, 3406-9
- 98 Vozzi, G., Flaim, C., Ahluwalia, A. and Bhatia, S. (2003) Fabrication of PLGA scaffolds using soft lithography and microsyringe deposition *Biomaterials* **24**, 2533-40
- 99 Vozzi, G., Flaim, C. J., Bianchi, F., Ahluwalia, A. and Bhatia, S. (2002) Microfabricated PLGA scaffolds: a comparative study for application to tissue engineering *Materials Science and Engineering: C* **20**, 43-7
- 100 Yang, F., Cui, W., Xiong, Z., Liu, L., Bei, J. and Wang, S. (2006) Poly(1,1-lactide-co-glycolide)/tricalcium phosphate composite scaffold and its various changes during degradation in vitro *Polymer Degradation and Stability* **91**, 3065-73
- 101 Pamula, E. and Menaszek, E. (2008) In vitro and in vivo degradation of poly(1-lactide-co-glycolide) films and scaffolds *Journal of Materials Science: Materials in Medicine* **19**, 2063-70
- 102 Mooney, D. J., Baldwin, D. F., P., S. N., Vacanti, J. P. and Langer, R. (1996) Novel approach to fabricate porous sponges of poly(D,L-lactic-co-glycolic acid) without the use of organic solvents *Biomaterials* **17**, 1417-22
- 103 Heden, P., Sellman, G., Von Wachenfeldt, M., Olenius, M. and Fagrell, D. (2009) Body Shaping and Volume Restoration: The Role of Hyaluronic Acid *Aesthetic Plastic Surgery* **33**, 274-82
- 104 Marcacci, M., Kon, E., Zaffagnini, S., Iacono, F., Filardo, G. and Delcogliano, M. (2006) Autologous Chondrocytes in a Hyaluronic Acid Scaffold *Operative Techniques in Orthopaedics* **16**, 266-70
- 105 Holzman, S. and Connolly, R. J. (1994) Effect of Hyaluronic Acid Solution on Healing of Bowel Anastomoses *Journal of Investigative Surgery* **7**, 431 - 7
- 106 Giordano, C., Sanginario, V., Ambrosio, L., Silvio, L. D. and Santin, M. (2006) Chemical-Physical Characterization and in vitro

REFERENCES

- Preliminary Biological Assessment of Hyaluronic Acid Benzyl Ester-Hydroxyapatite Composite *J Biomater Appl* **20**, 237-52
- 107 Zhong, S. P., Teo, W. E., Zhu, X., Beuerman, R., Ramakrishna, S. and Yung, L. Y. L. (2007) Development of a novel collagen-GAG nanofibrous scaffold via electrospinning *Materials Science and Engineering: C* **27**, 262-6
- 108 Mandal, B. B. and Kundu, S. C. (2009) Cell proliferation and migration in silk fibroin 3D scaffolds *Biomaterials* **15**, 2956-65
- 109 Motta, A., Migliaresi, C., Lloyd, A. W., Denyer, S. P. and Santin, M. (2002) Serum protein adsorption on silk fibroin fibres and membranes: surface opsonization and binding strength *Journal of bioactive and compatible polymers* **17**, 23-35
- 110 Silva, S. S., Motta, A., Rodrigues, M. T., Pinheiro, A. F., Gomes, M. E., Mano, J. F., et al. (2008) Novel genipin-cross-linked chitosan/silk fibroin sponges for cartilage engineering strategies *Biomacromolecules* **9**, 2764-74
- 111 Motta, A., Fambri, L. and Migliaresi, C. (2002) Regenerated silk fibroin films: Thermal and dynamic mechanical analysis *Macromolecular Chemistry Physics* **203**,
- 112 Kaur, L., Singh, J. and Liu, Q. (2007) Starch – A Potential Biomaterial for Biomedical Applications *Nanomaterials and Nanosystems for Biomedical Applications*,
- 113 Lam, C. X. F., Mox, M., Teoh, S. H. and Hutmacher, D. W. (2002) Scaffold development using 3D printing with a starch-based polymer *Materials Science and Engineering: C* **20**, 49-56
- 114 Pereira, C. S., Cunha, A. M., Reis, R. L., Vazquez, B. and San Roman, J. (1988) New starch-based thermoplastic hydrogels for use as bone cements or drug-delivery carriers *Journal of Materials Science: Materials in Medicine* **9**, 825-33
- 115 Duarte, A. R. C., Mano, J. F. and Reis, R. L. (2009) Preparation of starch-based scaffolds for tissue engineering by supercritical immersion precipitation *The Journal of Supercritical Fluids* **49**, 279-85
- 116 Buschmann, M. D., Gluzband, Y. A., Grodzinsky, A. J. and Hunziker, E. B. (1995) Mechanical compression modulates matrix biosynthesis in chondrocyte/agarose culture *J Cell Sci* **108**, 1497-508

REFERENCES

- 117 Rahfoth, B., Weisser, J., Sternkopf, F., Aigner, T., Von Der Mark, K. and Bräuer, R. (1998) Transplantation of allograft chondrocytes embedded in agarose gel into cartilage defects of rabbits *Osteoarthritis Cartilage* **6**, 50-65
- 118 Benya, P. D. and Shaffer, J. D. (1982) Dedifferentiated chondrocytes reexpress the differentiated collagen phenotype when cultured in agarose gels *Cell* **30**, 215-24
- 119 Wong, M. (2003) Alginates in Tissue Engineering 2003 238 77-86
- 120 Orive, G., Hernández, R. M., Gascón, A. R. and Pedraz, J. L. (2006) Encapsulation of Cells in Alginate Gels **22**, 345-55
- 121 Shapiro, L. and Cohen, S. (1997) Novel alginate sponges for cell culture and transplantation *Biomaterials* **18**, 583-90
- 122 Drury, J. L. and Mooney, D. J. (2003) Hydrogels for tissue engineering: scaffold design variables and applications *Biomaterials Synthesis of Biomimetic Polymers* **24**, 4337-51
- 123 Haycock, J. W. (2011) 3D cell culture: methods and protocols *Springer Protocols*, 17-39
- 124 Lv, Q. and Feng, Q. (2006) Preparation of 3-D regenerated fibroin scaffolds with freeze drying method and freeze drying/foaming technique *Journal of Materials Science: Materials in Medicine* **17**, 1349-56
- 125 Ma, D. and Mchugh, A. J. (2007) The interplay of phase inversion and membrane formation in the drug release characteristics of a membrane-based delivery system *Journal of Membrane Science* **298**, 156-68
- 126 Tsivintzelis, I., Pavlidou, E. and Panayiotou, C. (2007) Biodegradable polymer foams prepared with supercritical CO₂-ethanol mixtures as blowing agents *The Journal of supercritical fluids* **42**, 265-72
- 127 Tsivintzelis, I., Pavlidou, E. and Panayiotou, C. (2007) Porous scaffolds prepared by phase inversion using supercritical CO₂ as antisolvent: I. Poly(l-lactic acid) *The Journal of Supercritical Fluids* **40**, 317-22
- 128 Zong, X., Bien, H., Chung, C. Y., Yin, L., Fang, D., Hsiao, B. S., et al. (2005) Electrospun fine-textured scaffolds for heart tissue constructs *Biomaterials* **26**, 5330-8

REFERENCES

- 129 Liang, D., Hsiao, B. S. and Chu, B. (2007) Functional electrospun nanofibrous scaffolds for biomedical applications *Advanced Drug Delivery Reviews* **59**, 1392-412
- 130 Li, D. and Xia, Y. (2004) Electrospinning of Nanofibers: Reinventing the Wheel? *Advanced Materials* **16**, 1151-70
- 131 Huang, Z. M., Zhang, Y. Z., Kotaki, M. and Ramakrishna, S. (2003) A review on polymer nanofibers by electrospinning and their applications in nanocomposites *Composites Science and Technology* **63**, 2223-53
- 132 Hutmacher, D. W., Sittinger, M. and Risbud, M. V. (2004) Scaffold-based tissue engineering: rationale for computer-aided design and solid free-form fabrication systems *Trends in Biotechnology* **22**, 354-62
- 133 Vail, N. K., Swain, L. D., Fox, W. C., Aufdemorte, T. B., Lee, G. and Barlow, J. W. (1998) Solid Freeform fabrication proceedings *Materials for biomedical applications*, 621-8
- 134 Landers, R., John, H. and R., M. Scaffolds for tissue engineering applications fabricated by 3D plotting,
- 135 Sachs, E. M., Haggerty, J. S., Cima, M. J. and Williams, P. A. (1989) Three-dimensional printing techniques,
- 136 Masood, S. H. (2007) Application of fused deposition modelling in controlled drug delivery devices *Assembly Automation* **27**,
- 137 Rangamani, P. (2005) Bioprocessing conditions for improving material properties of tissue engineered cartilage *PhD thesis*, Georgia Institute of Technology,
- 138 Clark, C. C., Tolin, B. S. and Brighton, C. T. (1991) The effect of oxygen tension on proteoglycan synthesis and aggregation in mammalian growth plate chondrocytes *Journal of Orthopaedic Research* **9**, 477-84
- 139 Vittur, F., Grandolfo, M., Fragonas, E., Godeas, C., Paoletti, S., Pollesello, P., et al. (1994) Energy Metabolism, Replicative Ability, Intracellular Calcium Concentration, and Ionic Channels of Horse Articular Chondrocytes *Experimental Cell Research* **210**, 130-6
- 140 Coimbra, I. B., Jimenez, S. A., Hawkins, D. F., Piera-Velazquez, S. and Stokes, D. G. (2004) Hypoxia inducible factor-1 alpha

REFERENCES

- expression in human normal and osteoarthritic chondrocytes
Osteoarthritis and Cartilage **12**, 336-45
- 141 Lee, R. B. and Urban, J. P. (1997) Evidence for a negative Pasteur effect in articular cartilage *Biochem J.* **321**, 95-102
- 142 Obradovic, B., Carrier, R. L., Vunjak-Novakovic, G. and Freed, L. E. (1999) Gas exchange is essential for bioreactor cultivation of tissue engineered cartilage *Biotechnology and Bioengineering* **63**, 197-205
- 143 Rajpurohit, R., Koch, C. J., Tao, Z., Teixeira, C. M. and Shapiro, I. M. (1996) Adaptation of chondrocytes to low oxygen tension: relationship between hypoxia and cellular metabolism *J Cell Physiol* **168**, 424-32
- 144 Davisson, T., Sah, R. L. and Ratcliffe, A. (2002) Perfusion increases cell content and matrix synthesis in chondrocyte three-dimensional cultures *Tissue Engineering* **8**, 807-16
- 145 Vunjak-Novakovic, G., Martin, I., Obradovic, B., Treppo, S., Grodzinsky, A. J., Langer, R., et al. (1999) Bioreactor Cultivation Conditions Modulate the Composition and Mechanical Properties of Tissue-Engineered Cartilage *J Orthop Res* **17**, 130-8
- 146 Vunjak-Novakovic, G., Obradovic, B., Martin, I., Bursac, P. M., Langer, R. and Freed, L. E. (1998) Dynamic Cell Seeding of Polymer Scaffolds for Cartilage Tissue Engineering *Biotechnology Progress* **14**, 193-202
- 147 Blunk, T., Sieminski, A. L., Gooch, K. J., Courter, D. L., Hollander, A. P., Nahir, A. M., et al. (2002) Differential Effects of Growth Factors on Tissue-Engineered Cartilage *Tissue Engineering* **8**, 73-84
- 148 Gooch, K. J., Blunk, T., Courter, D. L., Sieminski, A. L., Bursac, P. M., Vunjak-Novakovic, G., et al. (2001) IGF-I and Mechanical Environment Interact to Modulate Engineered Cartilage Development *Biochemical and Biophysical Research Communications* **286**, 909-15
- 149 Sittinger, M., Bujia, J., Minuth, W. W., Hammer, C. and Burmester, G. R. (1994) Engineering of cartilage tissue using bioresorbable polymer carriers in perfusion culture *Biomaterials* **15**, 451-6

REFERENCES

- 150 Begley, C. M. and Kleis, S. J. (2000) The fluid dynamic and shear environment in the NASA/JSC rotating-wall perfused-vessel bioreactor *Biotechnology and Bioengineering* **70**, 32-40
- 151 Begley, C. M. and Kleis, S. J. (2002) RWPV bioreactor mass transport: Earth-based and in microgravity *Biotechnology and Bioengineering* **80**, 465-76
- 152 Saini, S. and Wick, T. M. (2003) Concentric Cylinder Bioreactor for Production of Tissue Engineered Cartilage: Effect of Seeding Density and Hydrodynamic Loading on Construct Development *Biotechnology Progress* **19**, 510-21
- 153 Prendergast, P. J. and Mchugh, P. E. (2004) Topics in Bio-Mechanical Engineering *Trinity Centre for Bioengineering & National Centre for Biomedical Engineering Science*, 94-146
- 154 Darling, E. M. and Athanasiou, K. A. (2003) Articular Cartilage Bioreactors and Bioprocesses *Tissue Engineering* **9**, 9-26
- 155 Kim, Y. J., Sah, R. L. Y., Grodzinsky, A. J., Plaas, A. H. K. and Sandy, J. D. (1994) Mechanical Regulation of Cartilage Biosynthetic Behavior: Physical Stimuli *Archives of Biochemistry and Biophysics* **311**, 1-12
- 156 Takahashi, I., Nuckolls, G. H., Takahashi, K., Tanaka, O., Semba, I., Dashner, R., et al. (1998) Compressive force promotes sox9, type II collagen and aggrecan and inhibits IL-1 β expression resulting in chondrogenesis in mouse embryonic limb bud mesenchymal cells *J Cell Sci* **111**, 2067-76
- 157 Lee, D. A., Noguchi, T., Frean, S. P., Lees, P. and Bader, D. L. (2000) The influence of mechanical loading on isolated chondrocytes seeded in agarose constructs *Biorheology* **37**, 149-61
- 158 Mauck, R. L., Soltz, M. A., Wang, C. C., Wong, D. D., Chao, P. H., Valhmu, W. B., et al. (2000) Functional tissue engineering of articular cartilage through dynamic loading of chondrocyte-seeded agarose gels *J Biomech Eng* **122**, 252-60
- 159 Démarteau, O., Wendt, D., Braccini, A., Jakob, M., Schäfer, D., Heberer, M., et al. (2003) Dynamic compression of cartilage constructs engineered from expanded human articular chondrocytes *Biochemical and Biophysical Research Communications* **310**, 580-8

REFERENCES

- 160 Démarteau, O., Jakob, M., Schäfer, D., Heberer, M. and Martin, I. (2003) Development and validation of a bioreactor for physical stimulation of engineered cartilage *Biorheology* **40**, 331-6
- 161 Lee, J. W., Kim, Y. H., Kim, S. H., Han, S. H. and Hahn, S. B. (2004) Chondrogenic differentiation of mesenchymal stem cells and its clinical applications *Yonsei Med J* **45**, 41-7
- 162 De Witt, M. T., Handley, C. J., Oakes, B. W. and Lowther, D. A. (1984) In vitro response of chondrocytes to mechanical loading. The effect of short term mechanical tension *Connective Tissue Research* **12**, 97-109
- 163 Parkkinen, J. J., Ikonen, J., Lammi, M. J., Laakkonen, J., Tammi, M. and Helminen, H. J. (1993) Effects of Cyclic Hydrostatic Pressure on Proteoglycan Synthesis in Cultured Chondrocytes and Articular Cartilage Explants *Archives of Biochemistry and Biophysics* **300**, 458-65
- 164 Ikenoue, T., Trindade, M. C. D., Lee, M. S., Lin, E. Y., Schurman, D. J., Goodman, S. B., et al. (2003) Mechanoregulation of human articular chondrocyte aggrecan and type II collagen expression by intermittent hydrostatic pressure in vitro *Journal of Orthopaedic Research* **21**, 110-6
- 165 Carver, S. E. and Heath, C. A. (1999) Increasing extracellular matrix production in regenerating cartilage with intermittent physiological pressure *Biotechnology and Bioengineering* **62**, 166-74
- 166 Heath, C. A. (2000) The effects of physical forces on cartilage tissue engineering *Biotechnol Genet Eng Rev* **17**, 533-51
- 167 Glowacki, J., Mizuno, S. and Greenberger, J. S. (1998) Perfusion Enhances Functions of Bone Marrow Stromal Cells in Three-Dimensional Culture *Cell Transplantation* **7**, 319-26
- 168 Sailon, A. M., Allori, A. C., Davidson, E. H., Reformat, D. D., Allen, R. J. and Warren, S. M. (2009) A novel flow-perfusion bioreactor supports 3D dynamic cell culture *J Biomed Biotechnol* **2009**, 1-7
- 169 Duncan, R. L. and Turner, C. H. (1995) Mechanotransduction and the functional response of bone to mechanical strain *Calcified Tissue International* **57**, 344-58

REFERENCES

- 170 Yang, Y., Magnay, J. L., Cooling, L. and El Haj, A. J. (2002) Development of a 'mechano-active' scaffold for tissue engineering *Biomaterials* **23**, 2119-26
- 171 Shelton, R. M. and El Haj, A. J. (1992) A novel microcarrier bead model to investigate bone cell responses to mechanical compression in vitro *Journal of Bone and Mineral Research* **7**, 403-5
- 172 Van't Hof, R. J. and Ralston, S. H. (2001) Nitric oxide and bone *Immunology* **103**, 255-61
- 173 Altman, G. H., Diaz, F., Jakuba, C., Calabro, T., Horan, R. L., Chen, J., et al. (2003) Silk-based biomaterials *Biomaterials* **24**, 401-16
- 174 Vepari, C. and Kaplan, D. L. (2007) Silk as a biomaterial *Progress in Polymer Science Polymers in Biomedical Applications* **32**, 991-1007
- 175 Kim, U.-J., Park, J. H., Joo Kim, H., Wada, M. and Kaplan, D. L. (2005) Three-dimensional aqueous-derived biomaterial scaffolds from silk fibroin *Biomaterials* **26**, 2775-85
- 176 Wang, Y., Kim, H.-J., Vunjak-Novakovic, G. and Kaplan, D. L. (2006) Stem cell-based tissue engineering with silk biomaterials *Biomaterials* **27**, 6064-82
- 177 Bostman, O., Partio, E., Hirvensalo, E. and Rokkanen, P. (1992) Foreign-body reactions to polyglycolide screws *Acta Orthopaedica* **63**, 173 - 6
- 178 Monteforte, S. (2005) Elettrofilatura (electrospinning) di polimeri di interesse biomedico *Università degli Studi di Trento, Master thesis*
- 179 Lanza, R., Langer, R. and Vacanti, J. (2007) Principles of Tissue Engineering (3rd Edition) *Elsevier Academic Press*
- 180 Pfaffla, M. W. (2001) A new mathematical model for relative quantification in real-time RT-PCR *Nucleic Acids Res* **29**, 2002-7
- 181 Livak, K. J. and Schmittgen, T. D. (2001) Analysis of Relative Gene Expression Data Using Real-Time Quantitative PCR and the 2- $^{-\Delta\Delta CT}$ Method *Methods* **25**, 402-8
- 182 Foss, C. (2008) Scaffold multicomponente per la rigenerazione del difetto osteocondrale: proprietà fisiche e biologiche in condizioni di coltura dinamiche *Università degli Studi di Trento, Master thesis*

REFERENCES

- 183 Carletti, E., Endogan, T., Hasirci, N., Hasirci, V., Maniglio, D., Motta, A., et al. (In press) Microfabrication of PDLLA Scaffolds *Tissue Engineering and Regenerative Medicine*
- 184 Hsu, S.-H., Tsai, I.-J., Lin, D.-J. and Chen, D. C. (2005) The effect of dynamic culture conditions on endothelial cell seeding and retention on small diameter polyurethane vascular grafts *Medical Engineering & Physics* **27**, 267-72
- 185 Mauck, R. L., Wang, C. C.-B., Oswald, E. S., Ateshian, G. A. and Hung, C. T. (2003) The role of cell seeding density and nutrient supply for articular cartilage tissue engineering with deformational loading *Osteoarthritis and Cartilage* **11**, 879-90
- 186 Stevens, M. M. and George, J. H. (2005) Exploring and Engineering the Cell Surface Interface *Science* **310**, 1135-8
- 187 Brown, T. D. (2000) Techniques for mechanical stimulation of cells in vitro: a review *Journal of Biomechanics* **33**, 3-14
- 188 Bancroft, G. N., Sikavitsas, V. I., Van Den Dolder, J., Sheffield, T. L., Ambrose, C. G., Jansen, J. A., et al. (2002) Fluid flow increases mineralized matrix deposition in 3D perfusion culture of marrow stromal osteoblasts in a dose-dependent manner *Proceedings of the National Academy of Sciences of the United States of America* **99**, 12600-5
- 189 Sittichokechaiwut, A., Scutt, A. M., Ryan, A. J., Bonewald, L. F. and Reilly, G. C. (2009) Use of rapidly mineralising osteoblasts and short periods of mechanical loading to accelerate matrix maturation in 3D scaffolds *Bone* **44**, 822-9
- 190 Setzer, B., Bächle, M., Metzger, M. C. and Kohal, R. J. (2009) The gene-expression and phenotypic response of hFOB 1.19 osteoblasts to surface-modified titanium and zirconia *Biomaterials* **30**, 979-90
- 191 Lecture of Prof. Scott J.Hollister, Biosolid Mechanics: Modeling and Applications, University of Michigan, USA.
- 192 Lecture of Prof. Ozan Akku, Biomedical Engineering: Cartilage, Purdue University, West Lafayette, IN, USA.
- 193 Lecture prof. Claudio Migliaresi, Cartilage and Cartilage repair, University of Trento, IT.

ACKNOWLEDGEMENTS

- My advisor, Dr. A. Motta for her assistance on the biological sections of this work;
- My co-advisor, Prof. C. Migliaresi for his intellectual and financial support;
- My parents, my brother and my friends, which have always supported, helped and encouraged me during these years;
- Lucia especially for her selfless help, support, assistance and food, without which I would never be able to finish;
- Eleonora for the support of my project and the thesis correction, Devid for the long discussions and suggestions, respectively;
- Matteo S. and Mike for giving me a hand with cell cultures and RT-PCR stuff;
- Alfredo and Lorenzo for the time spent to help me during the bioreactor production;
- My laboratory colleagues Matteo T., matteo D., Thiago, Andrea, Michele, Roberto, Beppe, Cristina, Gian, Fabio, Christian, Dario, Eva, Marta, LDB, Gas, Mari, Massimo, Walter for supporting and helping me during all these years.
- Virgin radio for the several hours spent on air, keeping me company.